# Synchrotron radiation and heritage materials

Loïc Bertrand
IPANEMA CNRS/MiC/UVSQ
Synchrotron SOLEIL

PAST

PRESENT

“Raw” material

“Ancient” material

**cultural heritage**
**archaeology**
**palaeontology**
**palaeo-environments**

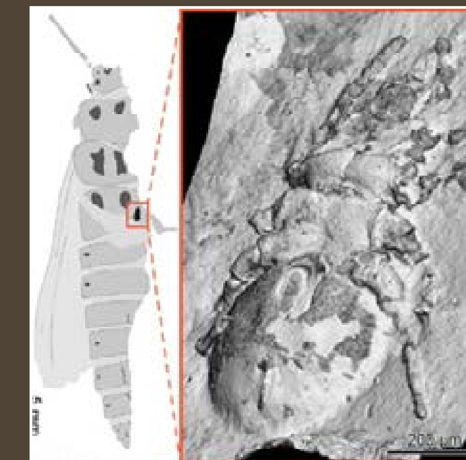

Origin of Life
Evolution / Development
Ecological affinities
Palaeo-environment

Sources of raw materials
Diffusion pathways
*“Chaînes opératoires”*

Technical art history
Chronology
Authentication

Alteration / Corrosion
Taphonomy
Exceptional preservations

PRESENT

FUTURE

"Ancient" material

"Future" material

Stabilisation
Consolidation
Restauration

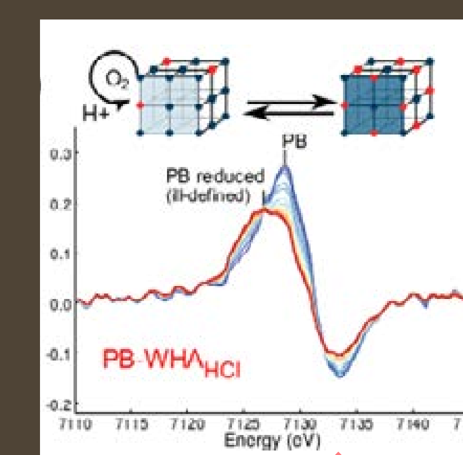


New analytical methods
Analogous materials
Long-term behaviour laws

**3 typical examples** illustrating the problematics at stake and the diversity of the approaches developed

**lute**, detail, Laux Maler (1485–1552), Bologna, 16th c., Musée de la musique, Paris, inv. num. E.2005.3.1 (*J-M. Anglès*)

**amulet**, Mehrgarh, Baluchistan, Pakistan, period III, 4500–3600 BCE, inv. no. MR.85.03.00.01 *(D. Bagault)*

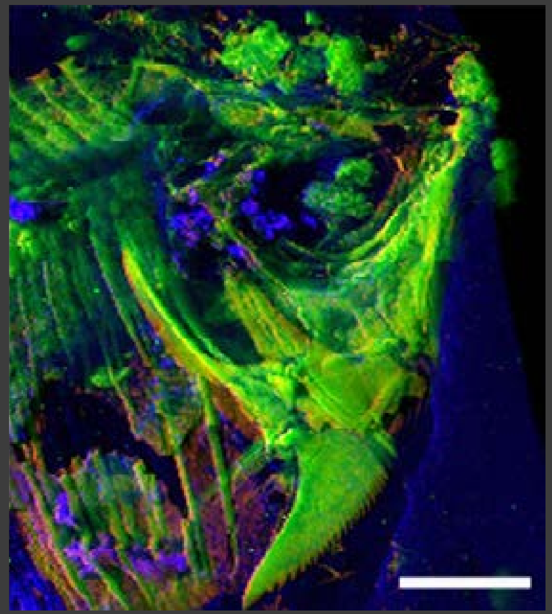

**fossil fish**, Late Cretaceous, -95 Myr, Djebel Oum Tkout Morocco (*P. Gueriau et al.*)

**lute**, Laux Maler (1485–1552), Bologna, 16th c., Musée de la musique, Paris, inv. num. E.2005.3.1 (*J.-M. Anglès*)

**Antonio Stradivari**, Provigny violin, 1716, inv. num. E.1730, Musée de la musique, Paris (*Cité de la musique, A. Giordan*)

oral tradition

Der Lautenmacher.

Gut Lauten hab ich lang gemacht
Auß Tannenholtz/gut vnd geschlacht/
Erstlich vber die Form gebogn/
Darnach mit Saiten vberzogn/
Vnd angestimmt mit süssem Klang/
Eben gleich figuriertem Gsang/
Gefürnist Kragen/Bodn vnd Stern/
Auch mach ich Geigen vnd Quintern.
D iij Der

historical sources

material evidence

light microscopy, Zeiss Axio Scope.A1, filter Fs05, 395–440 nm exc. 2-µm ultramicrotomed cross-section (Leica EM UC6, *J.-P. Échard*)

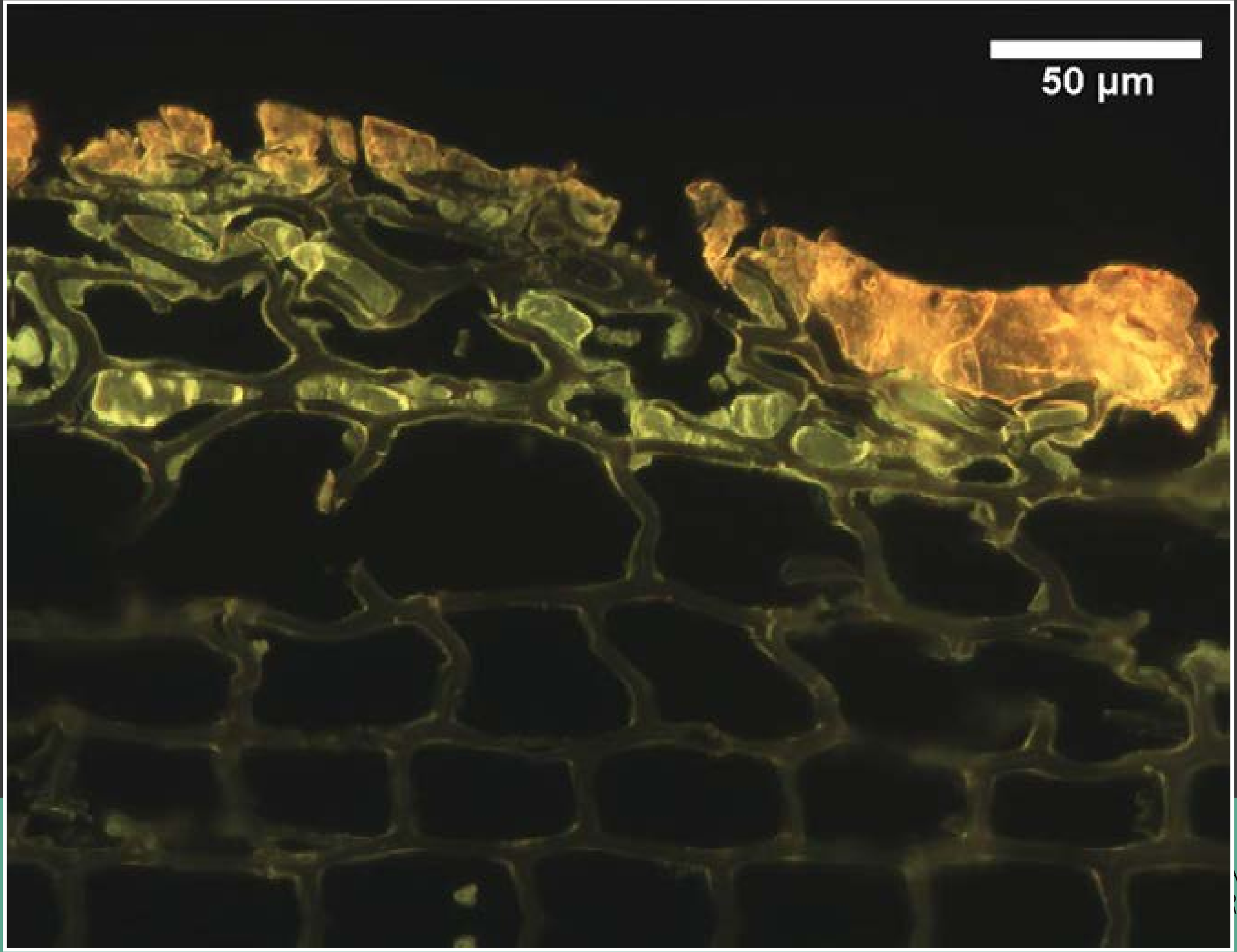


surface stratum

lower stratum

wood cell

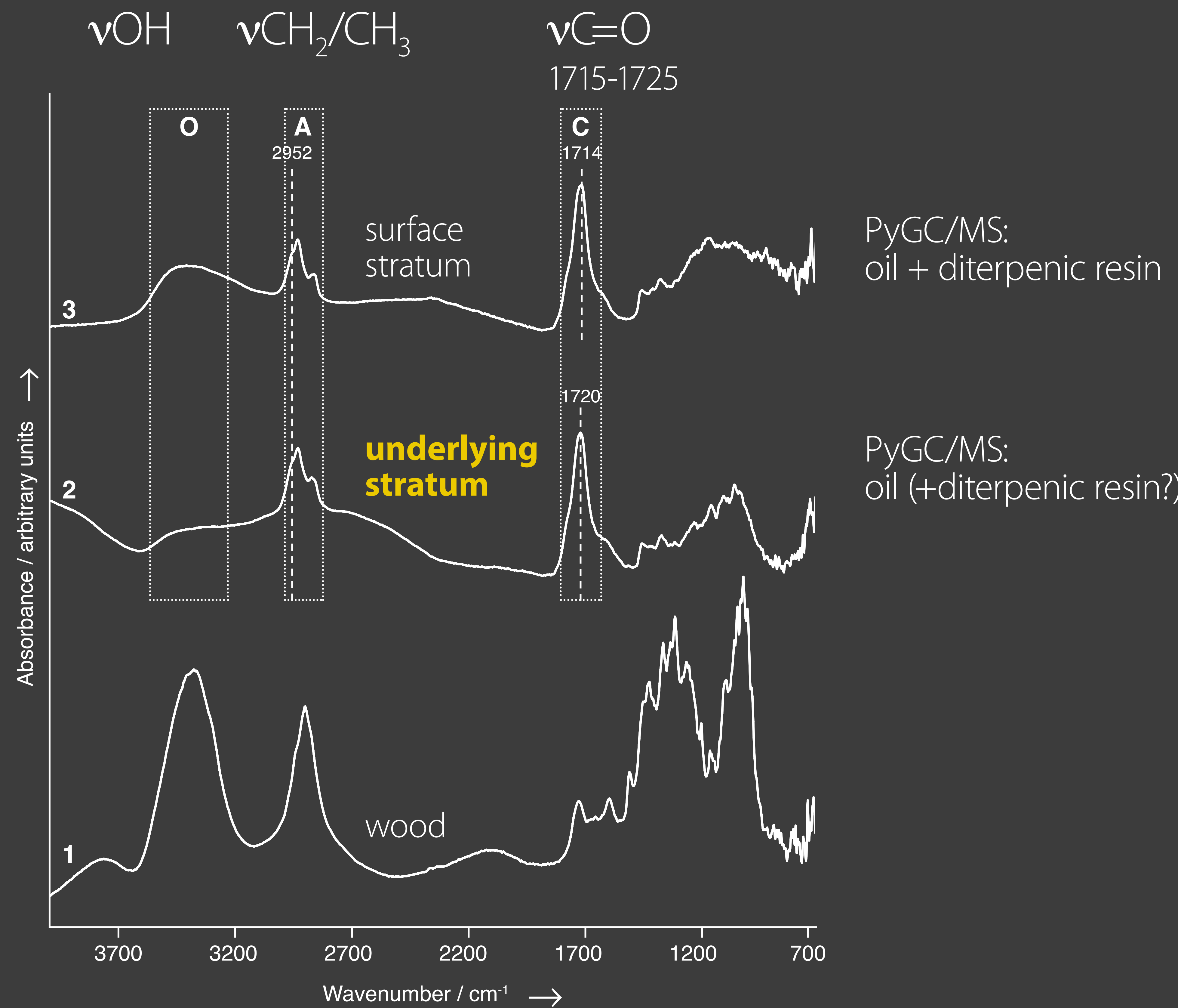
νOH
$\nu CH_2/CH_3$
νC=O
1715-1725
O
A
2952
C
1714
1720
surface stratum
underlying stratum
wood
3
2
1
Absorbance / arbitrary units
3700
3200
2700
2200
1700
1200
700
Wavenumber / cm$^{-1}$
PyGC/MS:
oil + diterpenic resin
PyGC/MS:
oil (+diterpenic resin?)

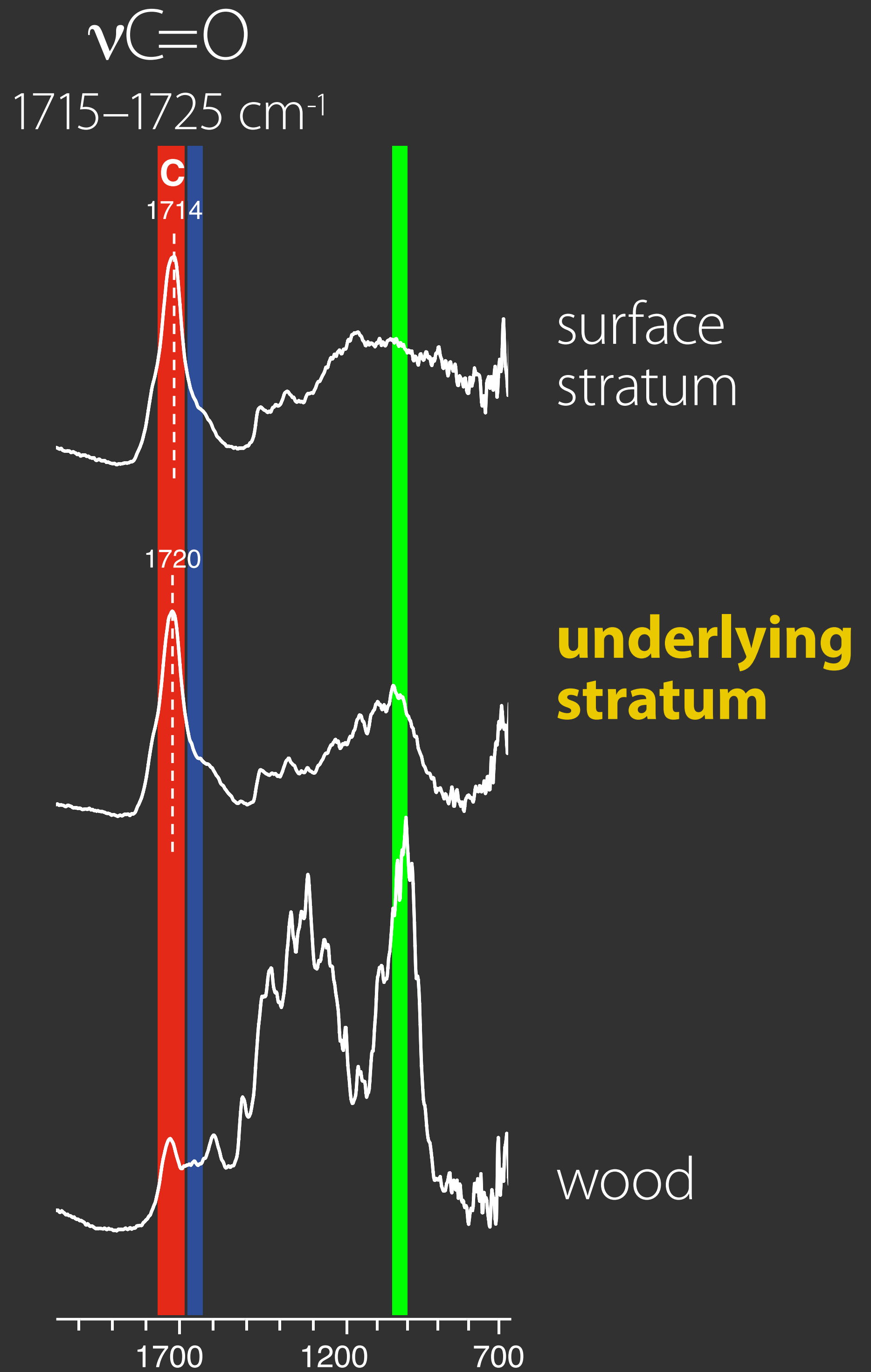


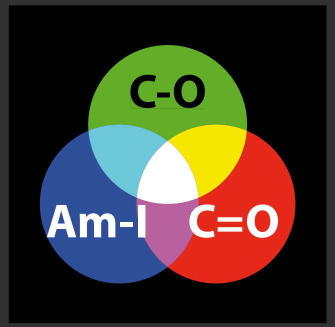


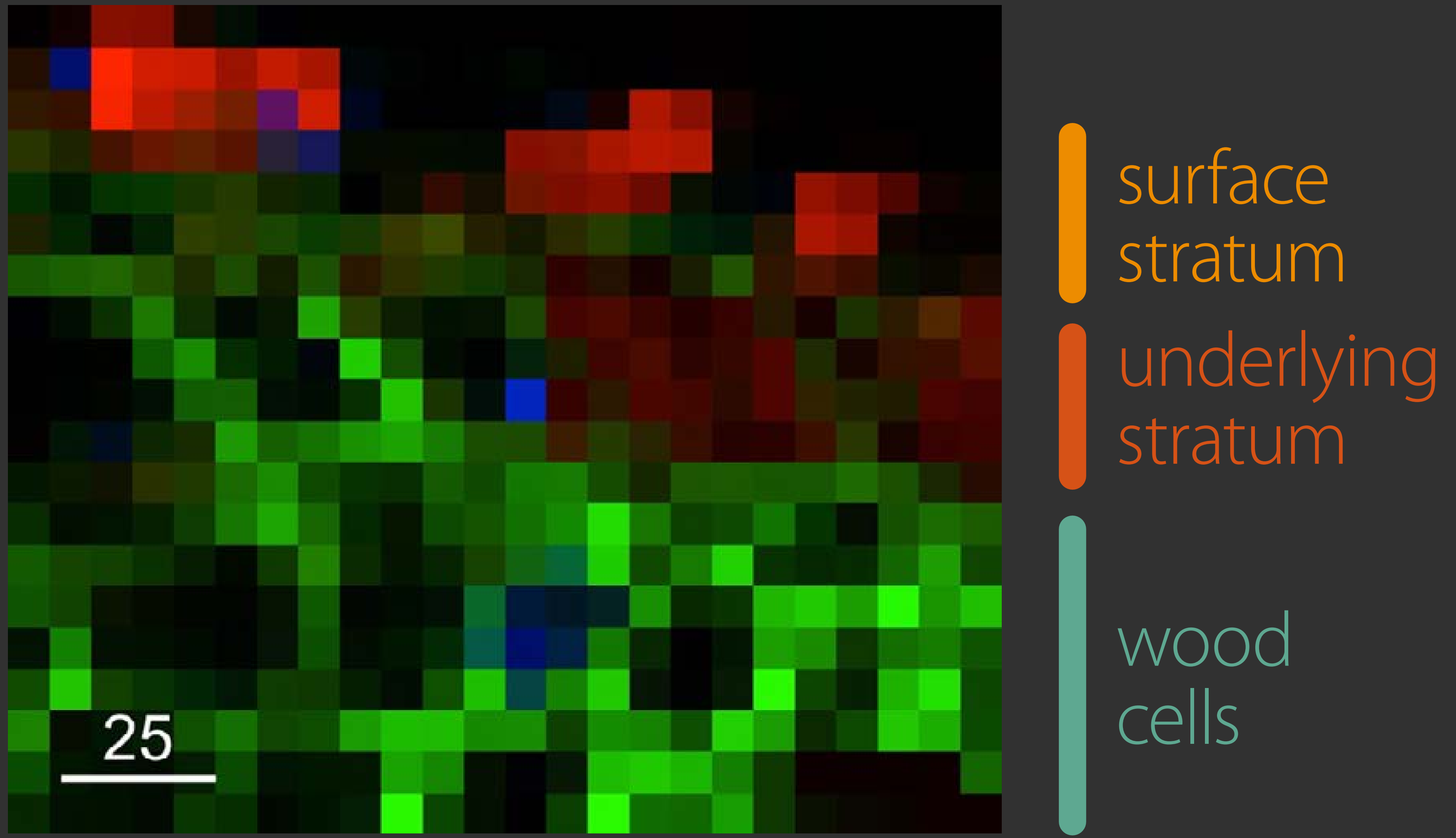


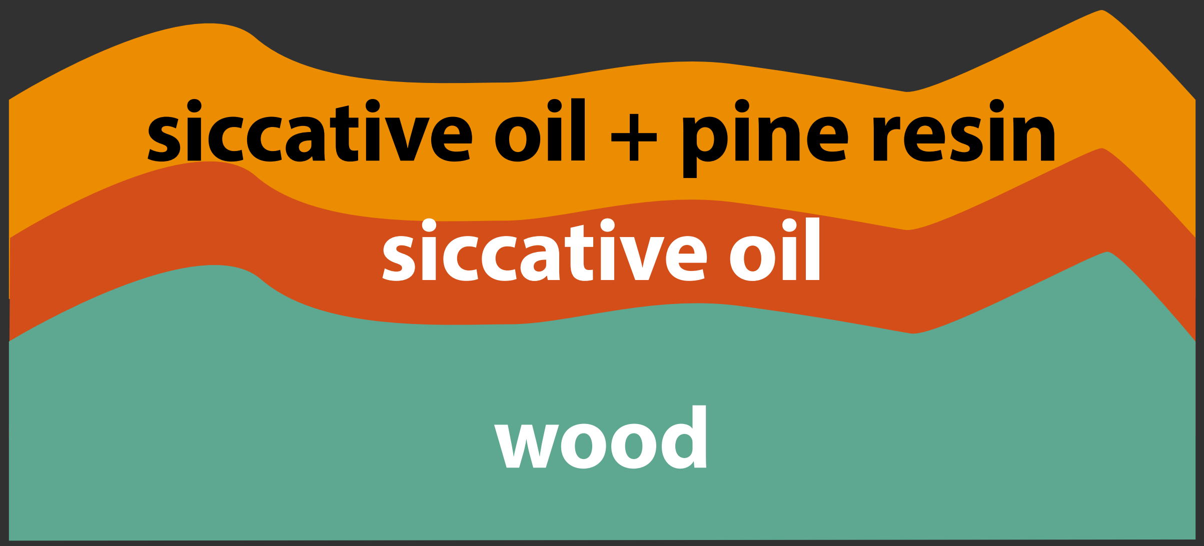


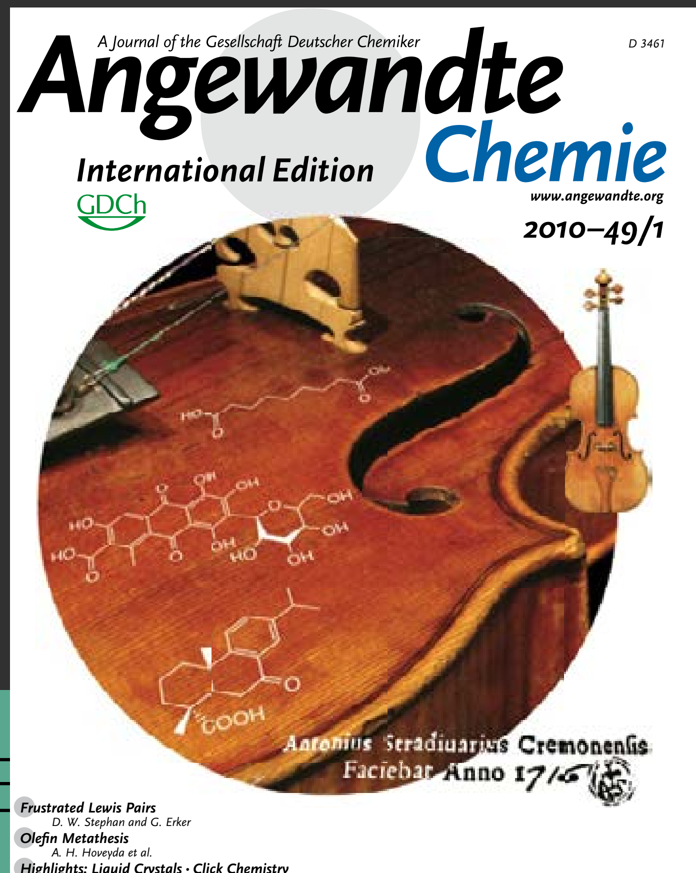




► J.-P. Echard et al. Angew Chem., 2010.

**cello**, Jacques Boquay, bef. 1715, Paris, priv. coll. (*B. Soulier*)

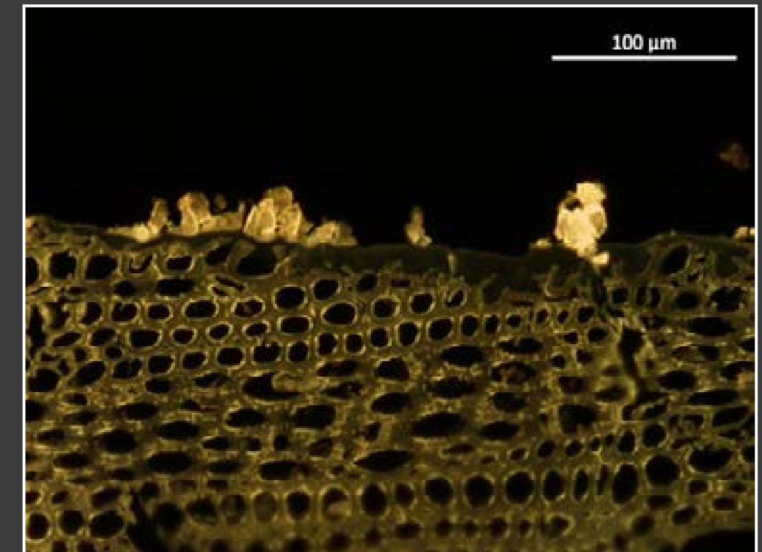


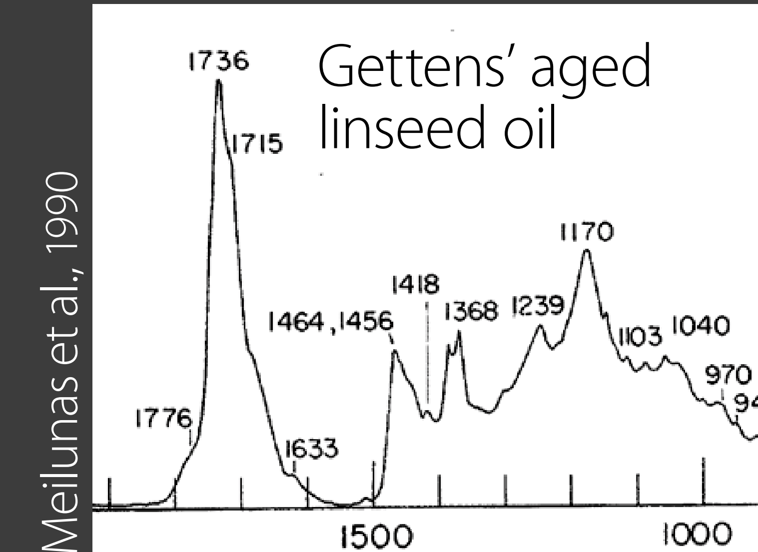


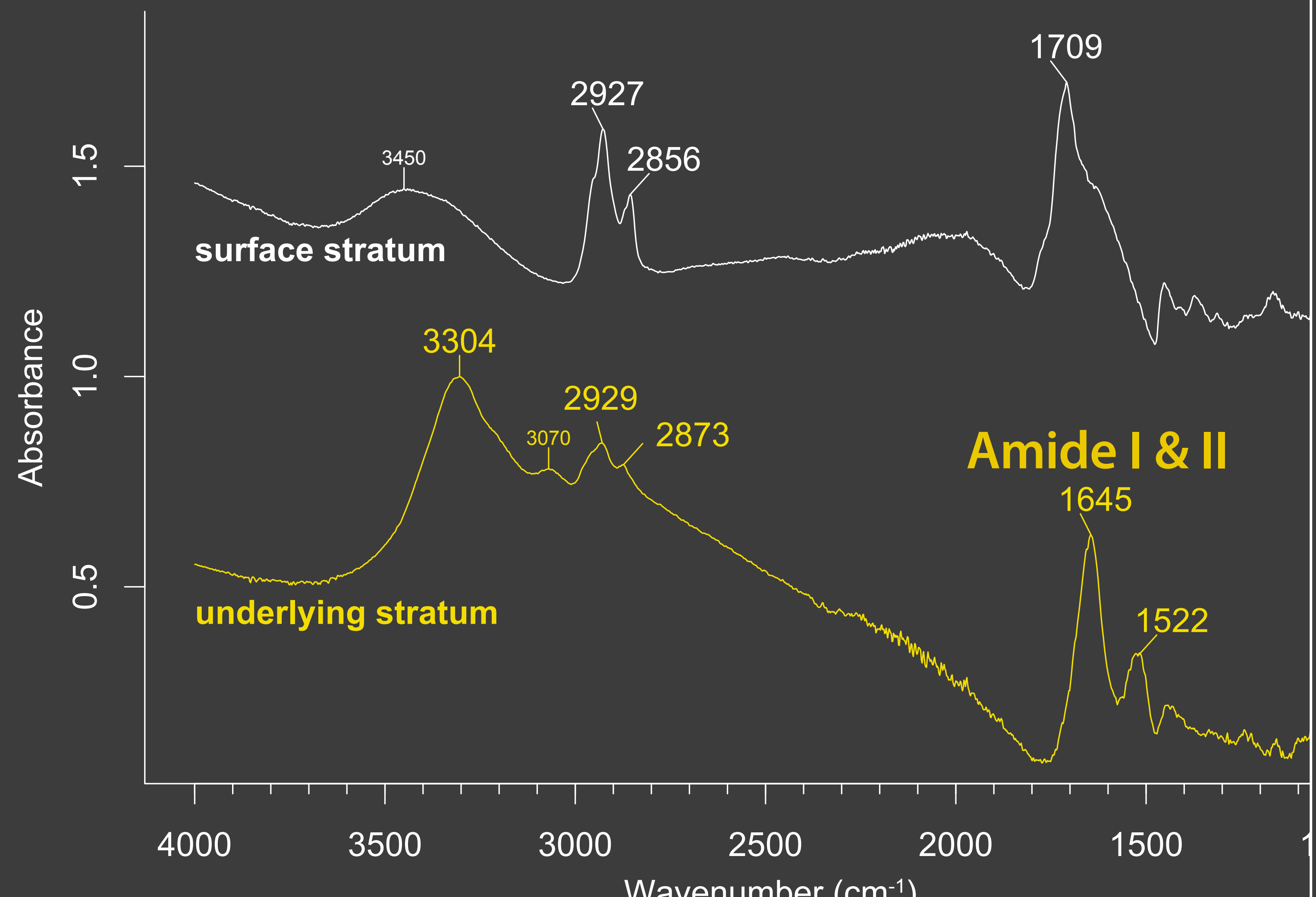


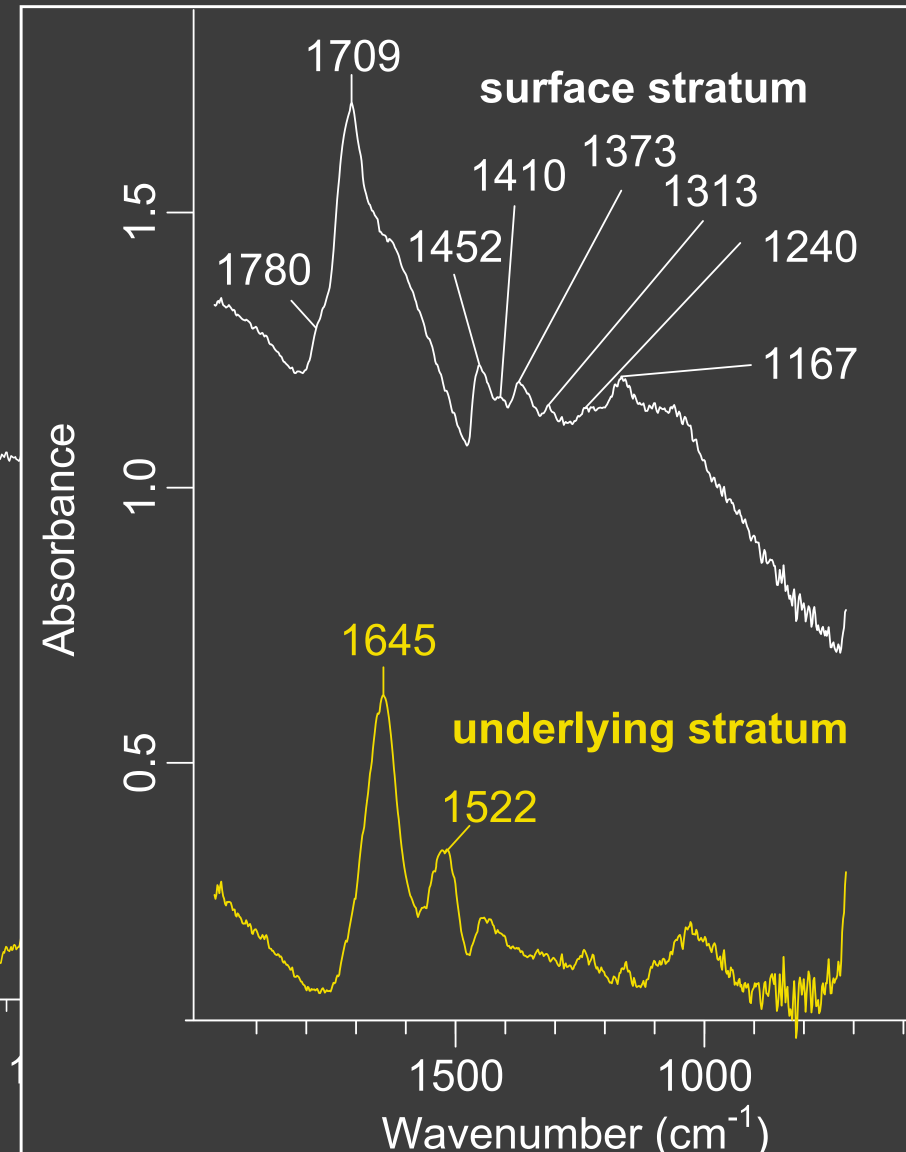


µFT-IR, SMIS (SOLEIL)
10x10 µm²

► L Bertrand et al. ABC, 2011.

# in the infrared, the specificity of the synchrotron source is not its high flux

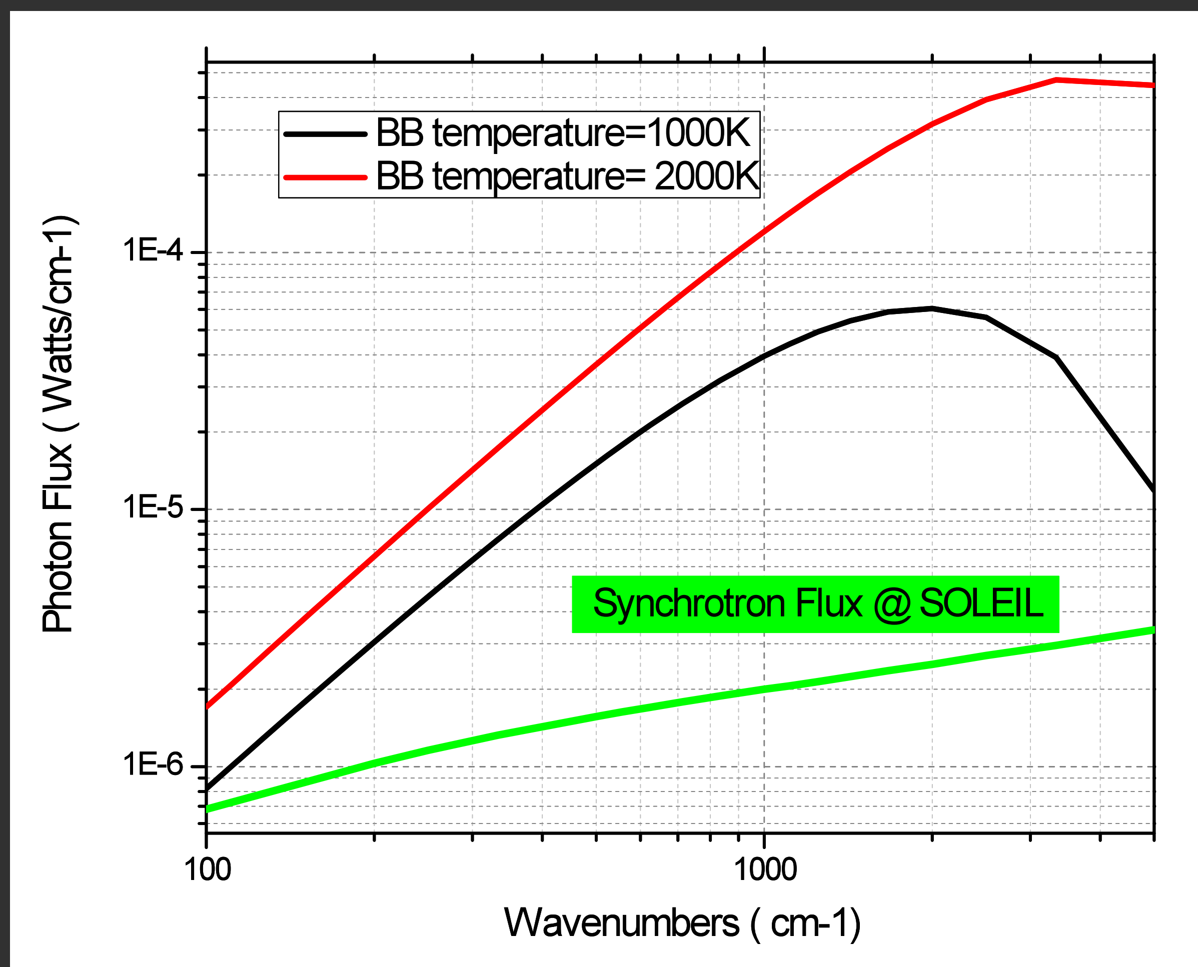


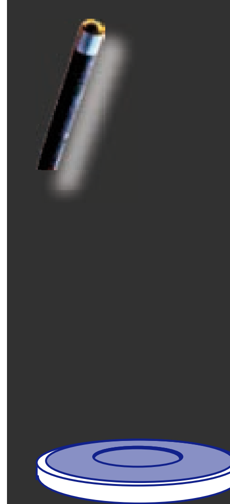

P. Dumas

# …but its brightness!

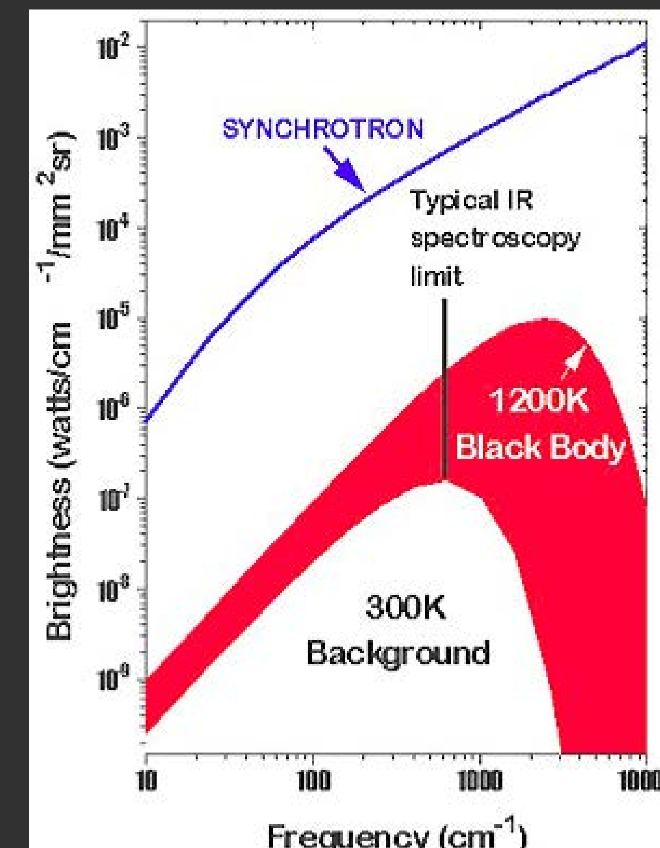


$10^{-3}$ $10^{-2}$ $10^{-1}$ 1

Energy (eV)

P. Dumas

E. Levenson et al. J. Synchrotron Rad., 2008.

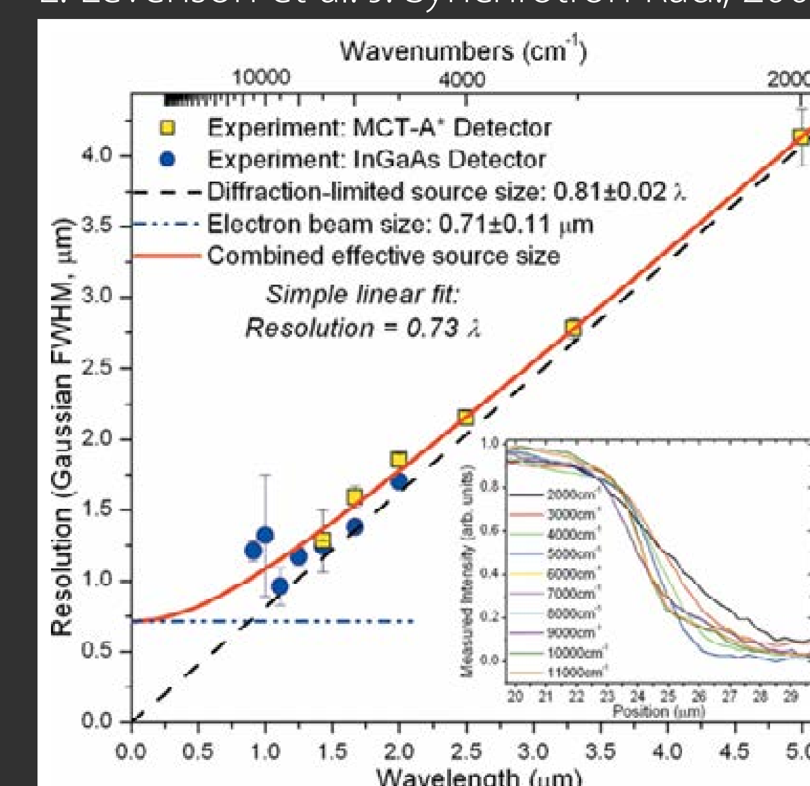

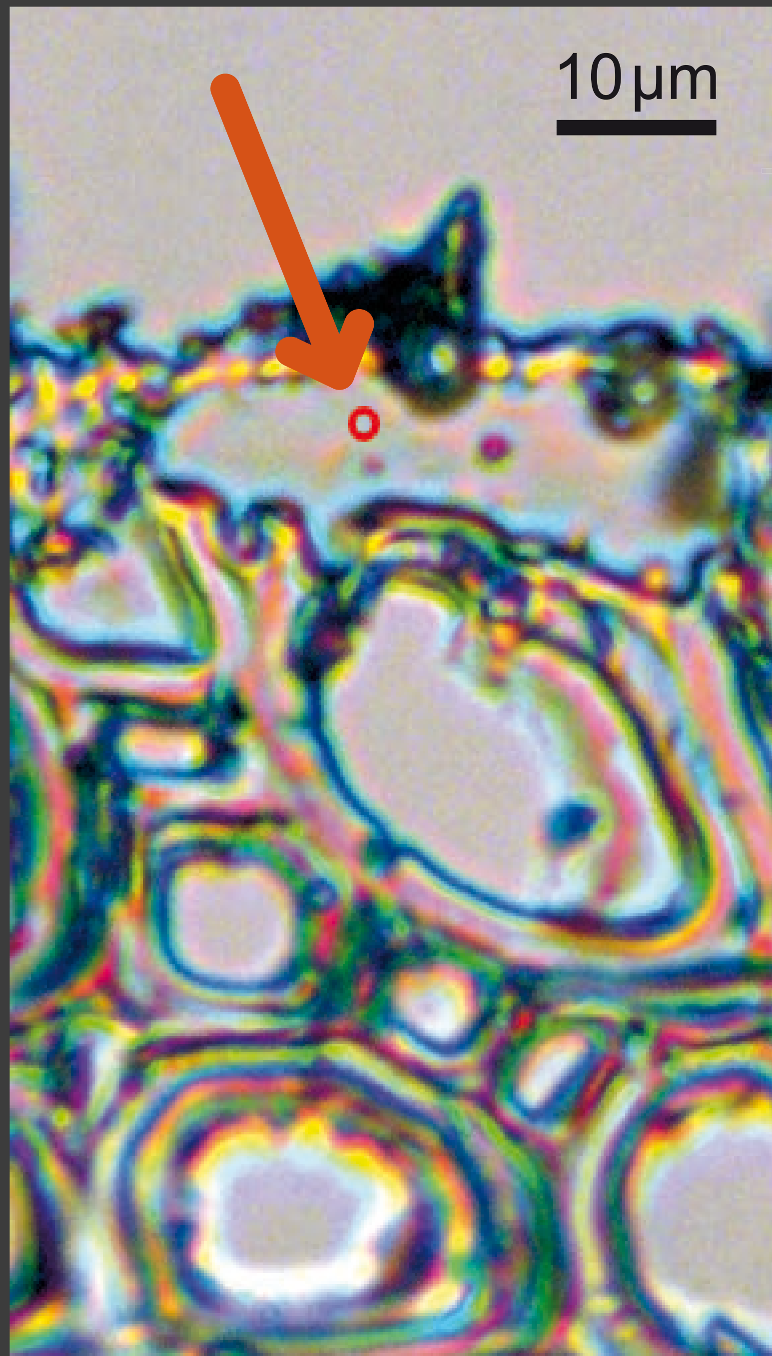


fragmentary surface stratum

underlying protein stratum

wood cell walls

thin section from the Boquay cello

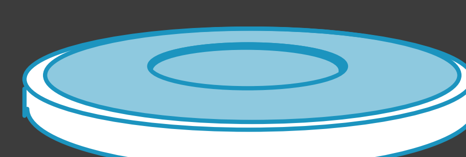

UV PL @ SOLEIL DISCO
B. 272 nm exc. 60s
C. 275 nm exc. 120s

hide glue reference:

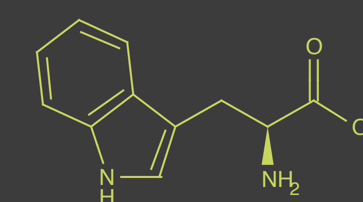


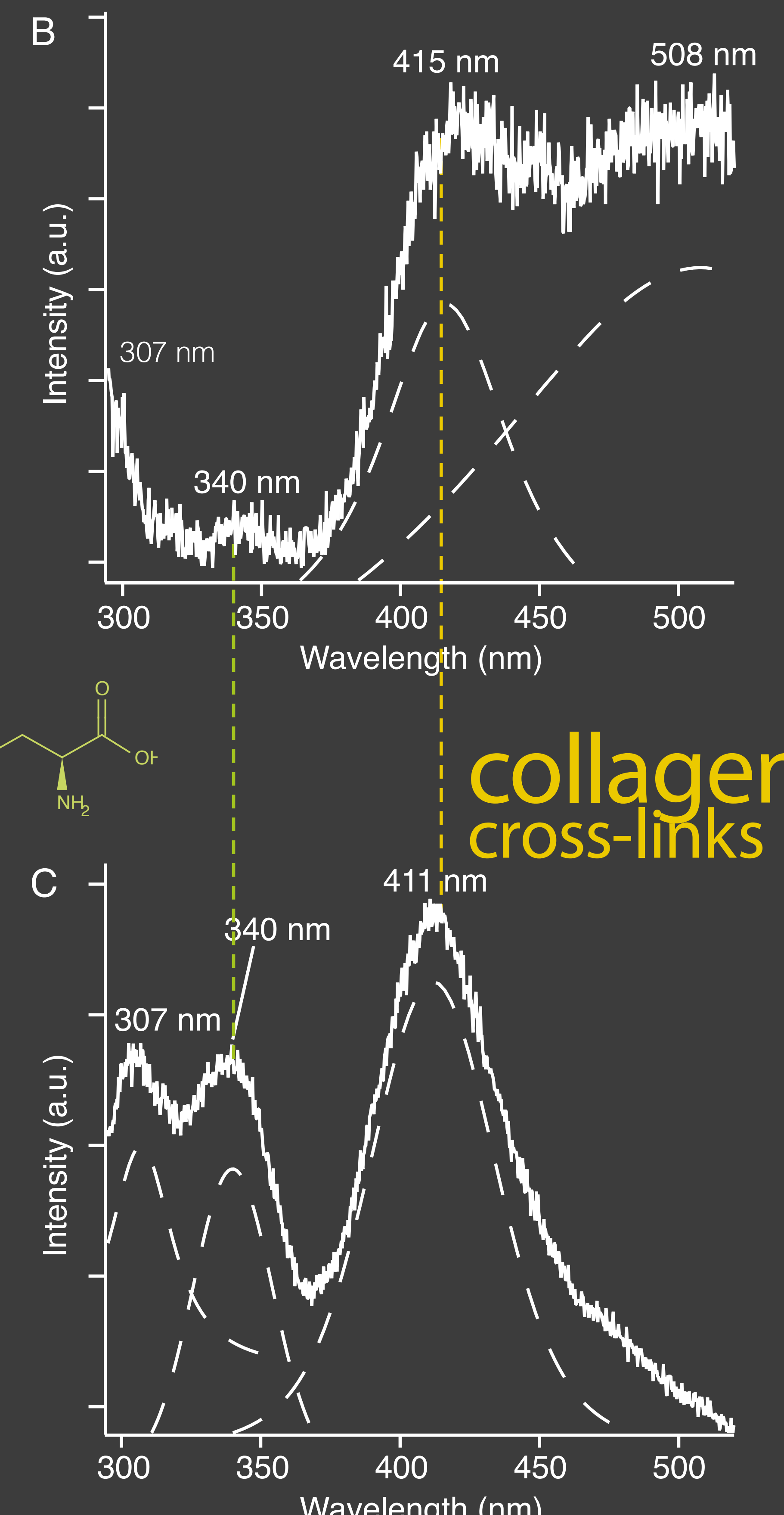




► M. Thoury et al. Anal. Chem., 2011.

**lute**, Laux Maler (1485–1552), Bologna, 16th c., Musée de la musique, Paris, inv. num. E.2005.3.1 (*J.-M. Anglès*)

one of the earliest surviving Italian lutes

**epiluminescence**
365 nm exc. (Hg)

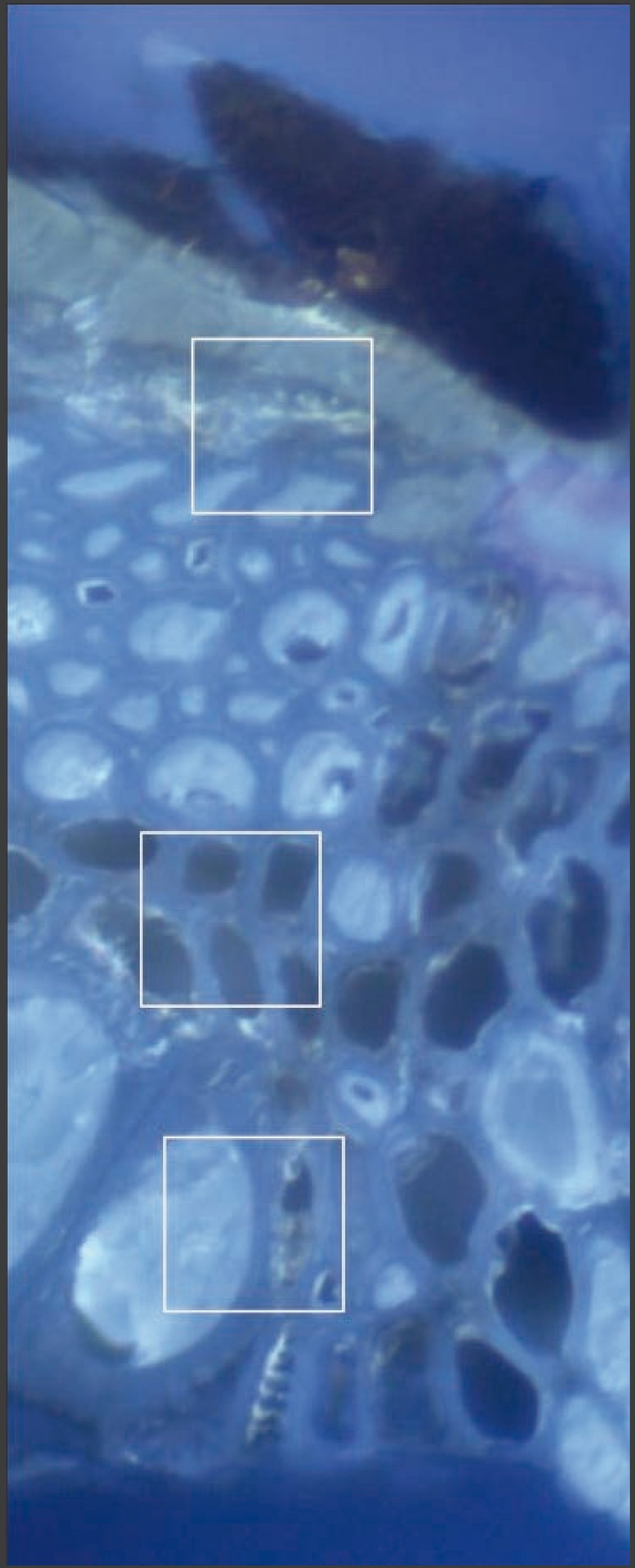

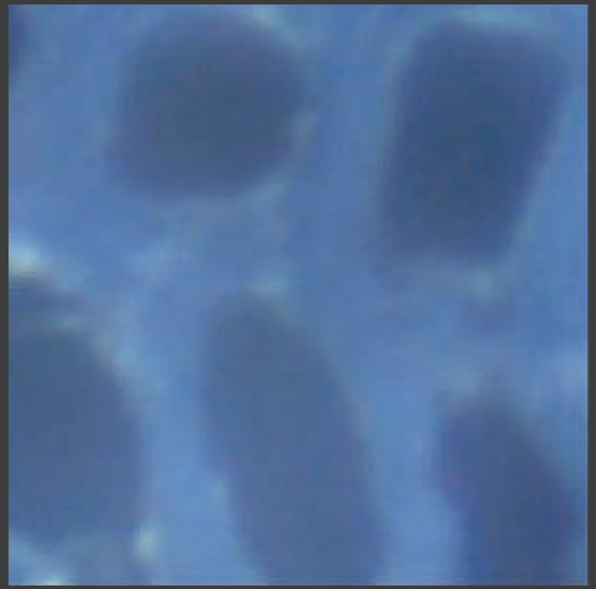

► M. Thoury et al. Anal. Chem., 2011.

**lute**, Laux Maler (1485–1552), Bologna, 16th c., Musée de la musique, Paris, inv. num. E.2005.3.1 (*J.-M. Anglès*)

light microscopy and Py-GC/MS:
surface stratum: drying oil + diterpenic Pinaceae resin
underlying stratum: drying oil
ash wood (Fraxinus sp.)

**Synchrotron deep UV PL @ SOLEIL DISCO**
275 nm exc. / 380, 465, 500 nm em.
313 nm proj. pixel size

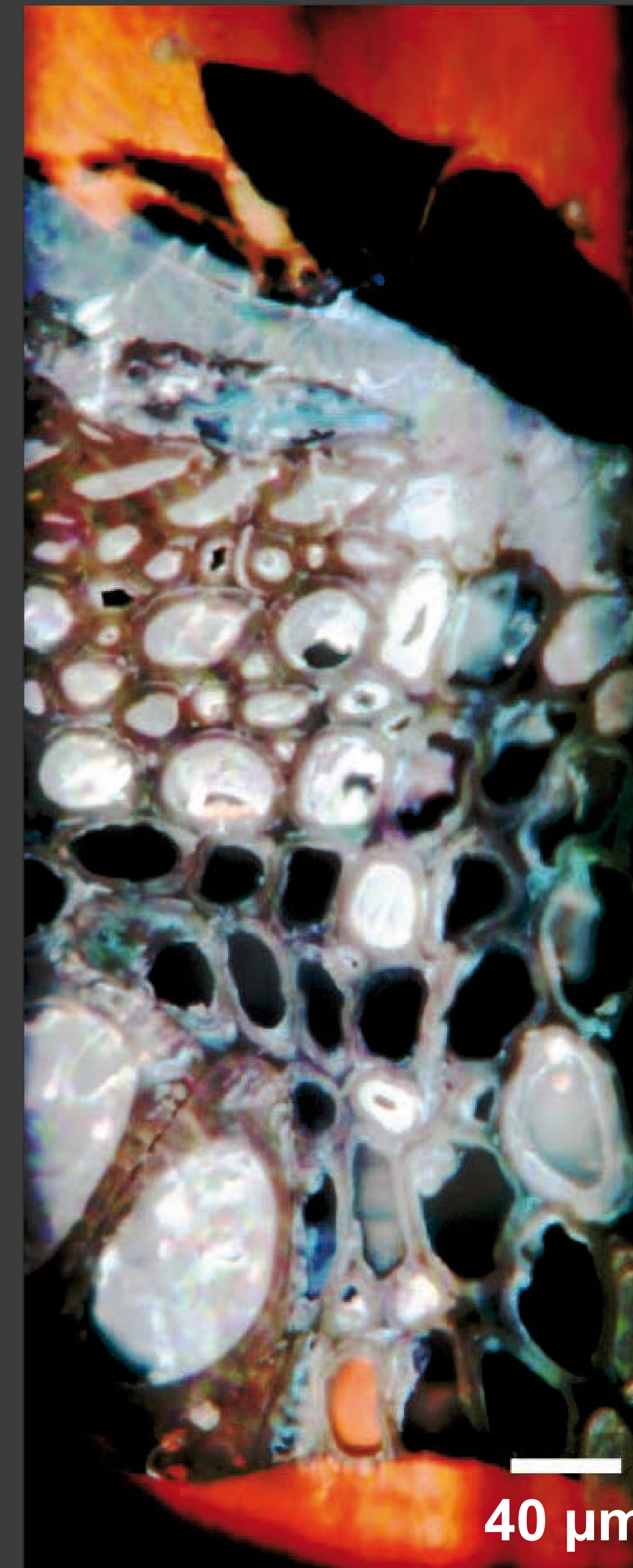


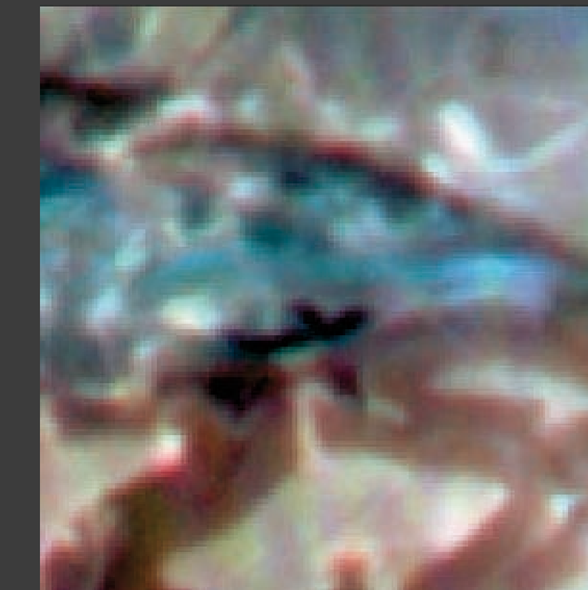

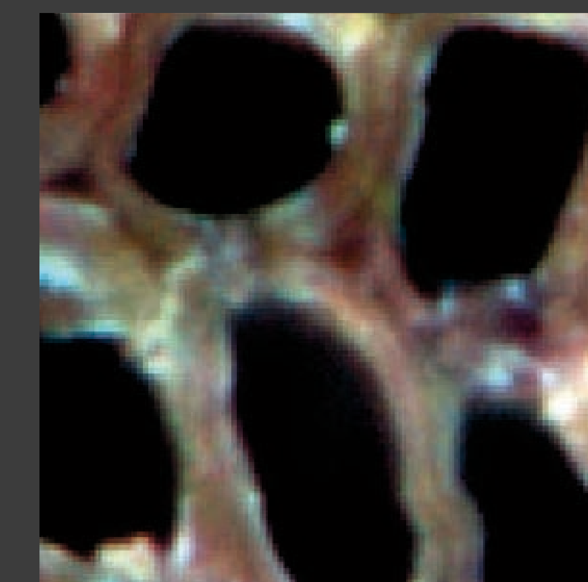

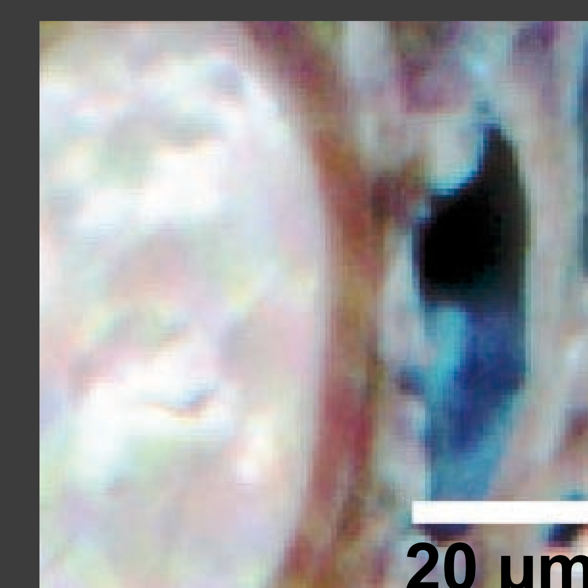


► J.-P. Échard et al., Analyst, 2015.

# Early lost-wax cast

M. Thoury, B. Mille, T. Séverin-Fabiani et al.

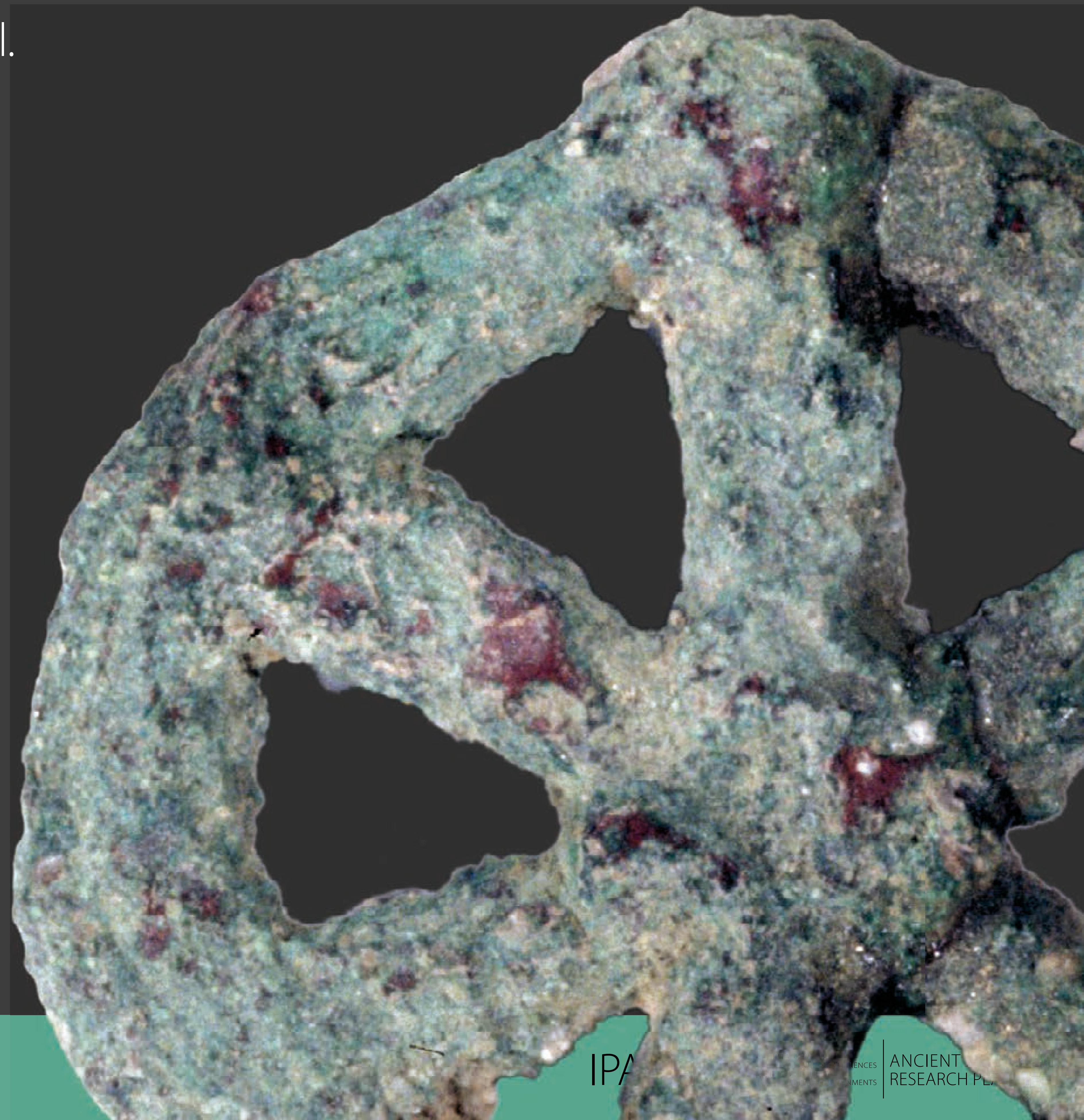

**amulet**, inv. no. MR.85.03.00.01,
Mehrgarh, Baluchistan, Pakistan,
period III, 4500–3600 BCE
*(C2RMF, D. Bagault)*

| | |
|---|---|
| Period I–II | 7500 – 5500 BCE |
| Period III | 4500 – 3600 BCE |
| Periods IV–V | 3600 – 3100 BCE |
| Periods VI–VII | 3100 – 2600 BCE |
| Period VIII | ca. 2100 – 1900 BCE |

1974: Discovery of the Mehrgarh site


Jean-François Jarrige

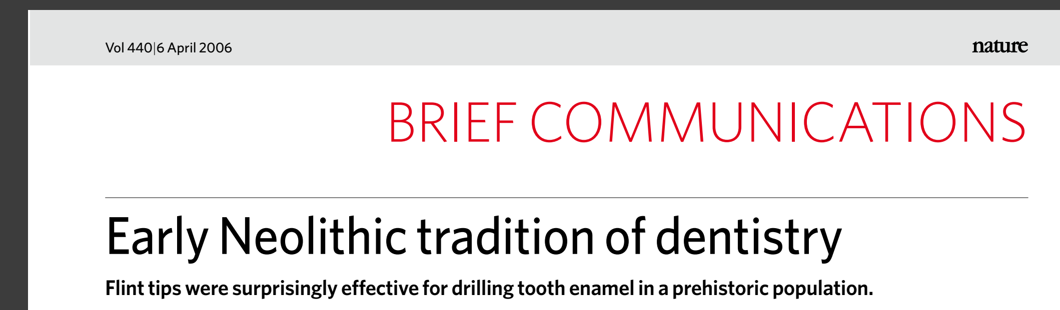

Vol 440|6 April 2006 nature

BRIEF COMMUNICATIONS

Early Neolithic tradition of dentistry

Flint tips were surprisingly effective for drilling tooth enamel in a prehistoric population.

Coppa *et al.*
7000–5500 BCE

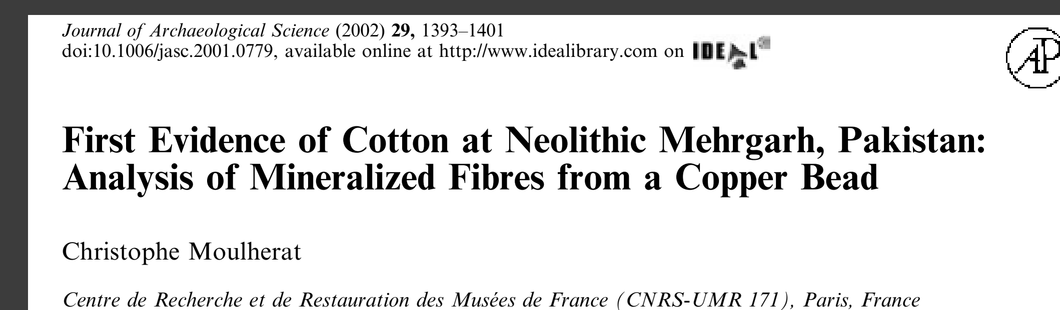

*Journal of Archaeological Science* (2002) **29**, 1393–1401
doi:10.1006/jasc.2001.0779, available online at http://www.idealibrary.com on IDEAL

**First Evidence of Cotton at Neolithic Mehrgarh, Pakistan: Analysis of Mineralized Fibres from a Copper Bead**

Christophe Moulherat

*Centre de Recherche et de Restauration des Musées de France (CNRS-UMR 171), Paris, France*

6th mill. BCE

**Togau ceramic vessel**, late 5th mill. BCE

**Figurine**, c. 3000 BCE (Musée Guimet)

**Polychrome ware**, c. 3600–3500 BCE

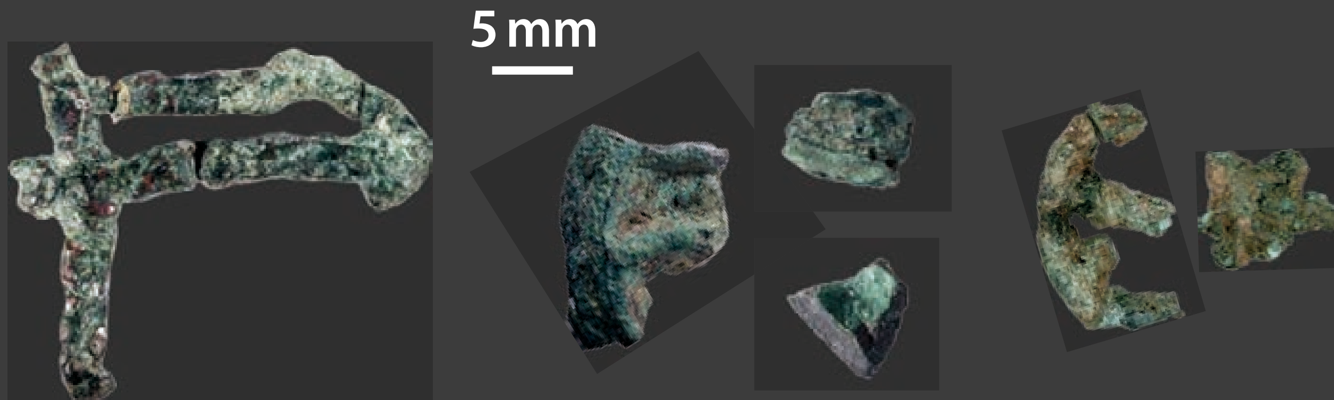


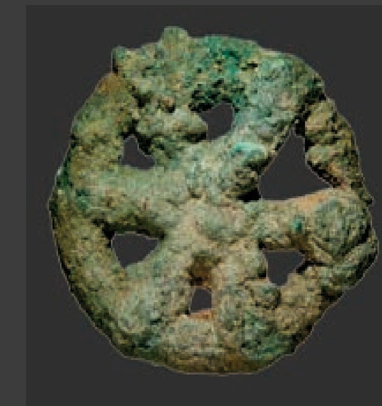

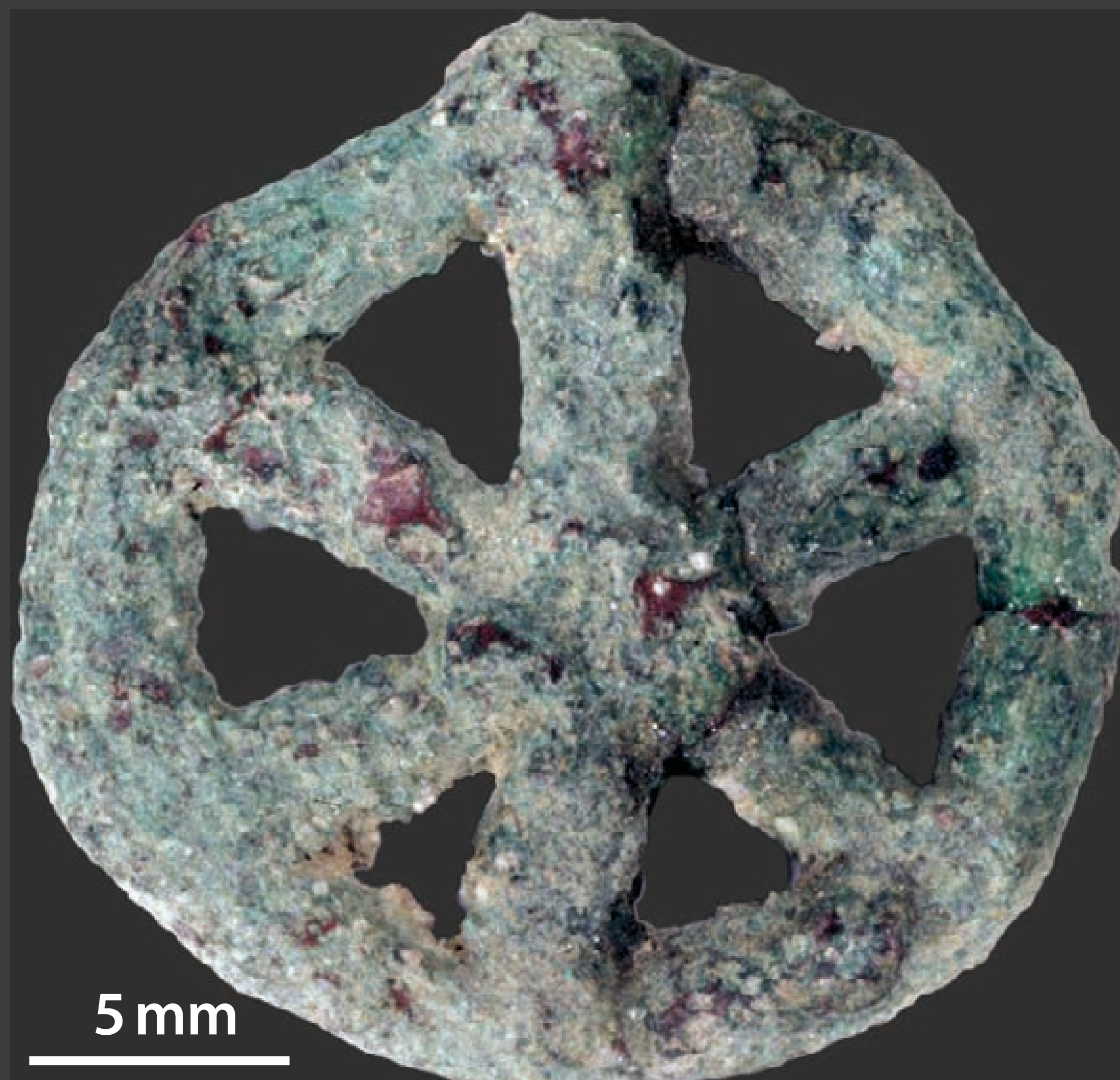


sector 10, MR2,
**Mehrgarh**,
Baluchistan, Pakistan,
period III,
4500–3600 BCE

**amulet**, inv. no. MR.85.03.00.01,
Mehrgarh, Baluchistan, Pakistan,
period III, 4500–3600 BCE
*(C2RMF, D. Bagault)*

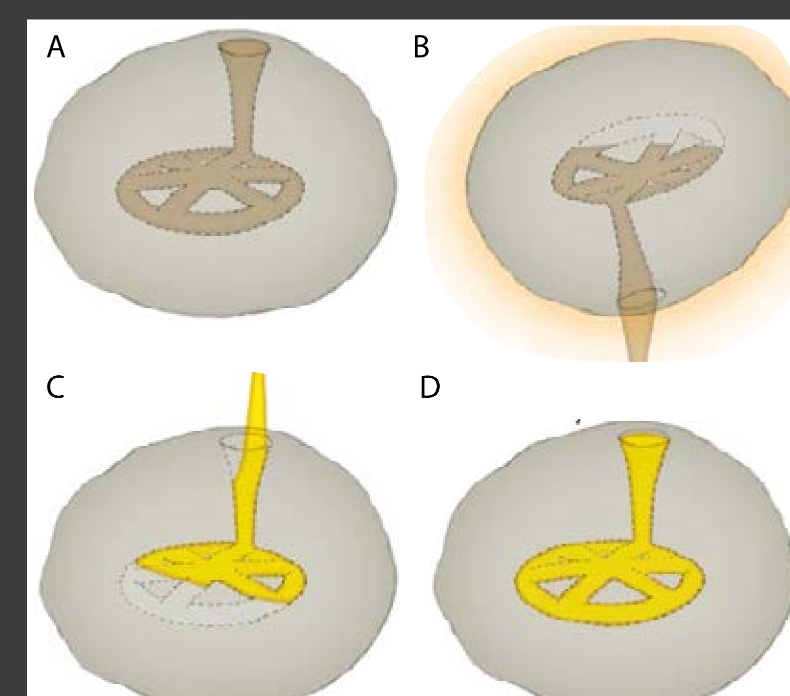


# **Early emergence of lost-wax casting**

3 independent inventions in Eurasia?

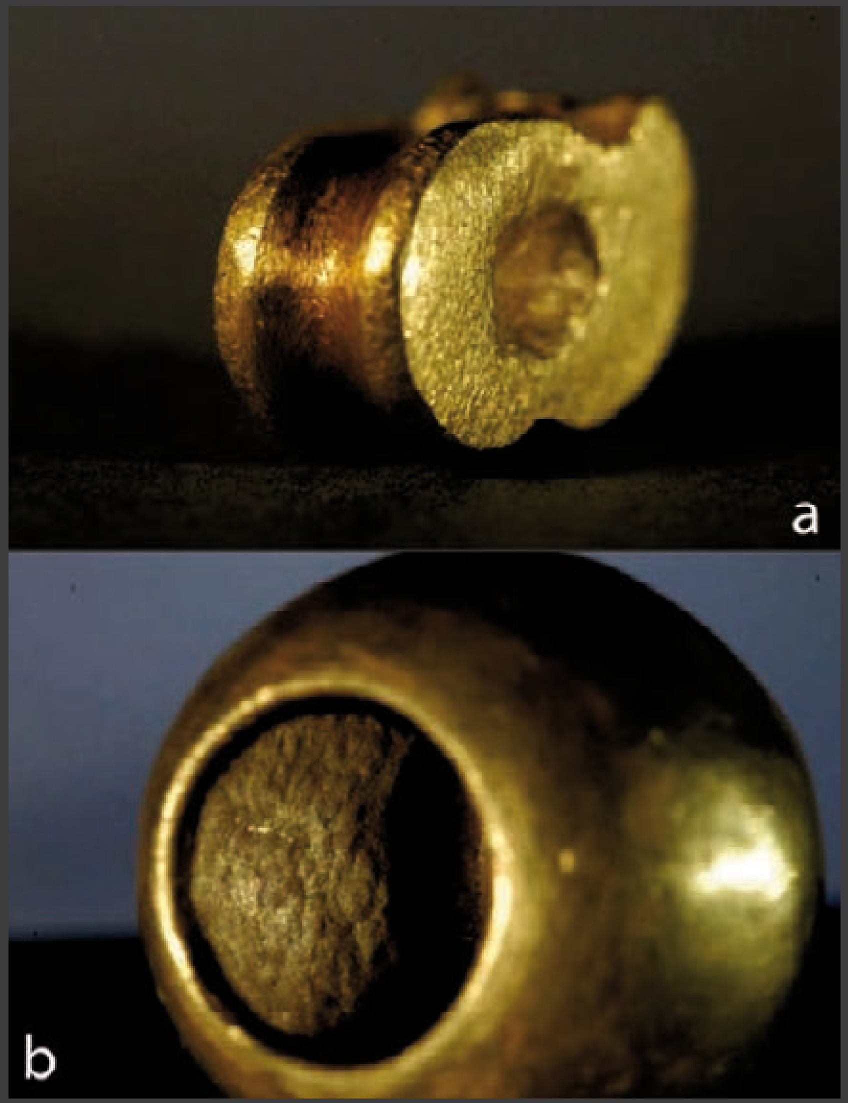


Artefacts, **Varna Cemetery I**, Bulgaria
4550-4450 BCE
(Leusch, Armbruster, Pernicka & Slavcev 2015)

Artefacts, **Mehrgarh MR2**, Pakistan
4500–3600 BCE
(Thoury, Mille et al., 2016)

Hoard, **Nahal Mishmar**, Israel
4200 or 3800 BCE
(Bar-Adon 1980, Klimscha 2013)


VARTA

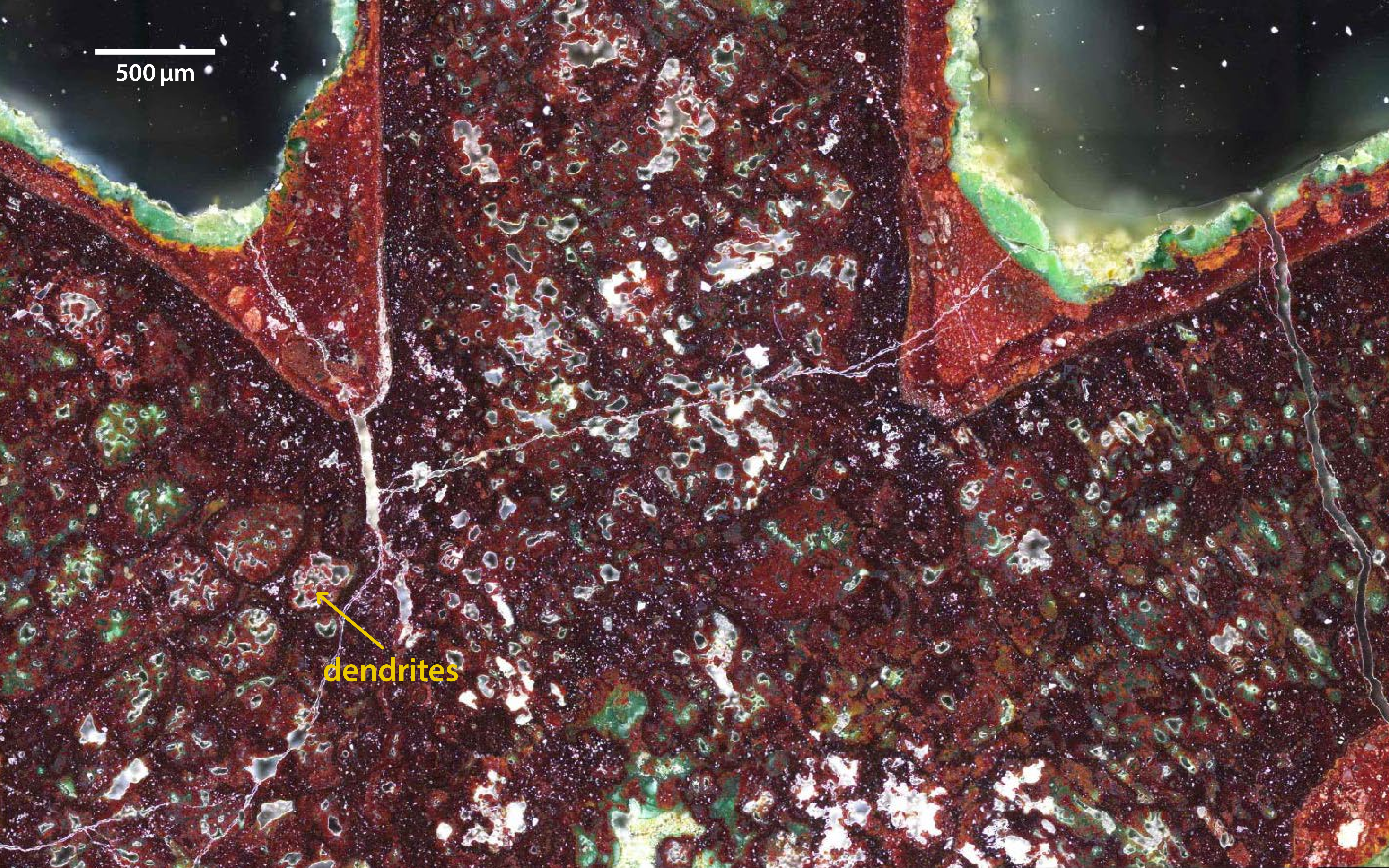
500 µm
dendrites

Synchrotron **XRF** mapping
DiffAbs, SOLEIL synchrotron

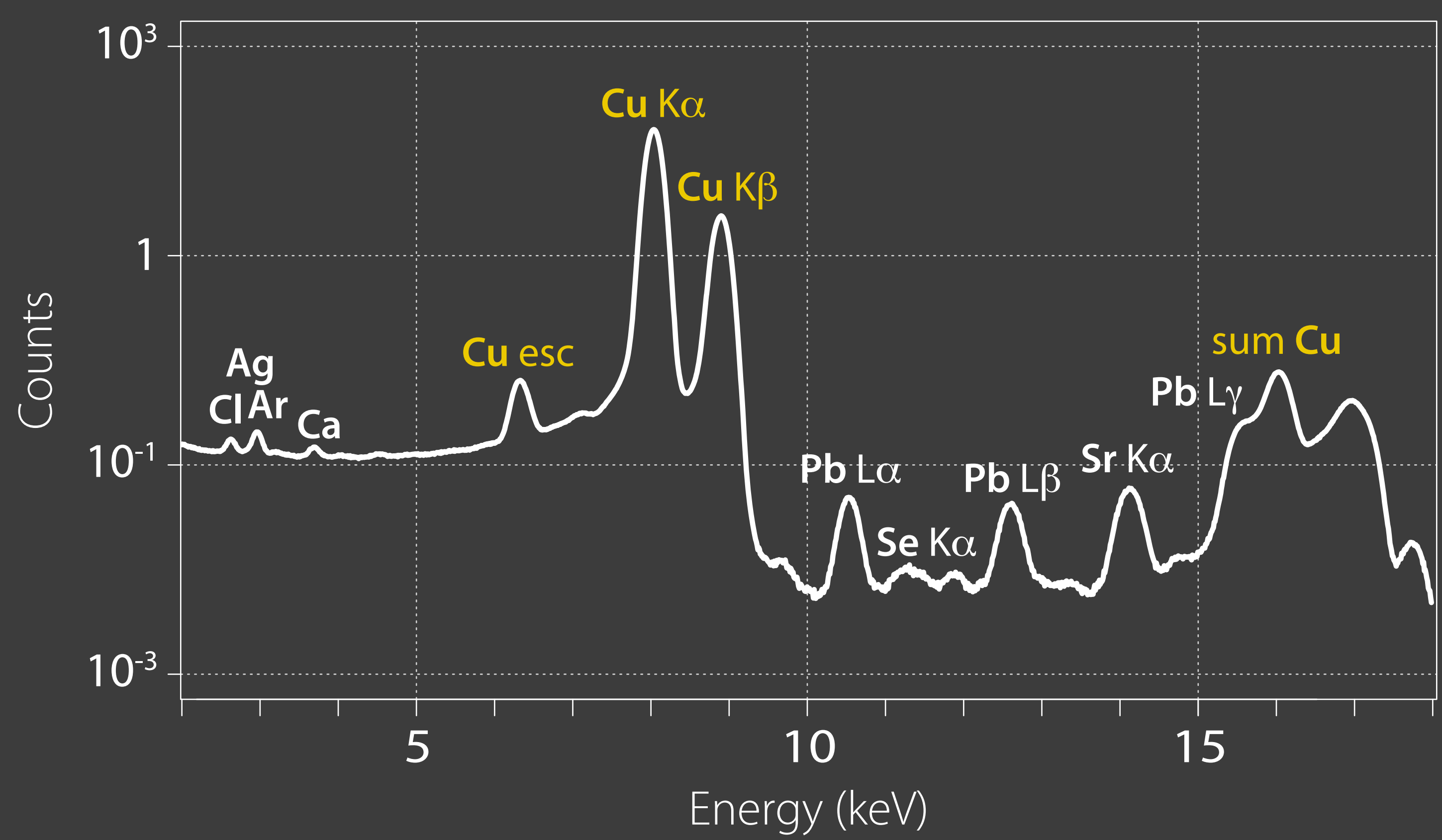


<u>bulk:</u>
[Ag] < 0.2%wt
[Au] = ~300 ppm
[Pb] ~ ppm
As, Se: traces
**no signif. As, Sn, Pb**

<u>dendrites:</u>
Cl

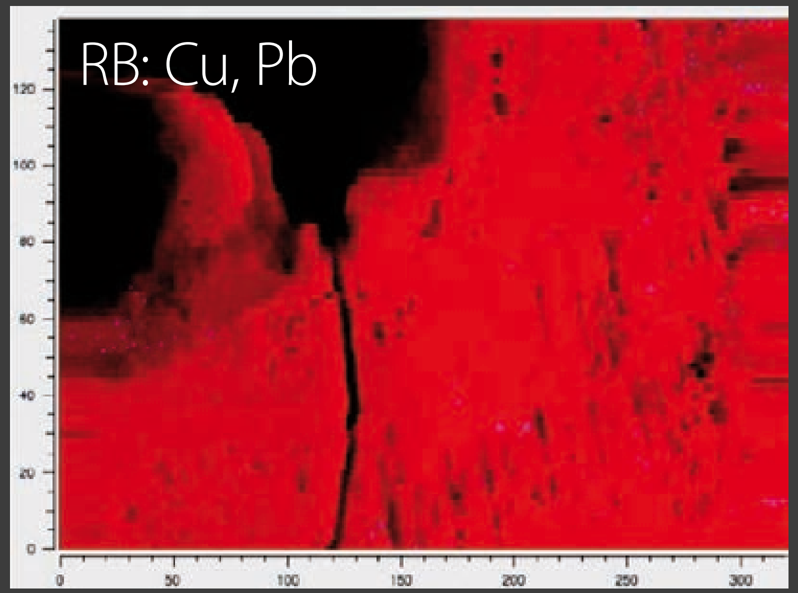


Inverse pole figure, **EBSD**, pixel step: 744 nm
local misorientation < 3.5°

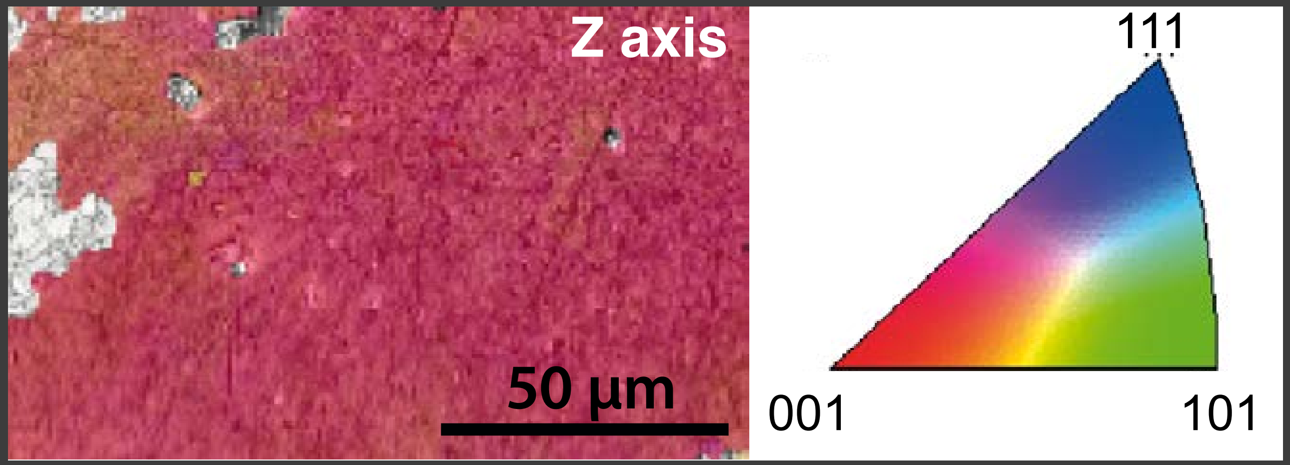


**Raman** spectroscopy
RGB: 632, 416, 218 $cm^{-1}$

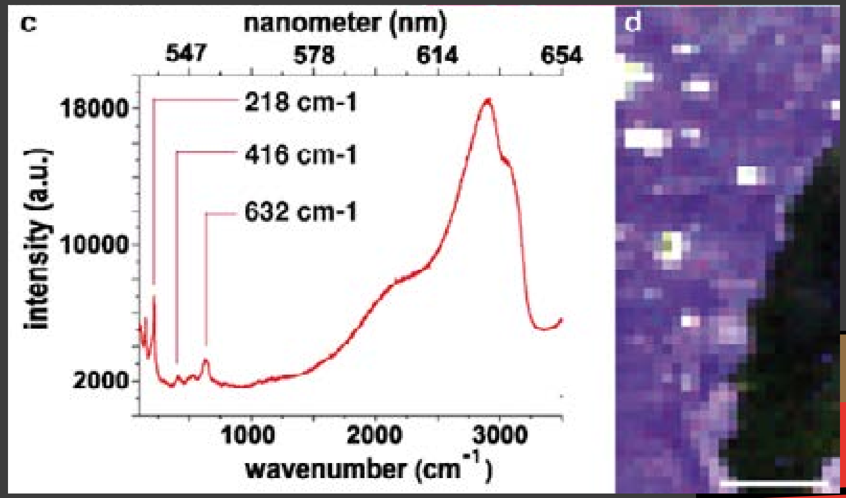


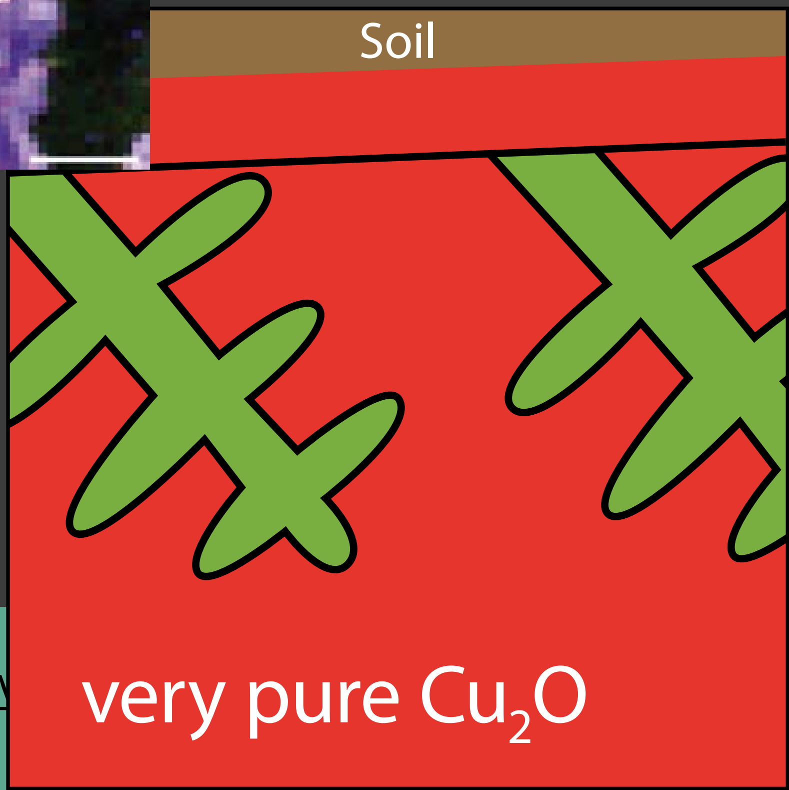

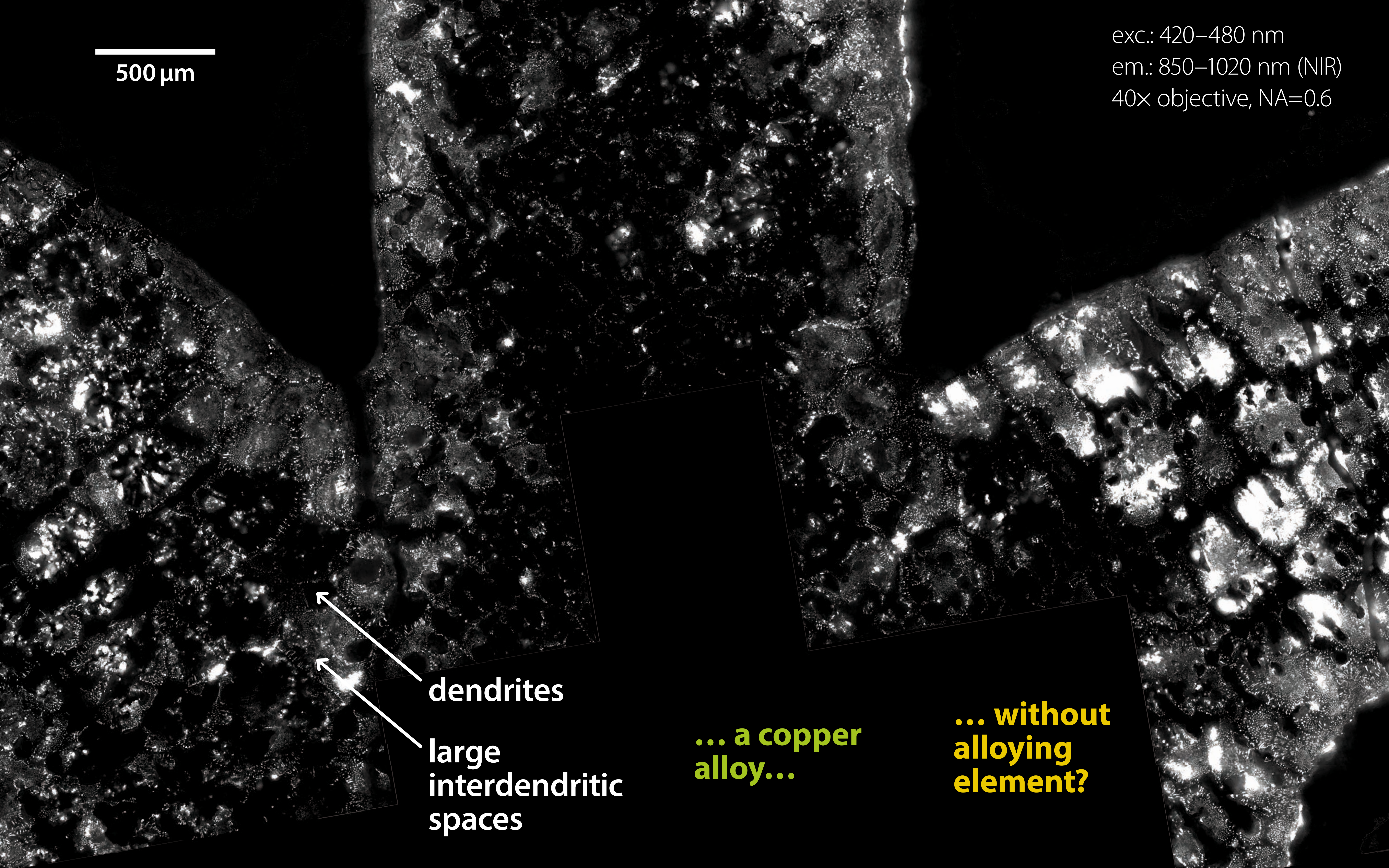
500 µm
exc.: 420–480 nm
em.: 850–1020 nm (NIR)
40× objective, NA=0.6
dendrites
large interdendritic spaces
… a copper alloy…
… without alloying element?

synchrotron UV/visible photoluminescence
TELEMOS instrument, DISCO beamline, SOLEIL (M. Réfrégiers et al.)

synchrotron UV/visible photoluminescence
TELEMOS instrument, DISCO beamline, SOLEIL (M. Réfrégiers et al.)

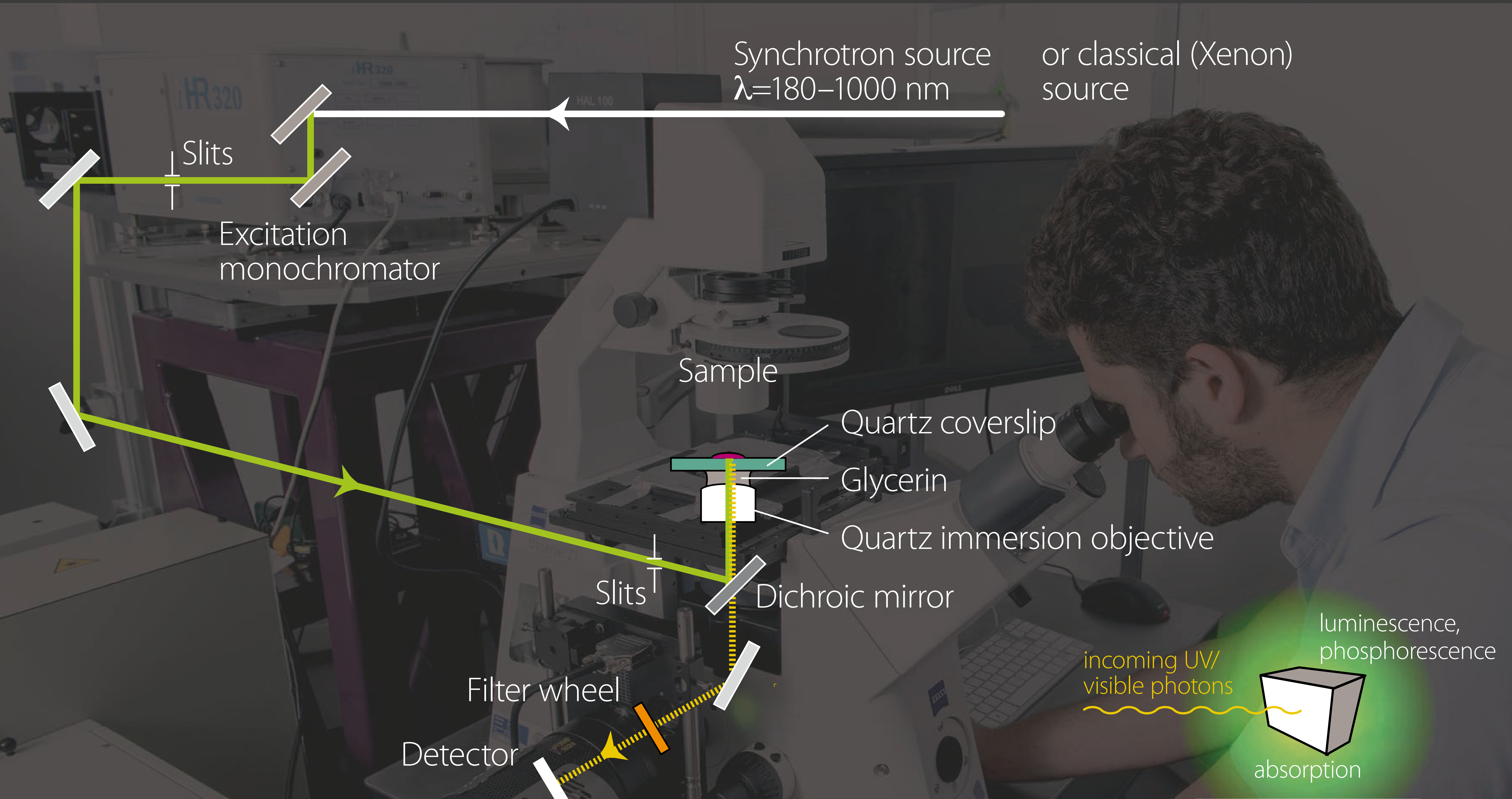

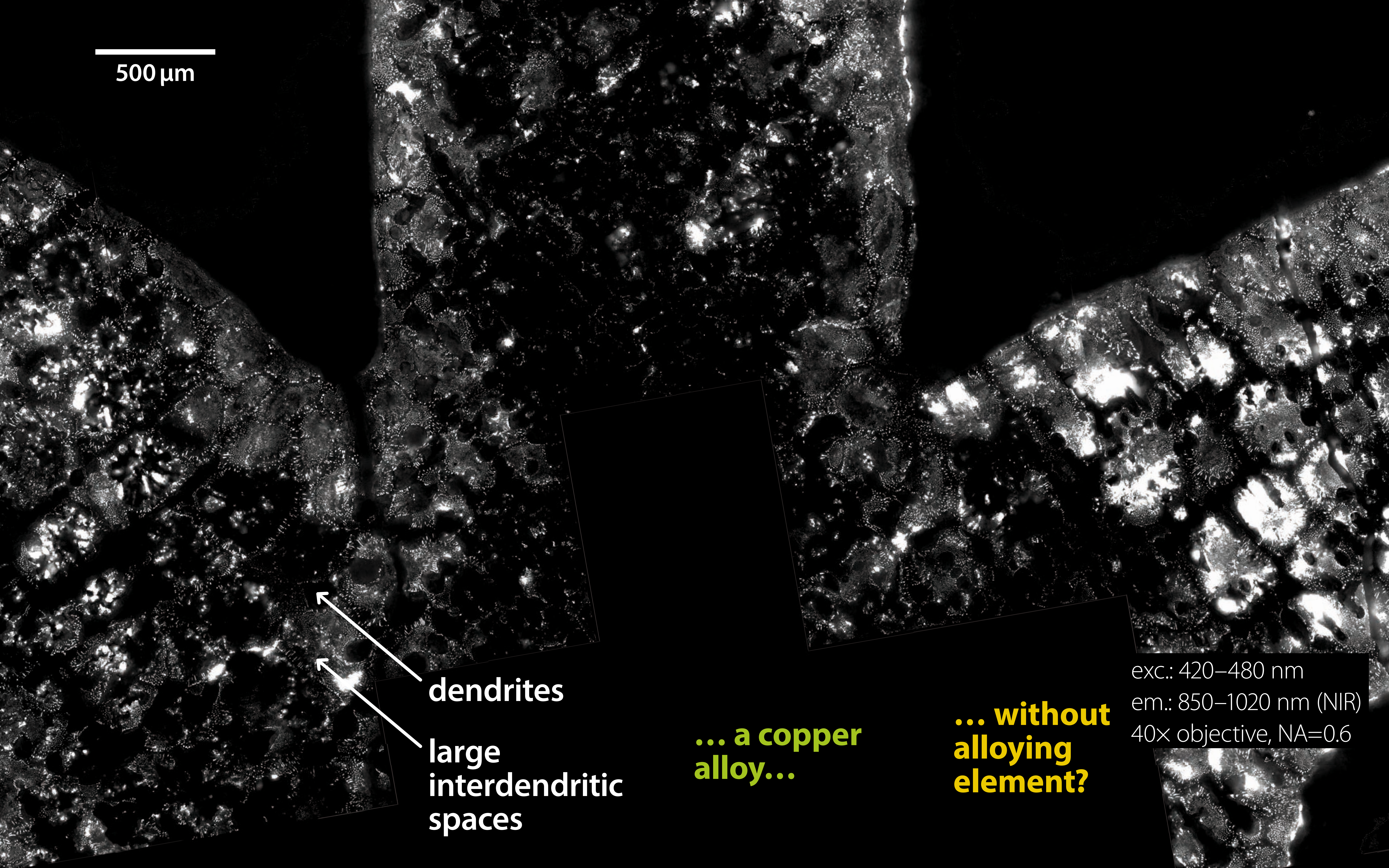
500 µm
dendrites
large interdendritic spaces
… a copper alloy…
… without alloying element?
exc.: 420–480 nm
em.: 850–1020 nm (NIR)
40× objective, NA=0.6

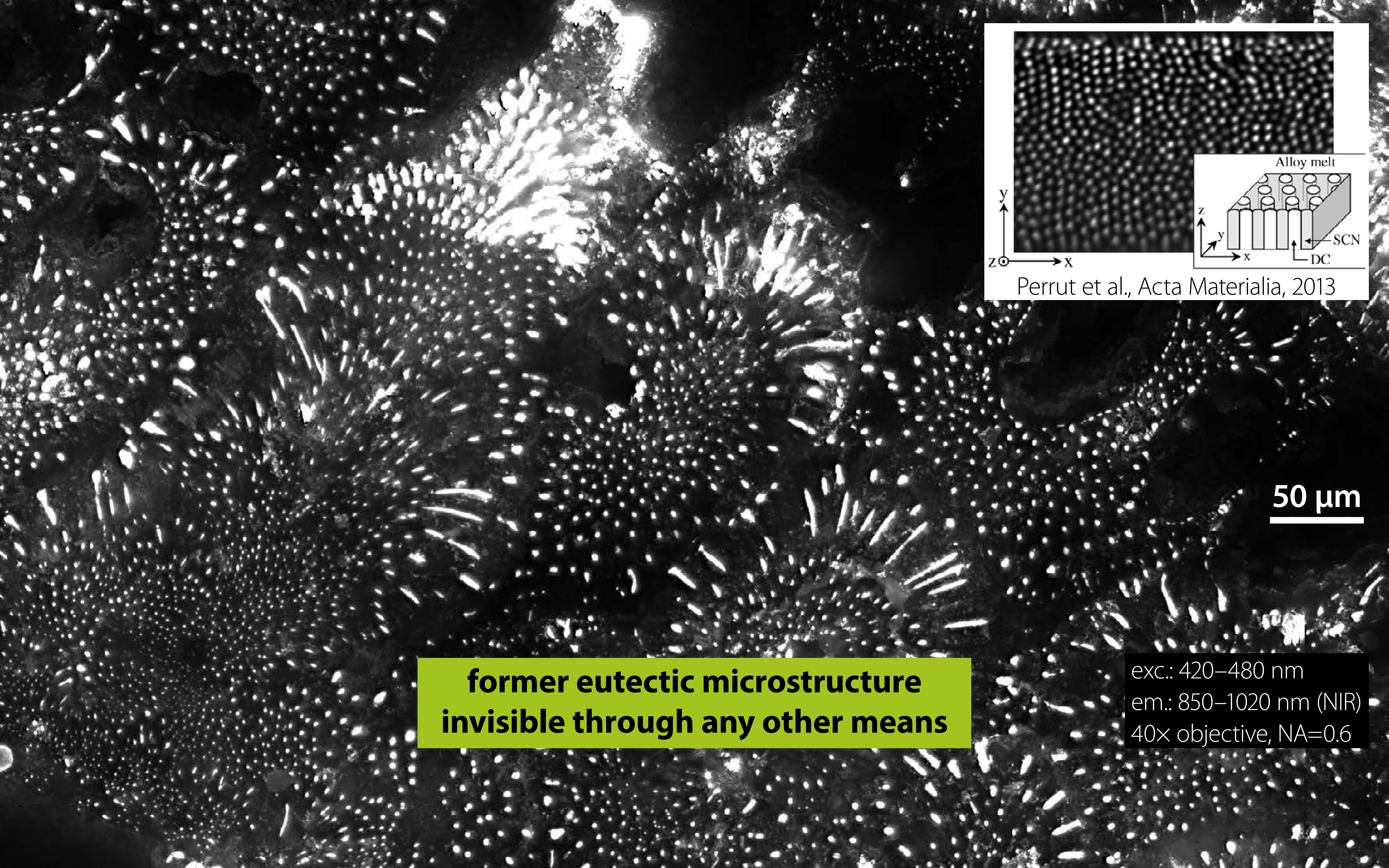

Alloy melt
y
z
x
SCN
DC
Perrut et al., Acta Materialia, 2013
50 µm
former eutectic microstructure
invisible through any other means
exc.: 420–480 nm
em.: 850–1020 nm (NIR)
40× objective, NA=0.6

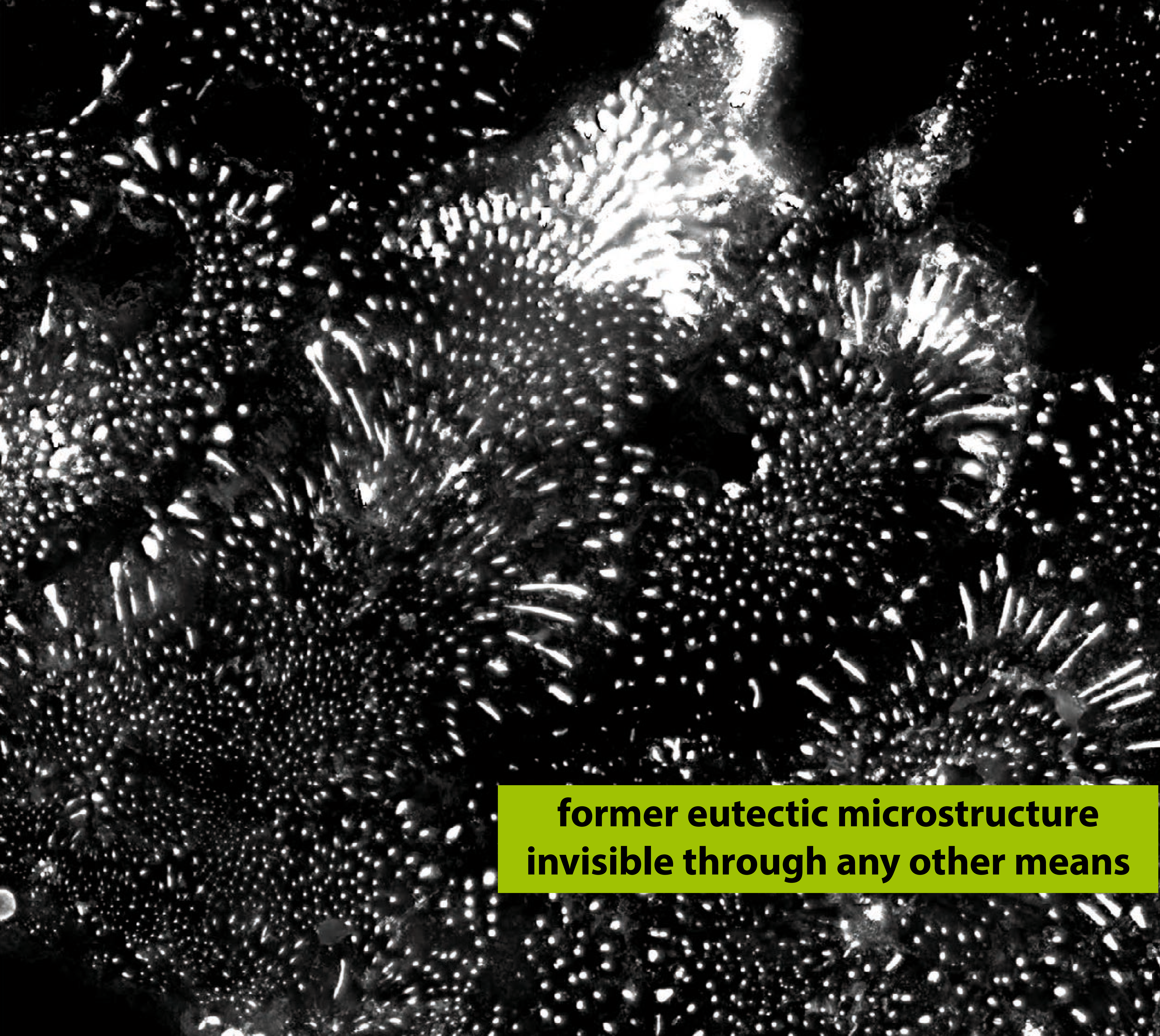

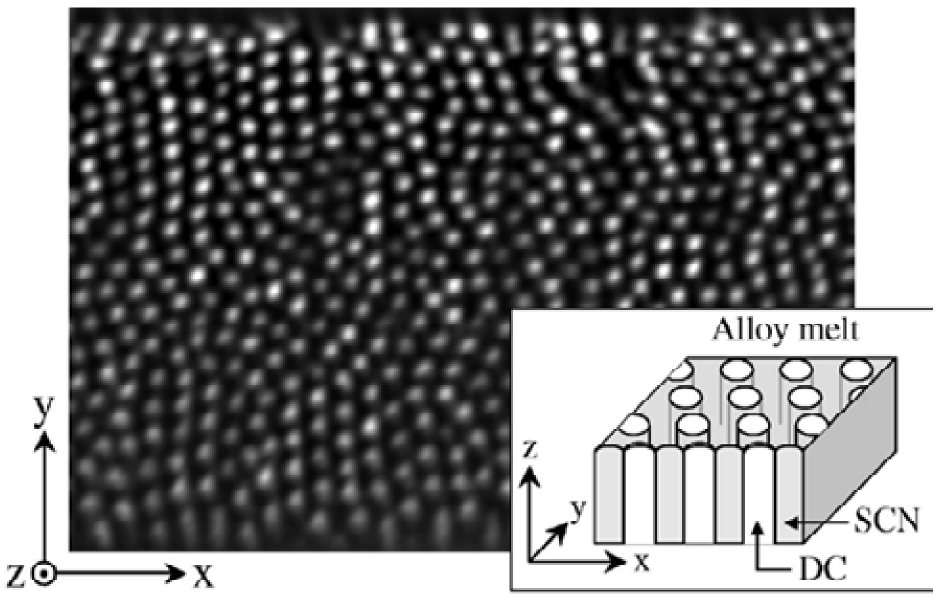


Perrut et al., Acta Materialia, 2013

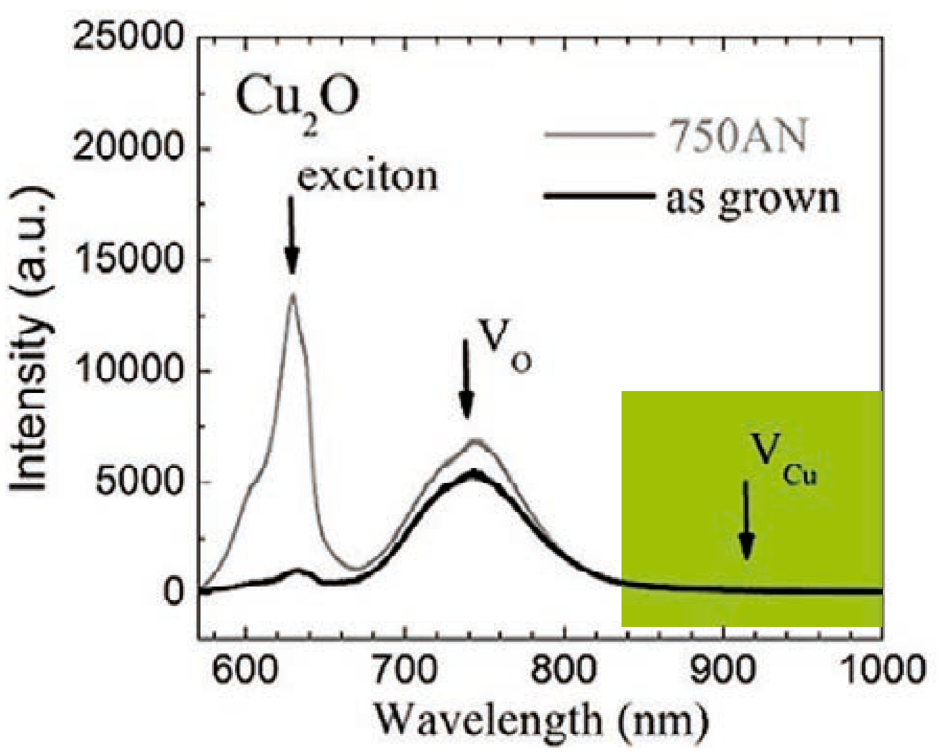


**former eutectic microstructure invisible through any other means**

exc.: 420–480 nm
em.: 850–1020 nm (NIR)
40× objective, NA=0.6

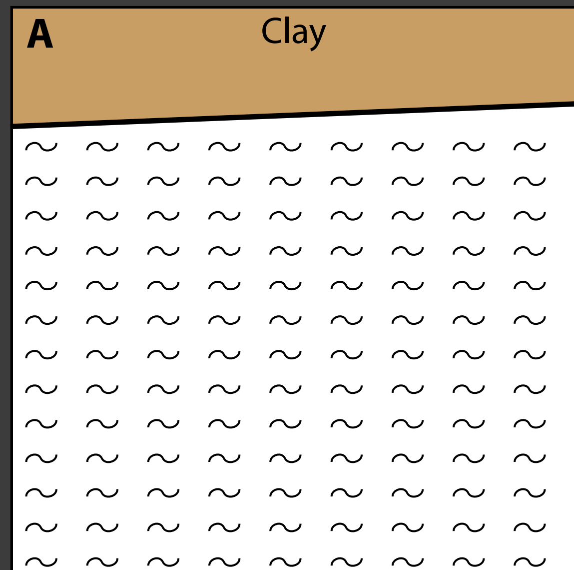


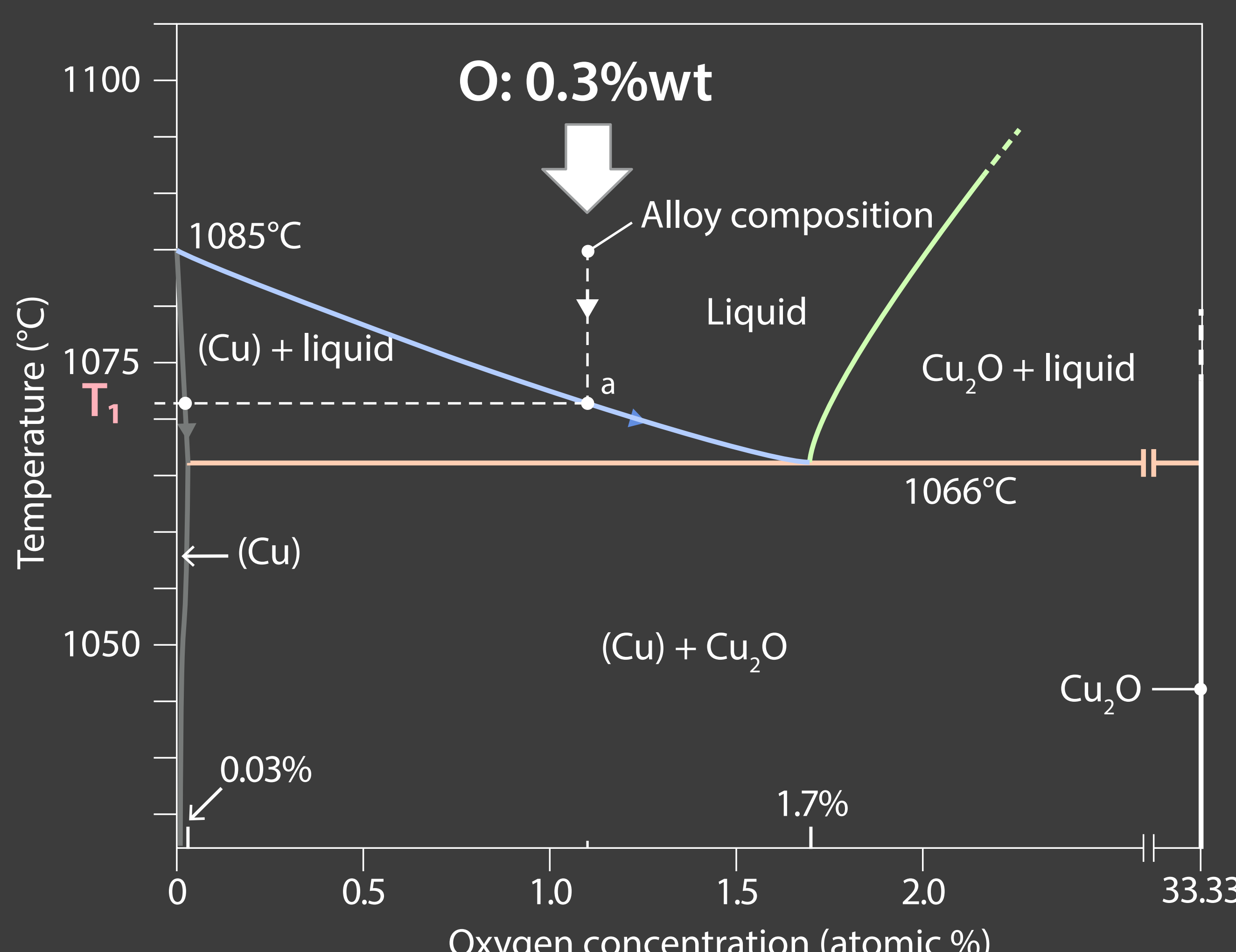


**Chalcolithic workers melted very pure copper**

From $\mathcal{A}$(eu-$Cu_2$0)/$\mathcal{A}$(eu-Cu): **O content 0.3%wt**

No significant As, Sb, Sn, Pb

High melting temperature: **> 1085°C**

**Native ore?**

Trace elements: Ag >> Au >> Pb >> As, Se, Hg

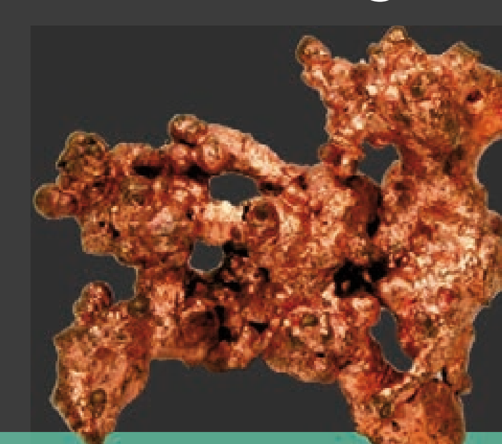



► M. Thoury et al. Nat. Comm., 2016.

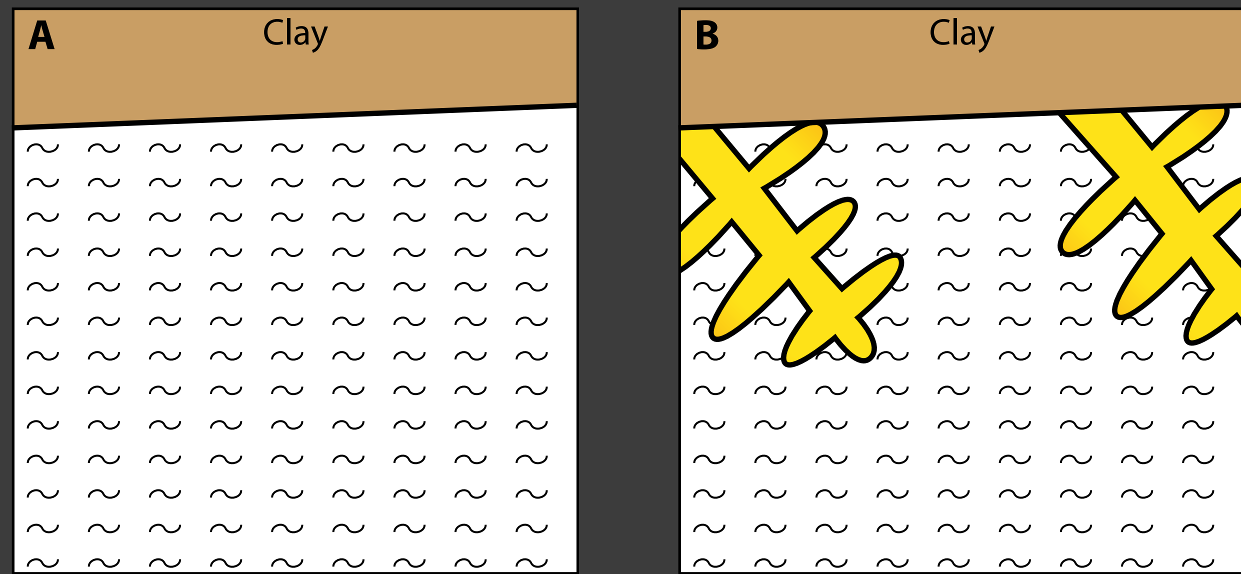


~1072°C

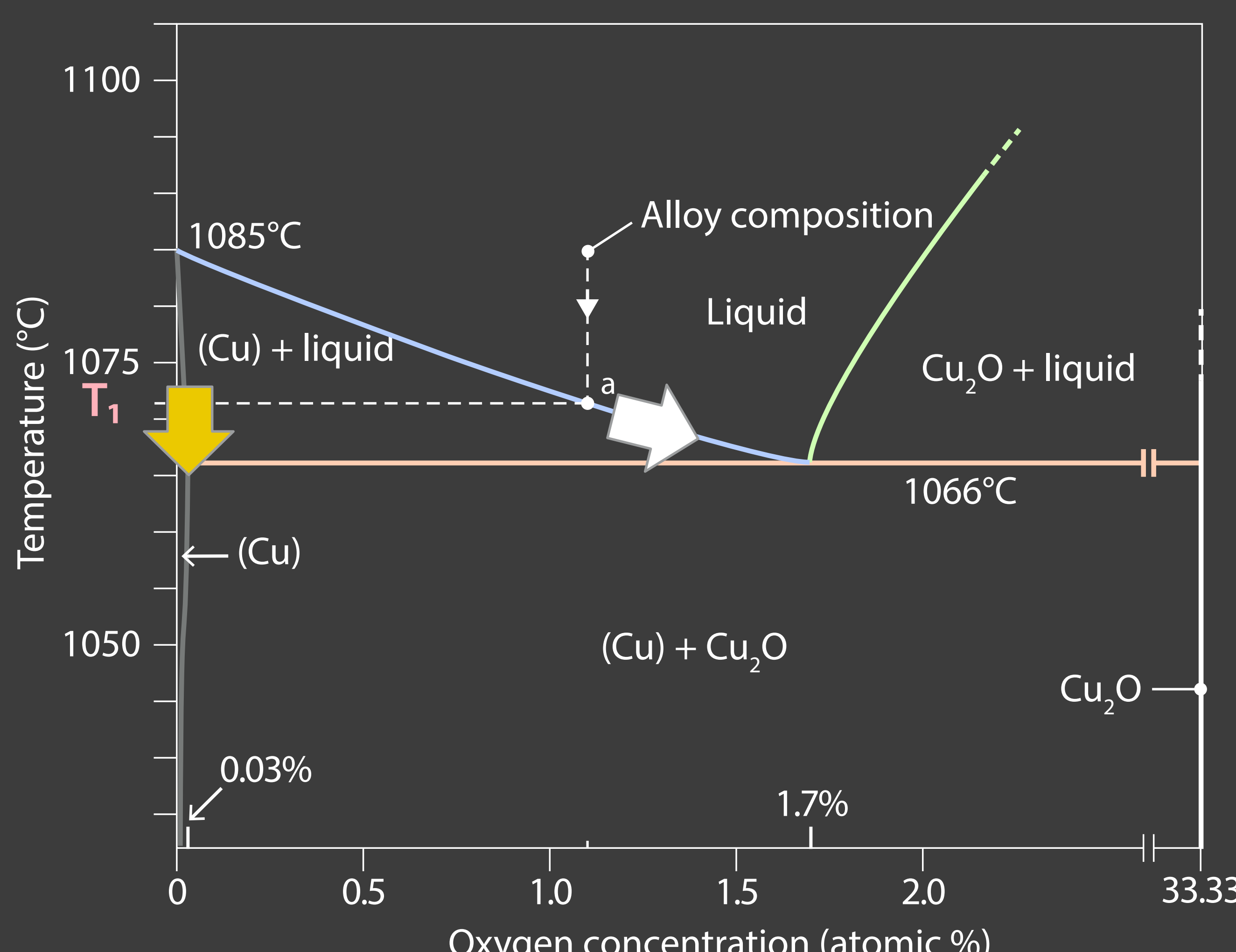


Solidification started at **1072°C**

**Bad castability**

A very atypical ore… **Specific status?**

A glimpse in the innovation process?

Towards Cu–Pb (10–30%wt) then Cu–Sn alloys



► M. Thoury et al. Nat. Comm., 2016.

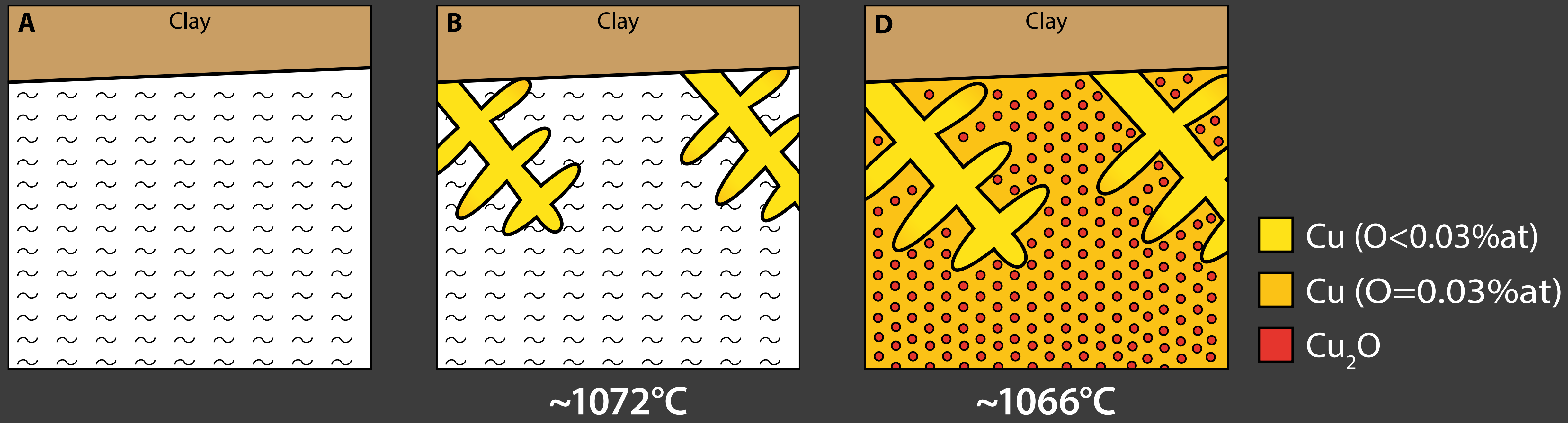


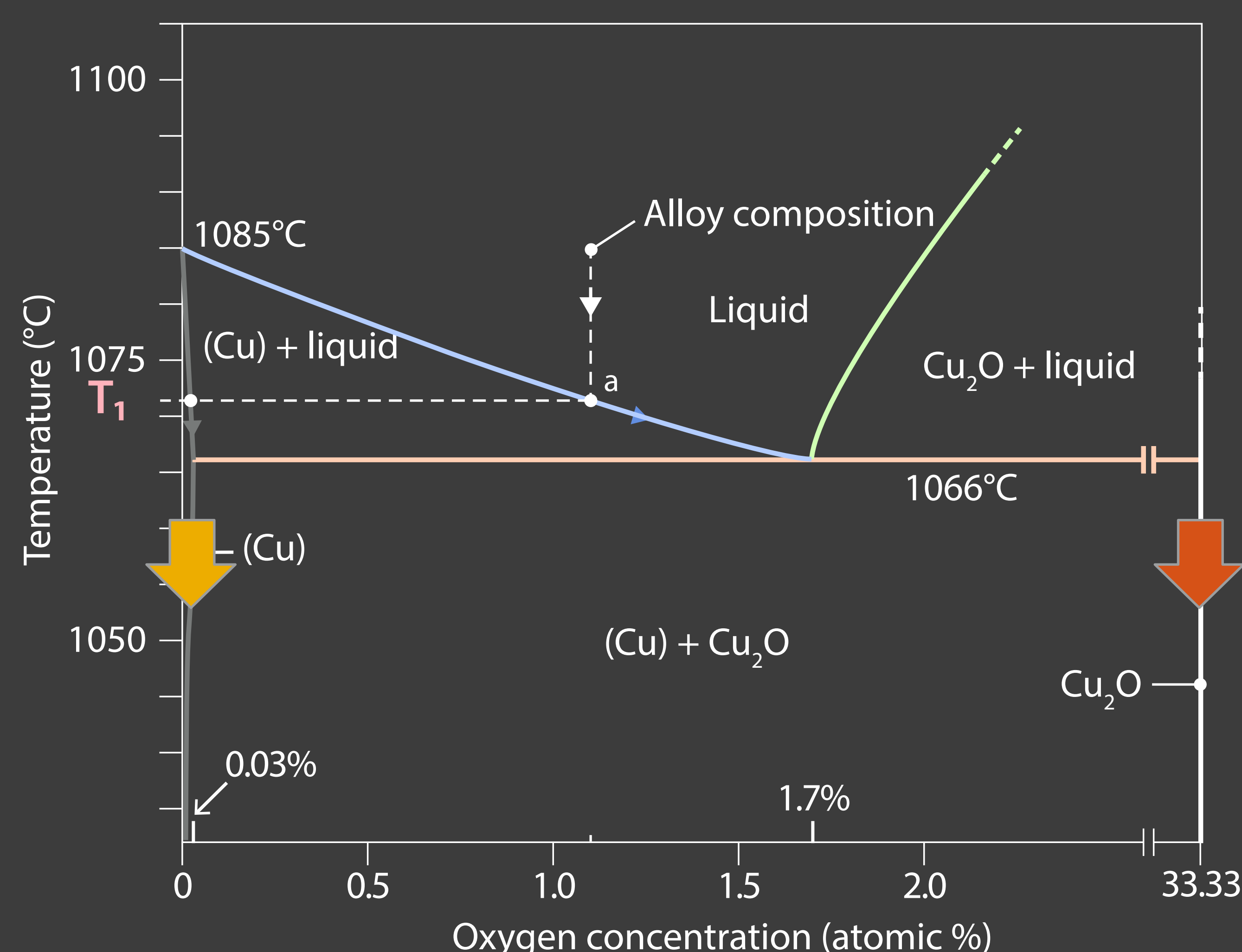


## Hypo-eutectic microstructure

Complete solidification at **1066°C**

$Cu_2O$ in a Cu (O=0.03%wt) matrix

The melt cools down and the mould is broken to release the artefact



► M. Thoury et al. Nat. Comm., 2016

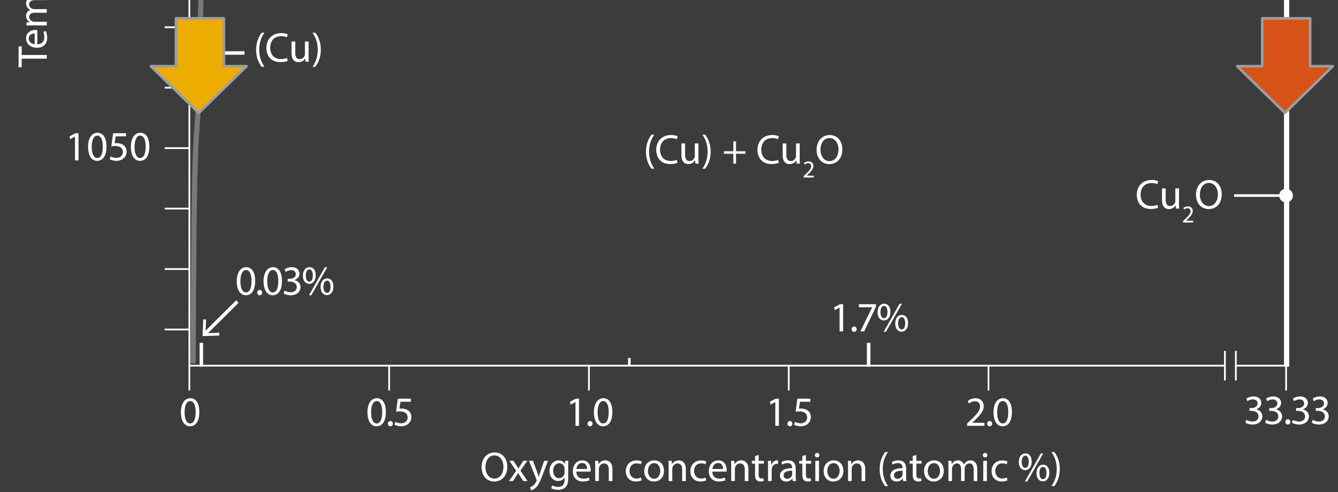


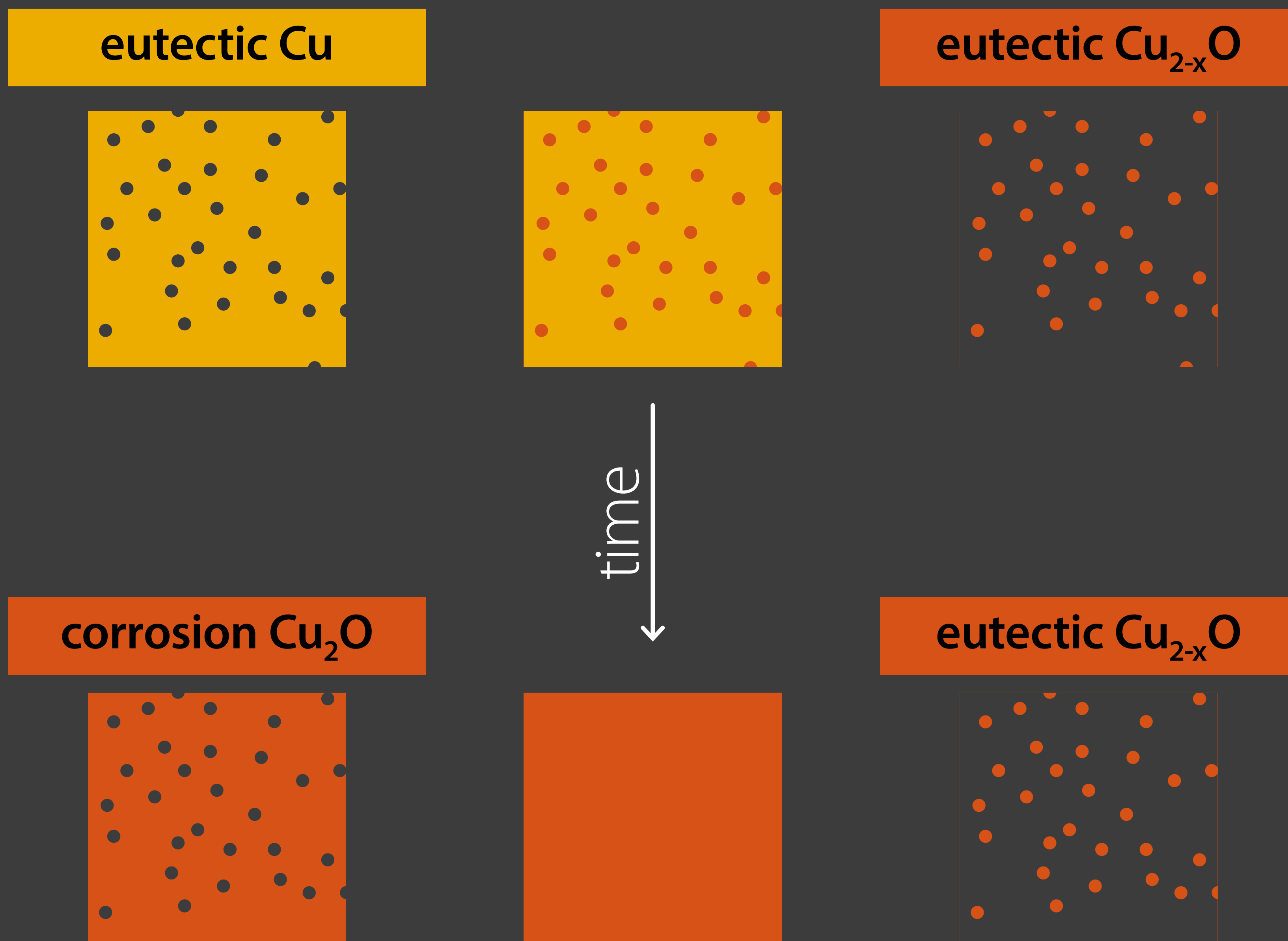


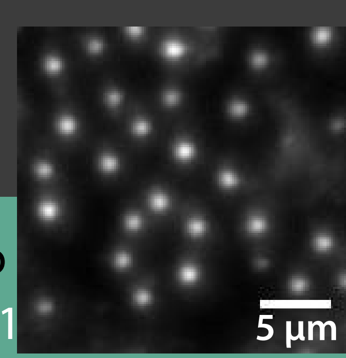


**Slow corrosion to cuprite $Cu_2O$**

Relatively **dry sandy clayey soil**

1 µm / year?

6 millennia later: **a single mineral phase**

Full preservation of the ghost morphology of the eutectic



► M. Thoury et al. Nat. Comm., 2016.

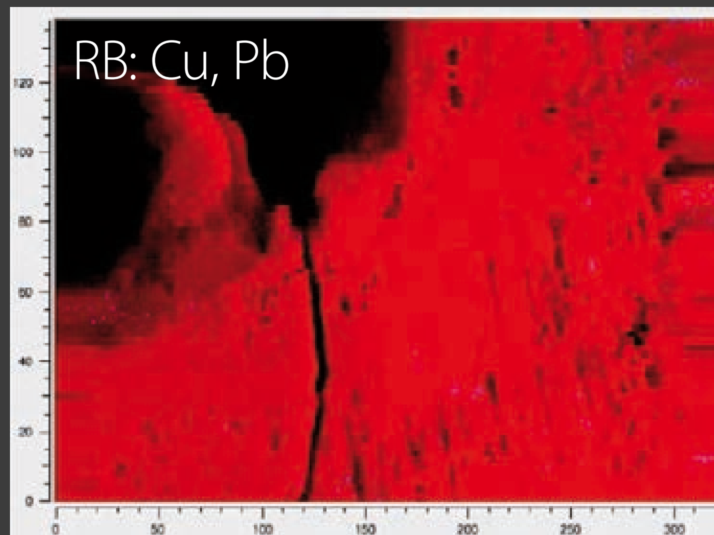


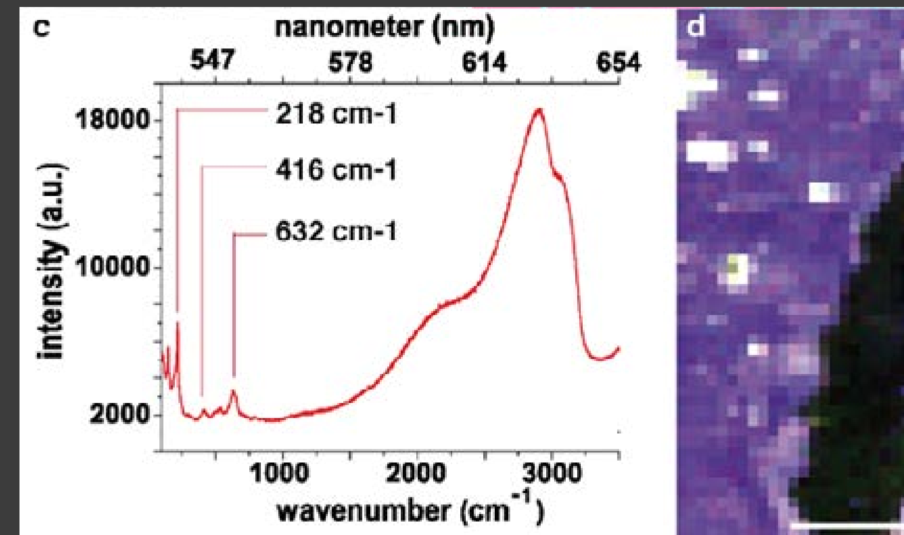


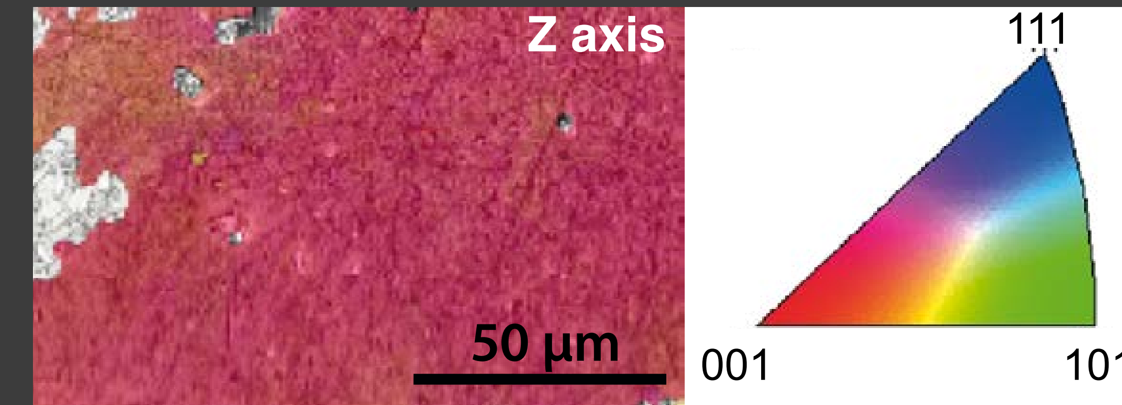


Inverse pole figure, **EBSD**, pixel step: 744 nm
local misorientation < 3.5°

no elemental contrast

no molecular contrast

no texture contrast!

# A "new" source of contrast

corrosion
$Cu_2O$

eutectic
$Cu_{2-x}O$

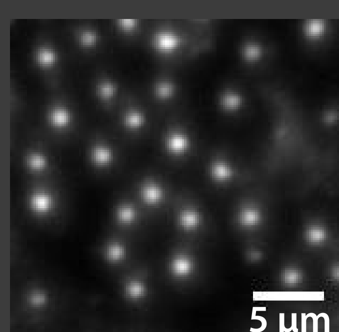


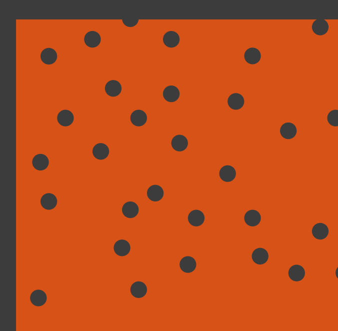

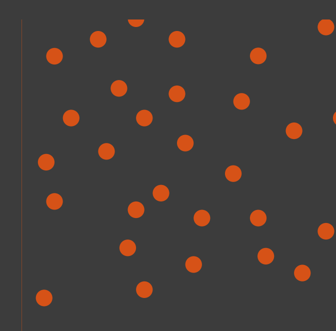

emission
$V_O$

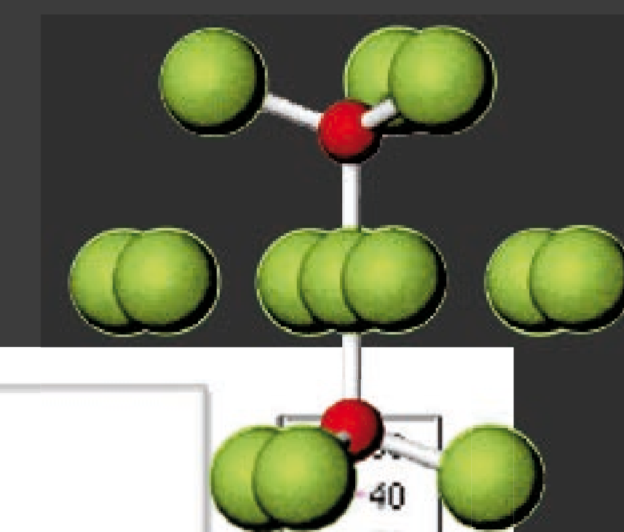

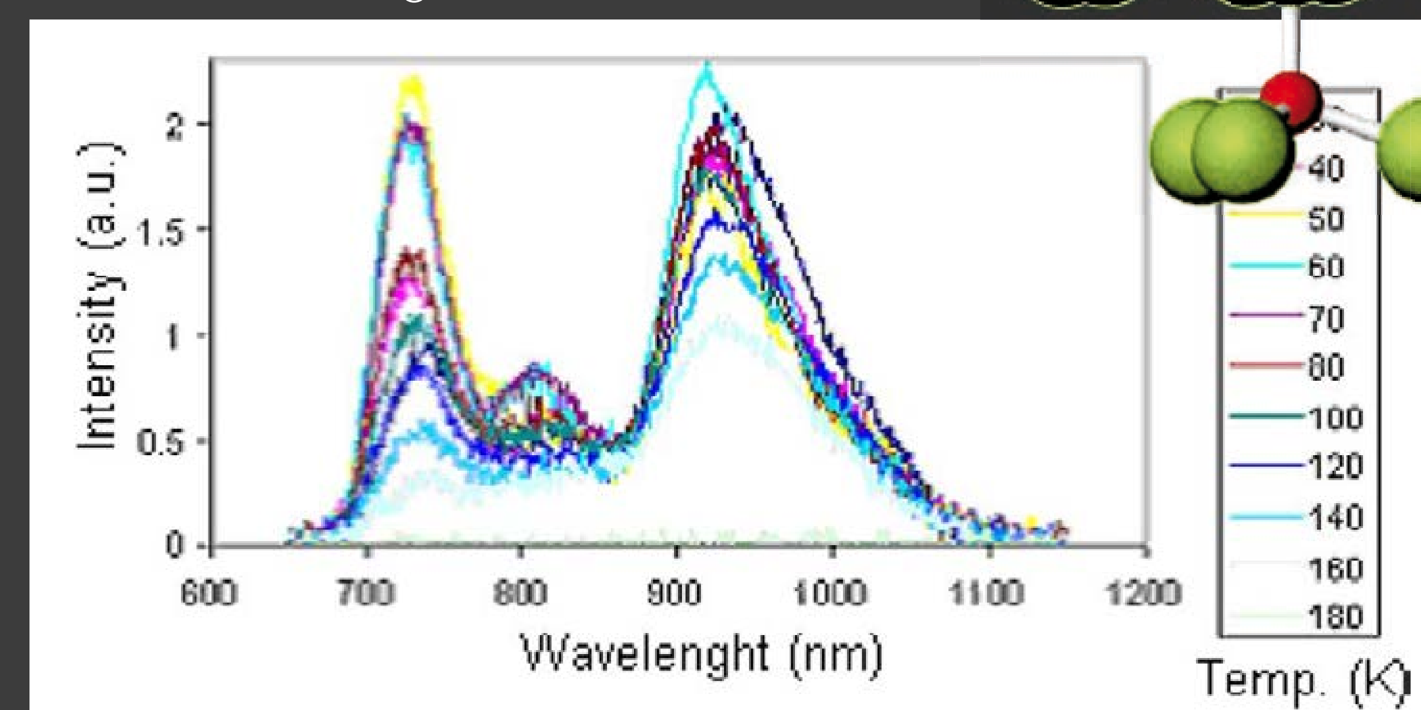


H. Solache-Carranco, 2009



► M. Thoury et al. Nat. Comm., 2016

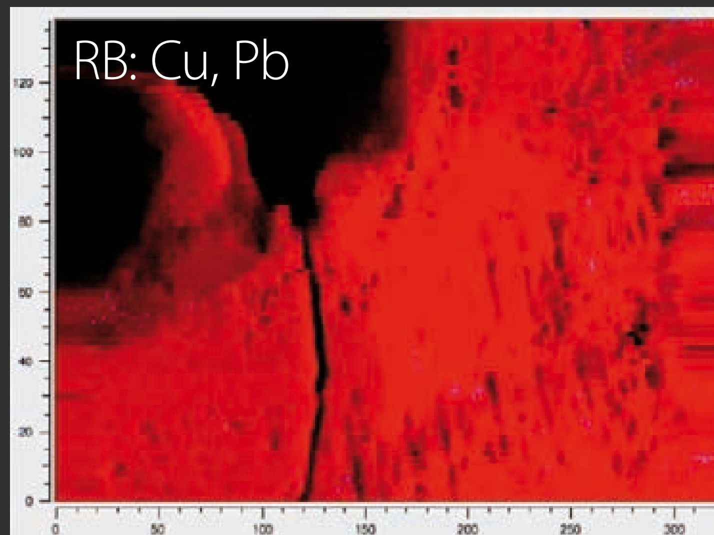


no elemental contrast

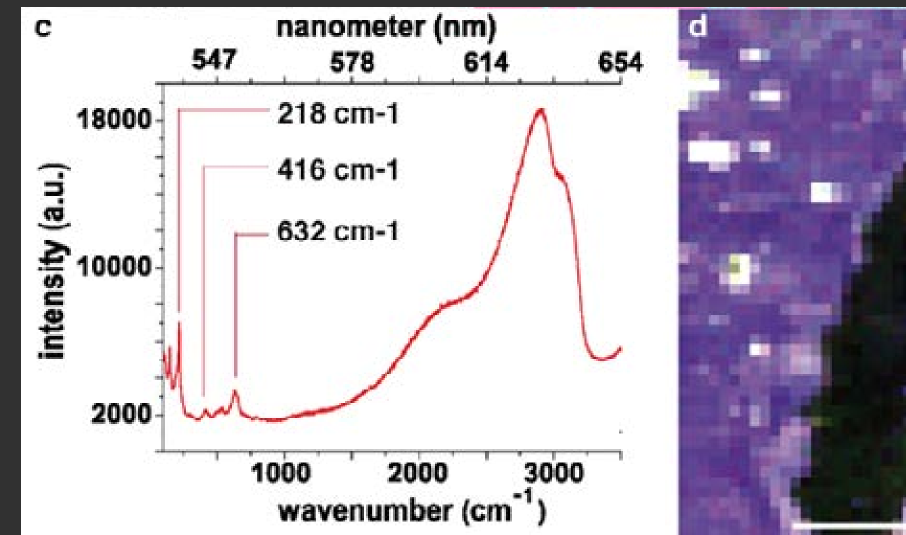


no molecular contrast

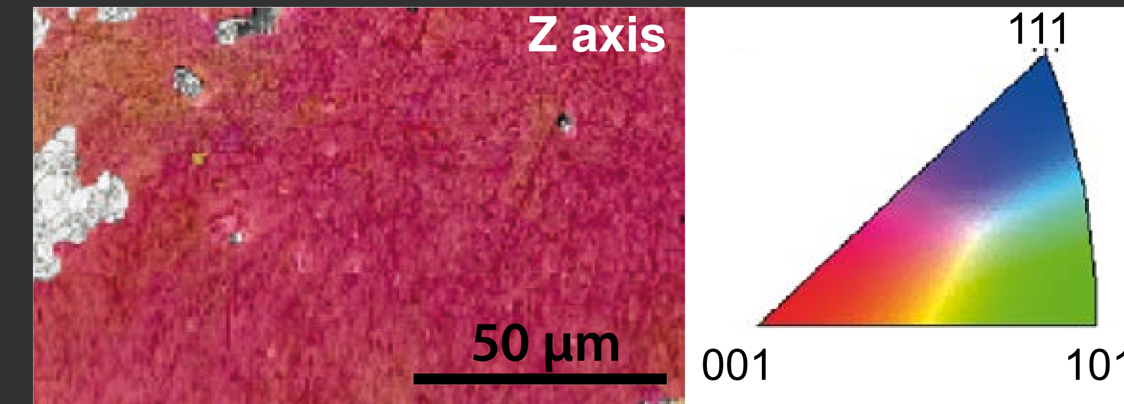


Inverse pole figure, **EBSD**, pixel step: 744 nm
local misorientation < 3.5°

no texture contrast!

## A “new” source of contrast

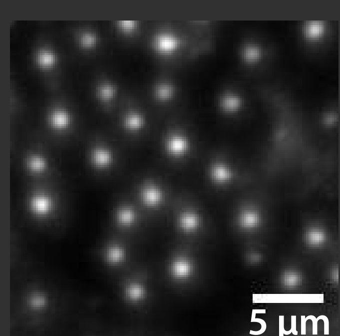


corrosion
$Cu_2O$

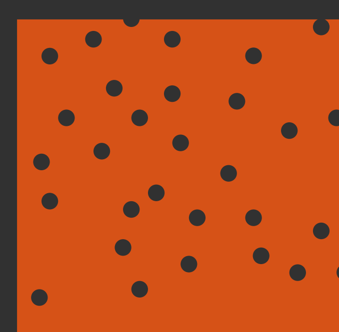

eutectic
$Cu_{2-x}O$

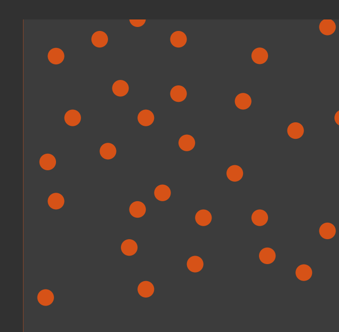

the morphology is only visible though a contrast in **atomic defect density** (Cu stoichiometry) in the $Cu_{2-x}O$ cubic lattice!

emission $V_O$ emission $V_{Cu}$

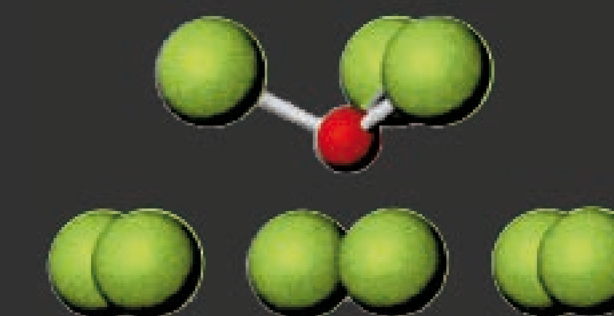

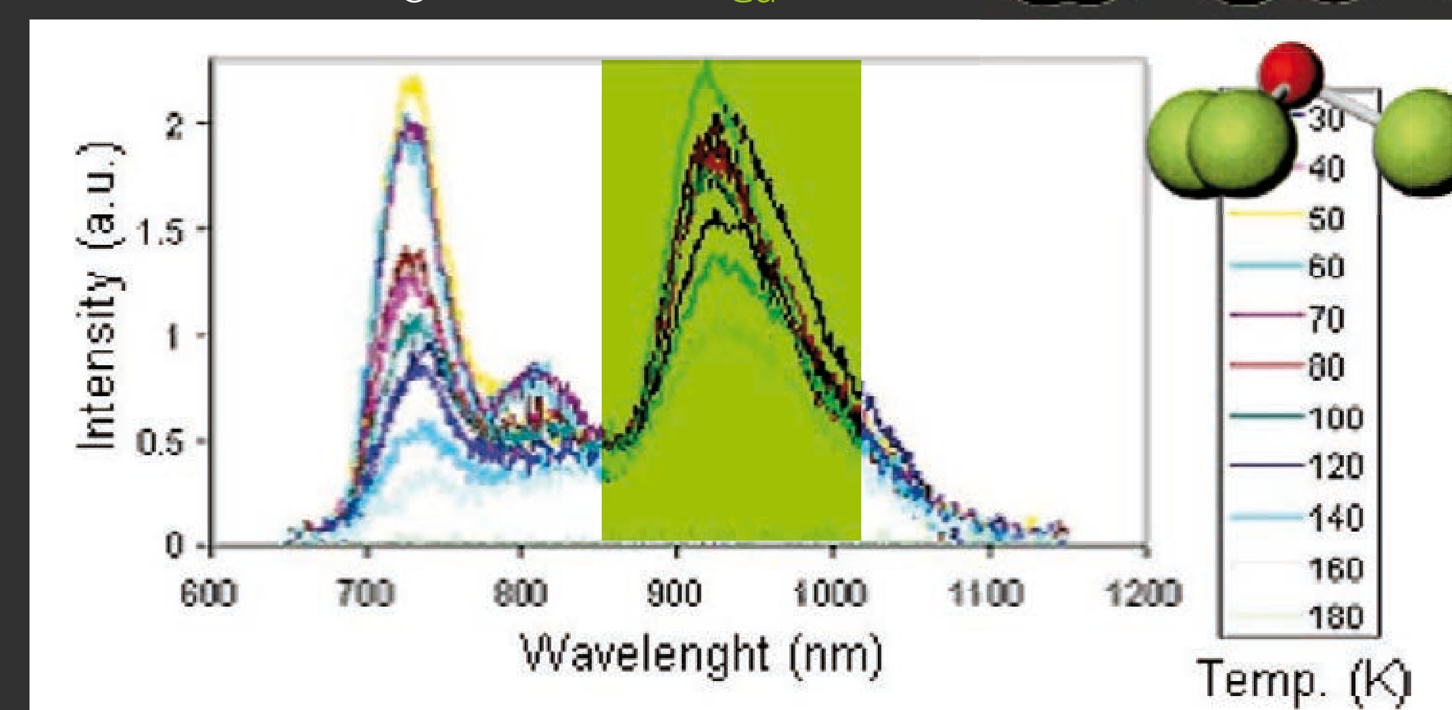


H. Solache-Carranco, 2009



► M. Thoury et al. Nat. Comm., 2016.

# historical zinc whites (ZnO) artists' pigments


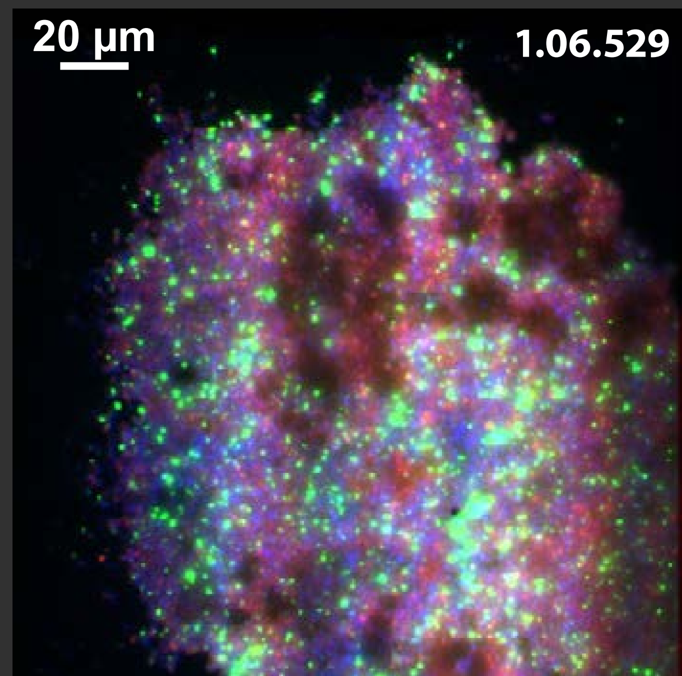


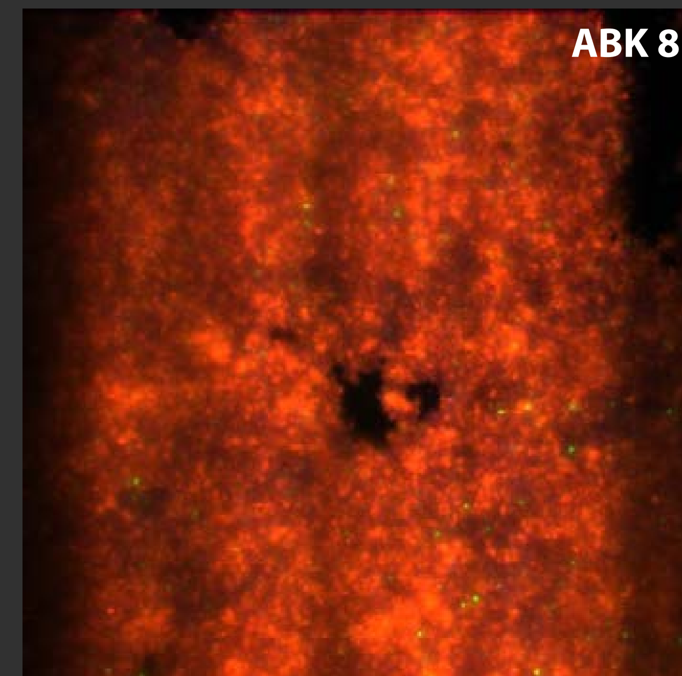


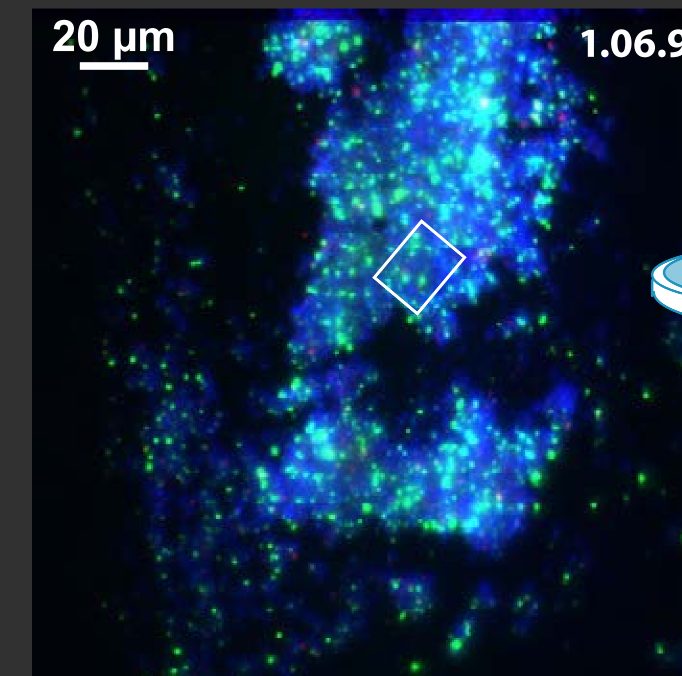


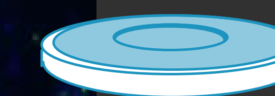

40× obj.
pps: 320 nm

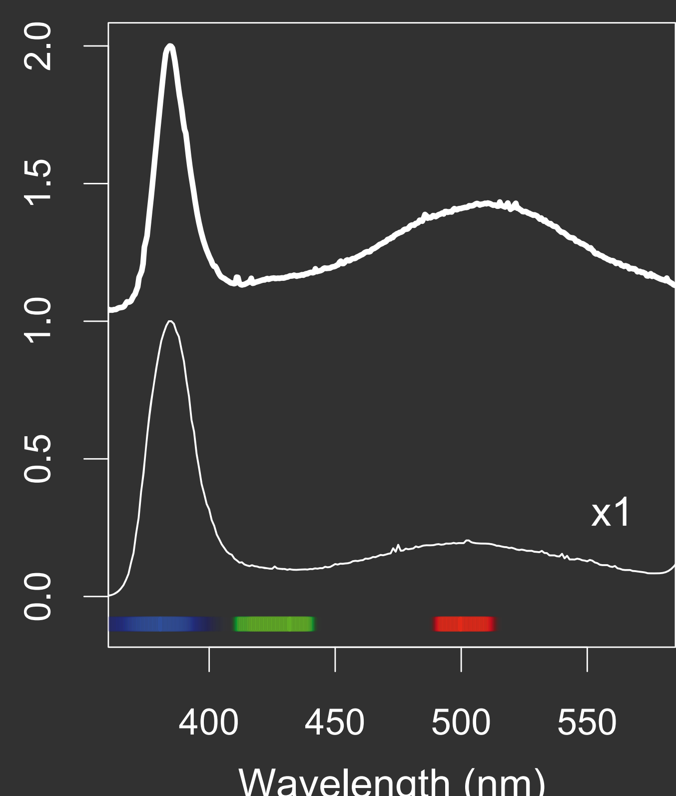


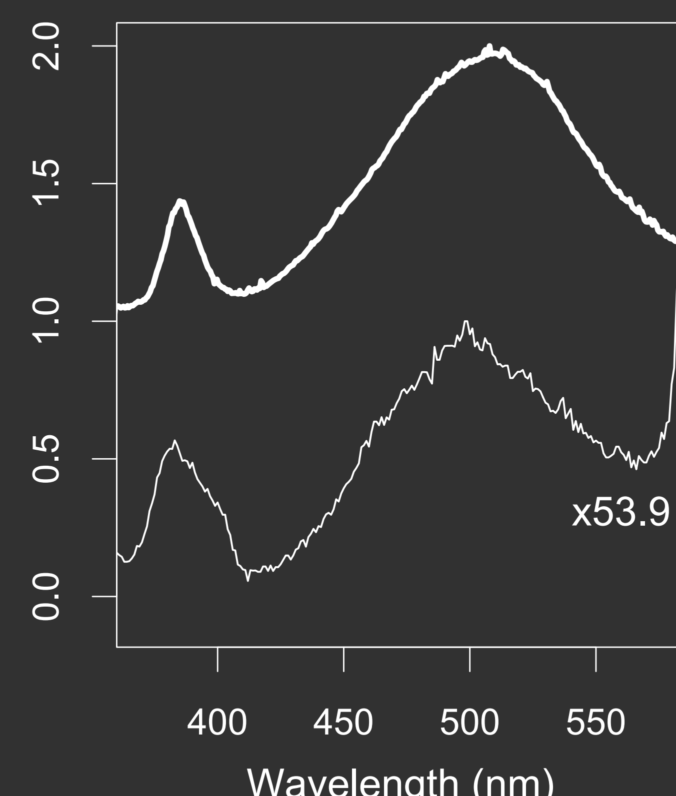


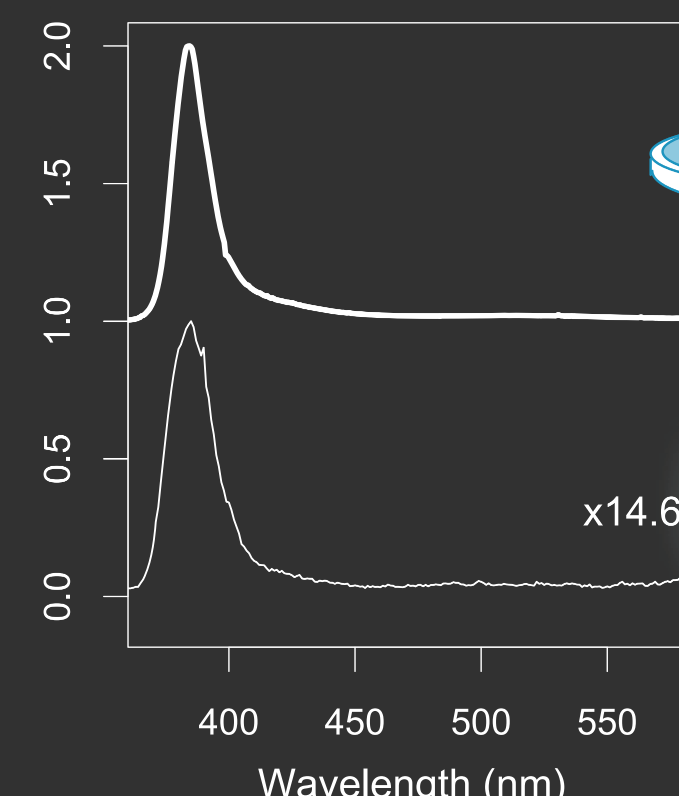


40× obj.
(20 µm)$^2$

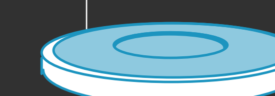

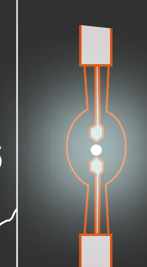

optical fibre
6 mm$^2$

$\lambda_{exc} = 275$ nm



► M. Thoury et al. Anal. Chem, 2011.
► L. Bertrand et al. Analyst, 2013.

the clue to the question is as much in the **chemical composition** as in the **multiscale microstructure**

**high spatial dynamics in spectral imaging**

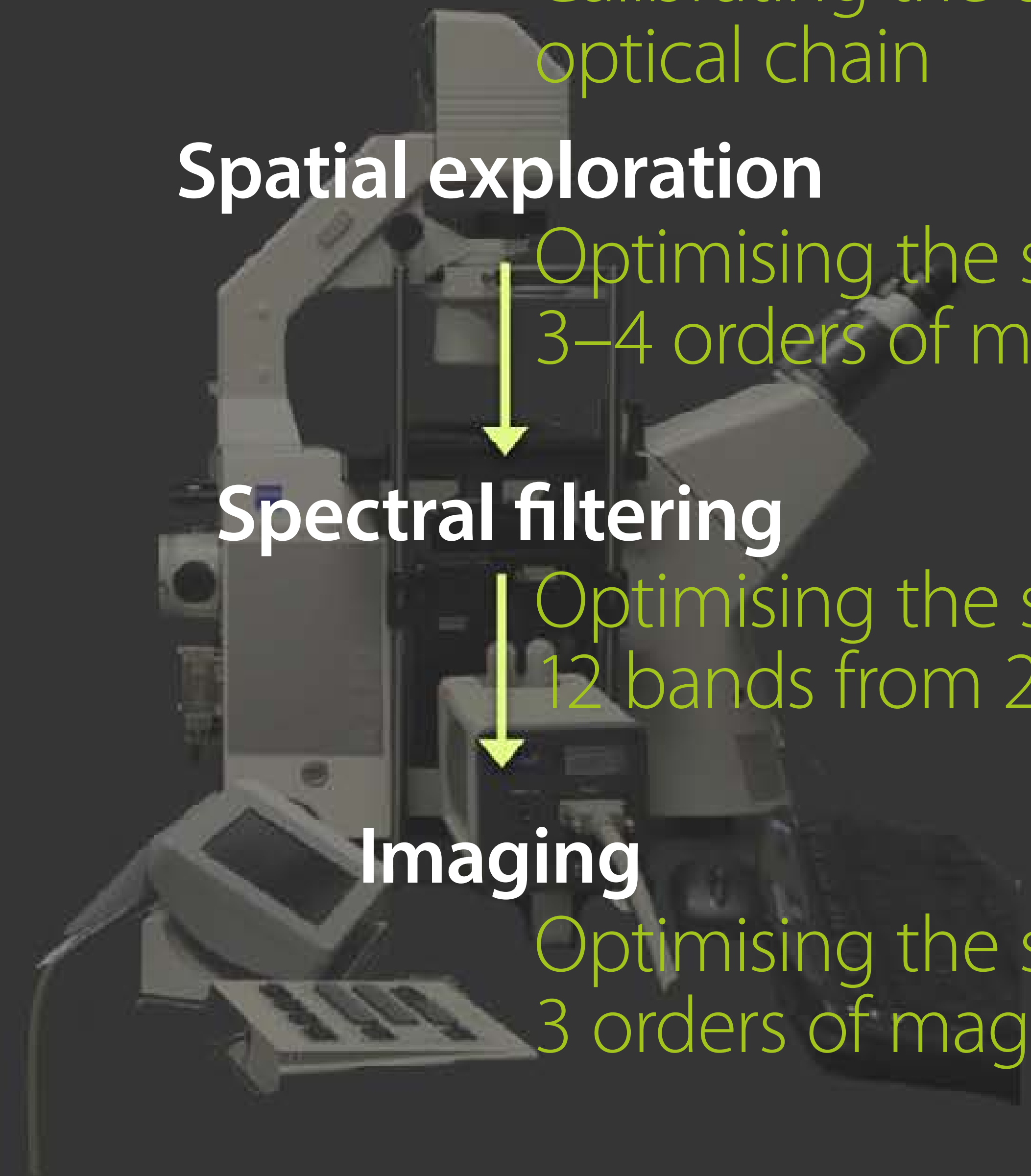

Calibrating the detection optical chain

**Spatial exploration**

Optimising the spatial dynamics: 3–4 orders of magnitude

**Spectral filtering**

Optimising the spectral dynamics: 12 bands from 260 to 1020 nm

**Imaging**

Optimising the signal dynamics: 3 orders of magnitude

► T. Séverin-Fabiani's Ph.D., 2012–2016

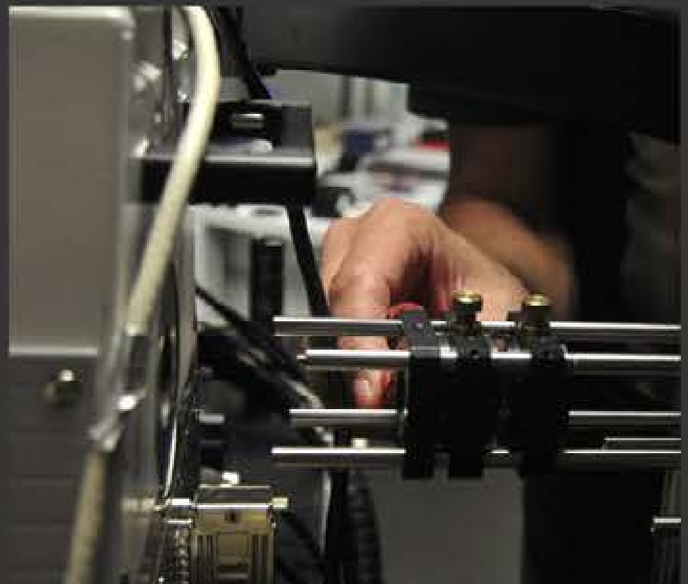

## Description and environment of Cretaceous fossils

P. Gueriau, S. Cohen, C. Mocuta, L. Bertrand

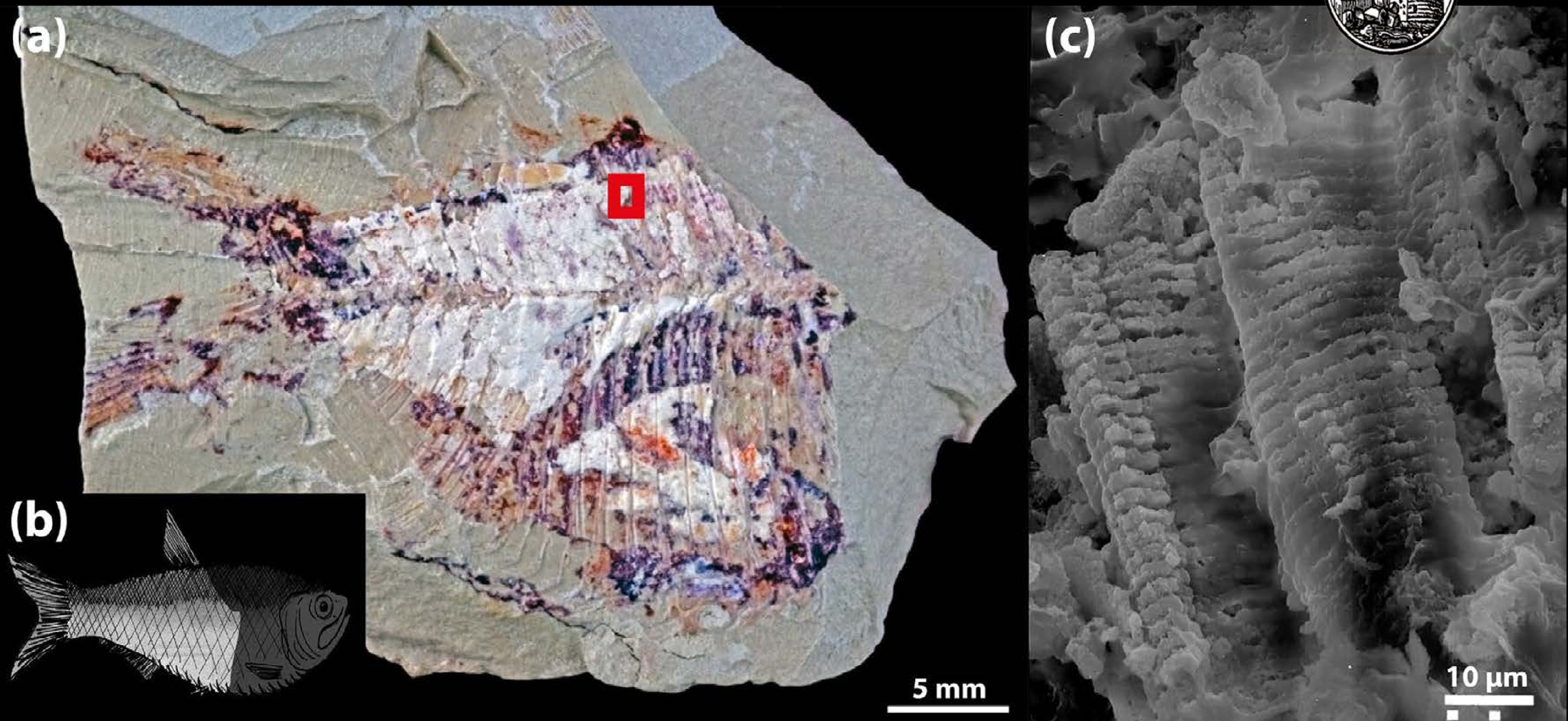


► P. Gueriau and L. Bertrand. Microsc. Today, 2015.

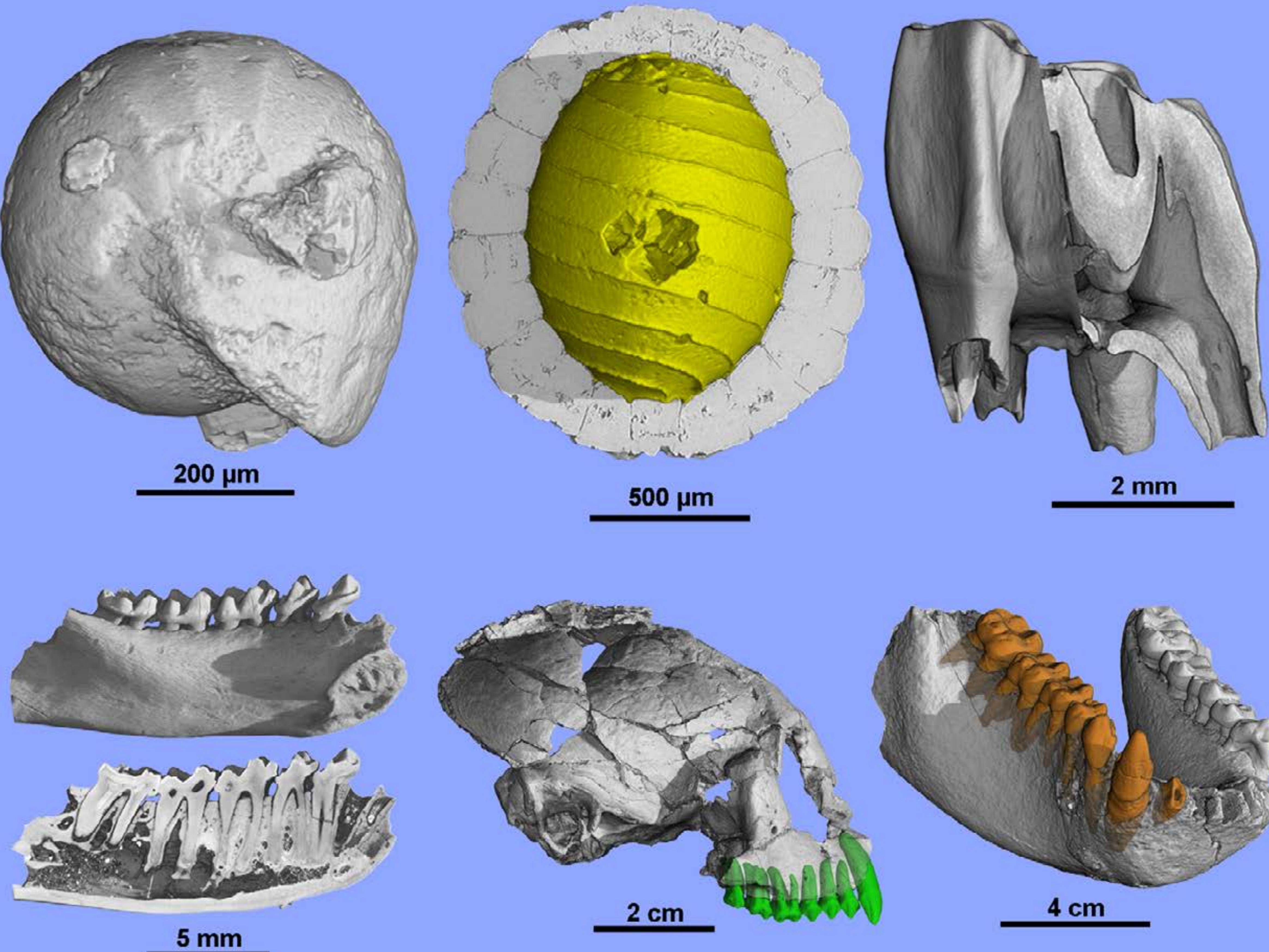


**Paul Tafforeau, ESRF**

# Discovery of two complete skeletons of animals that should have never been together in a 250 Ma-old burrow in South Africa

Vincent Fernandez, Kris Carlson, Nestor Abdala, Adam Yates, Bruce Rubidge and Paul Tafforeau

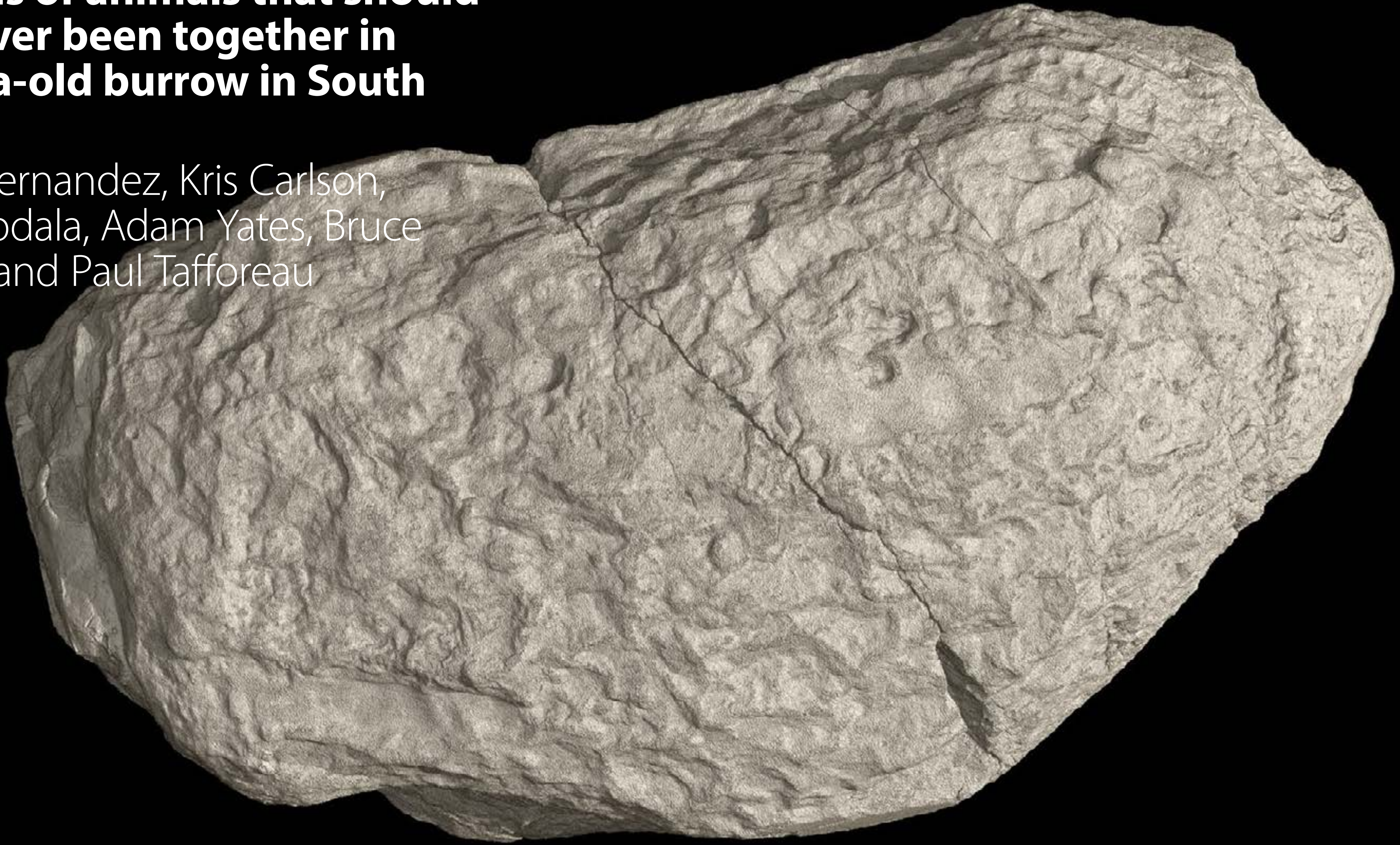

Paul Tafforeau, ESRF

Paul Tafforeau, ESRF

# *Thrinaxodon* : Mammalian reptile, close to the origin of mammals

Paul Tafforeau, ESRF

*Broomistega* : Temnospondyl amphibian, aquatic predator, the best skeleton ever discovered

Paul Tafforeau, ESRF

Paul Tafforeau, ESRF


VORTEX®-EX
MADE IN USA
A 0
B -80
C -200
D -170
SDD Thickness µm
MRSN8 25
ESP
COMPATIBLE

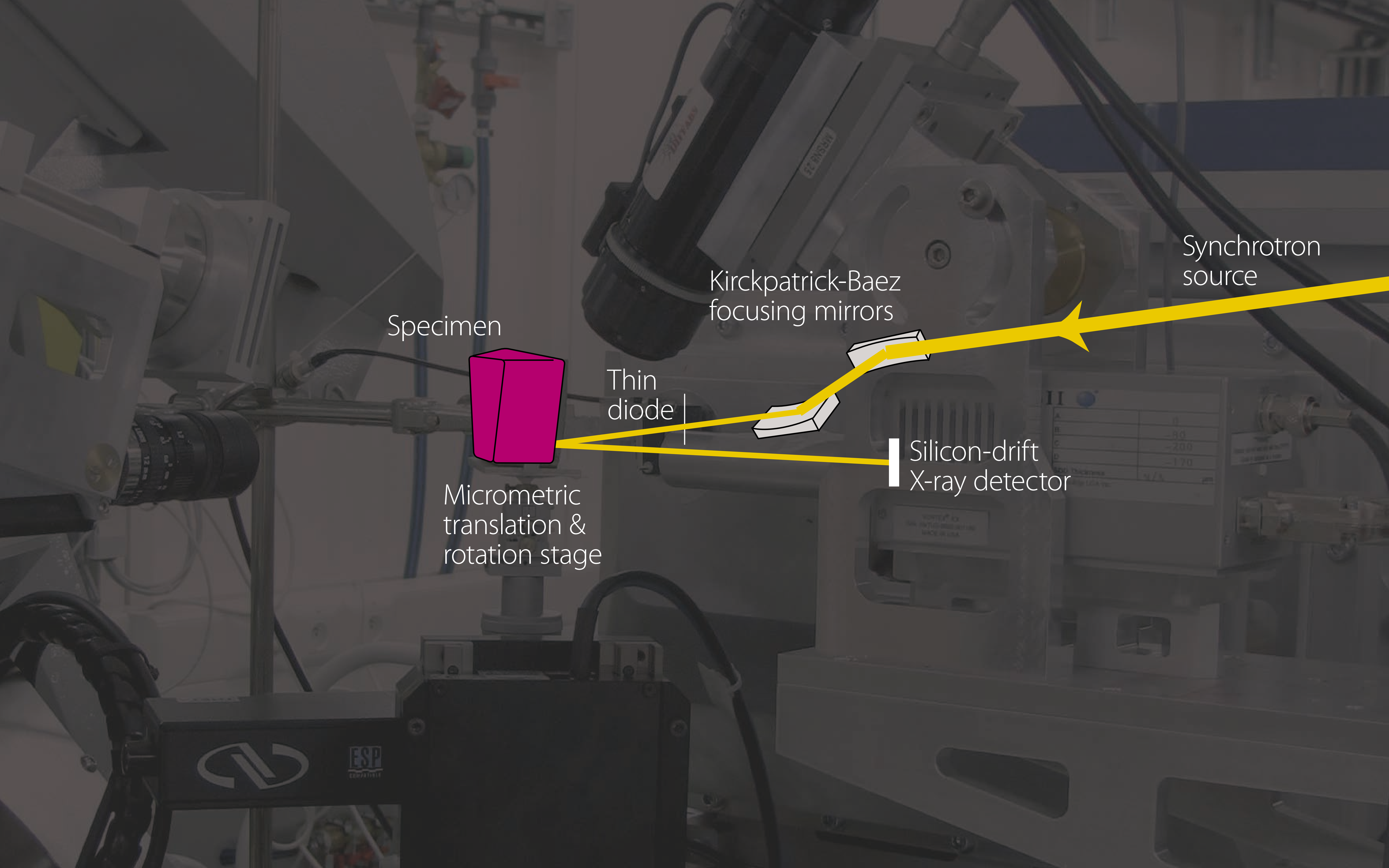
Synchrotron
source
Kirckpatrick-Baez
focusing mirrors
Specimen
Thin
diode
Silicon-drift
X-ray detector
Micrometric
translation &
rotation stage

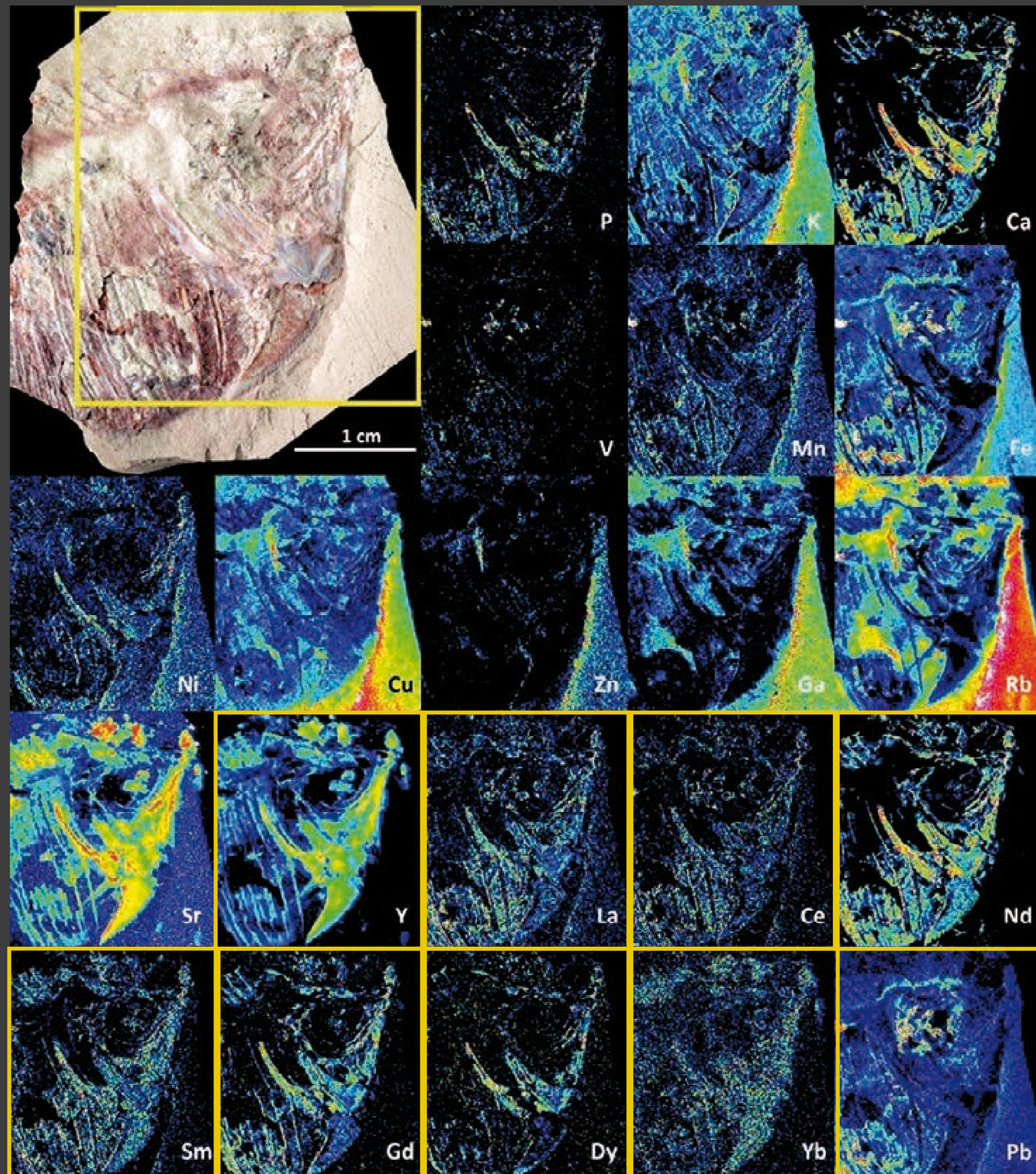


**Fish**, Late Cretaceous, -95 Myr, Djebel Oum Tkout Morocco

# Cretaceous fossils from Morocco (95 Myr old)

strong contrast in elemental distributions!

alkaline earths: Ca, Sr
pnictogen: P
transition metals: V, Mn, Fe, Ni, Cu, Zn

heavy metals: Pb
alkali metals: K, Rb
other metals: Ga

**rare earths:** Y, La, Ce, Nd, Sm, Gd, Dy, Yb

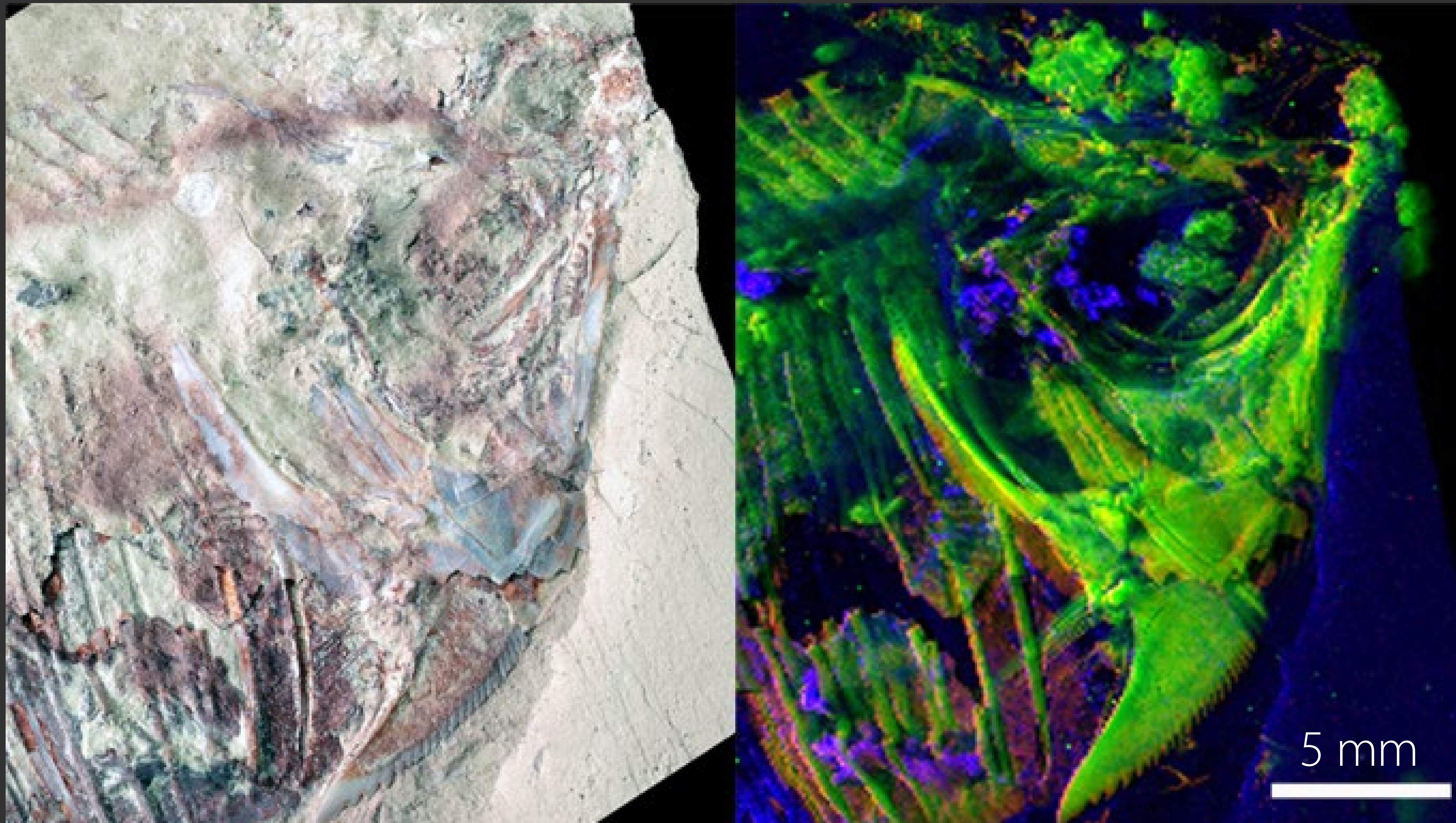


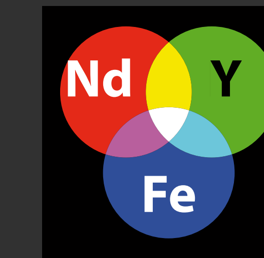


**XRF @ SOLEIL Diffabs**

17.2 keV, beam 10×7 µm² (H×V, FWHM), 100 µm-step;
4-element Vortex ME4 SDD; step-by-step 500ms/pt

**Fish**, Late Cretaceous, -95 Myr, Djebel Oum Tkout Morocco



► P. Gueriau et al. Elements, 2016.
► P. Gueriau et al. Plos One, 2014.

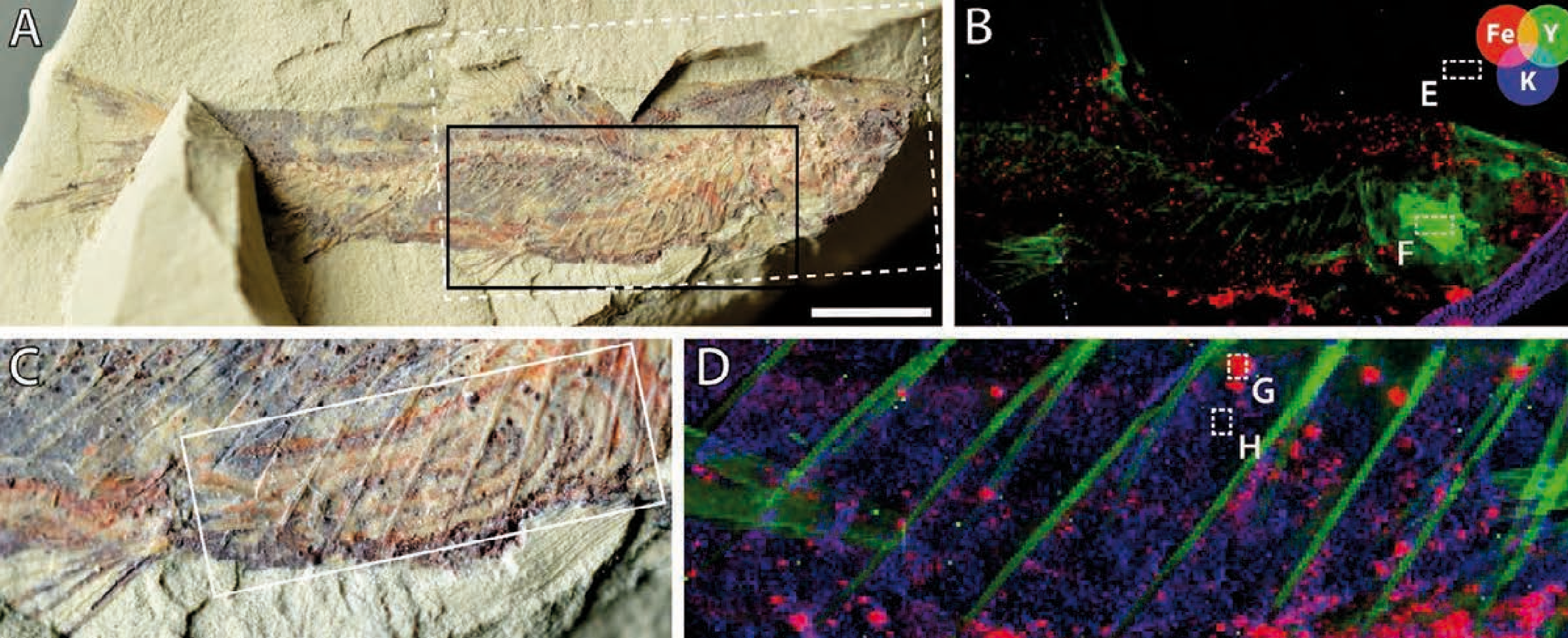


**Freshwater acanthomorph**, Late Cretaceous -95 Ma, Djebel Oum Tkout, Morocco

**XRF @ SOLEIL Diffabs**

17.2 keV, beam 11×7 µm$^2$ (H×V, FWHM), 100 µm (B) and 30 µm-step (D); single element Vortex SDD, step-by-step 500ms/pt

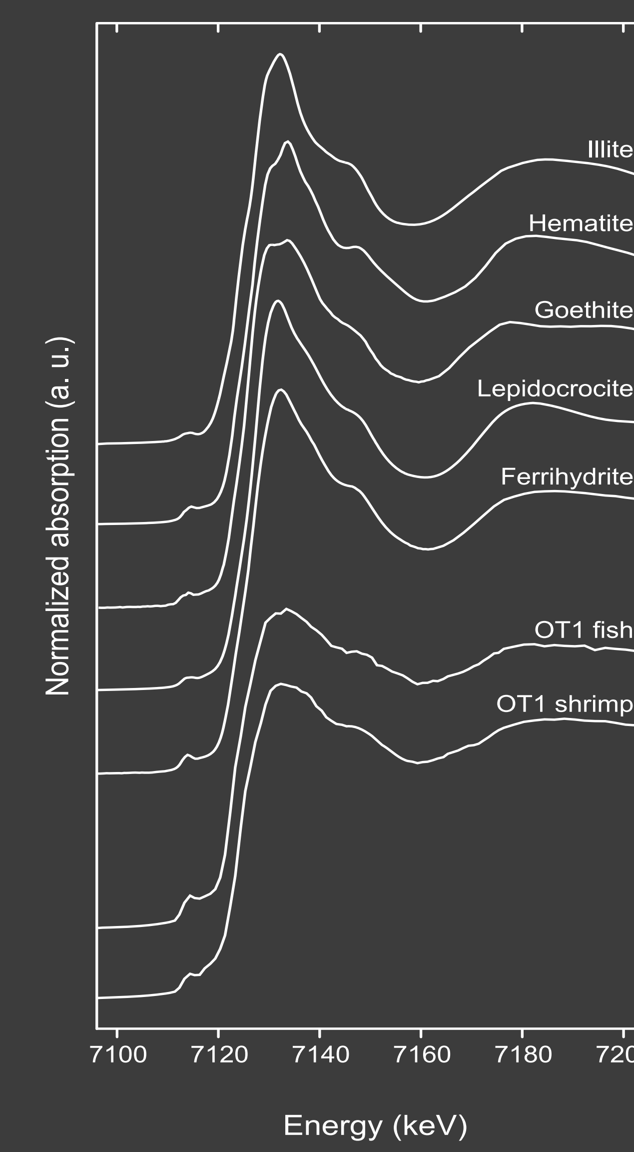


phosphatisation of a gut from bacterial activity in presence of $PO_4^{3-}$ anions released by carcasses ⟶ **anoxic environment**

yet…

Fe(III) compounds forms, typically ferrihydrite $Fe_2O_3{\cdot}0.5H_2O$

⟶ **oxic environment**

**local change of environment from anoxic to oxic due to microbial mats formed at early fossilisation stages?**

► P. Gueriau et al. in preparation.


A
2 cm
Phillip L. Manning

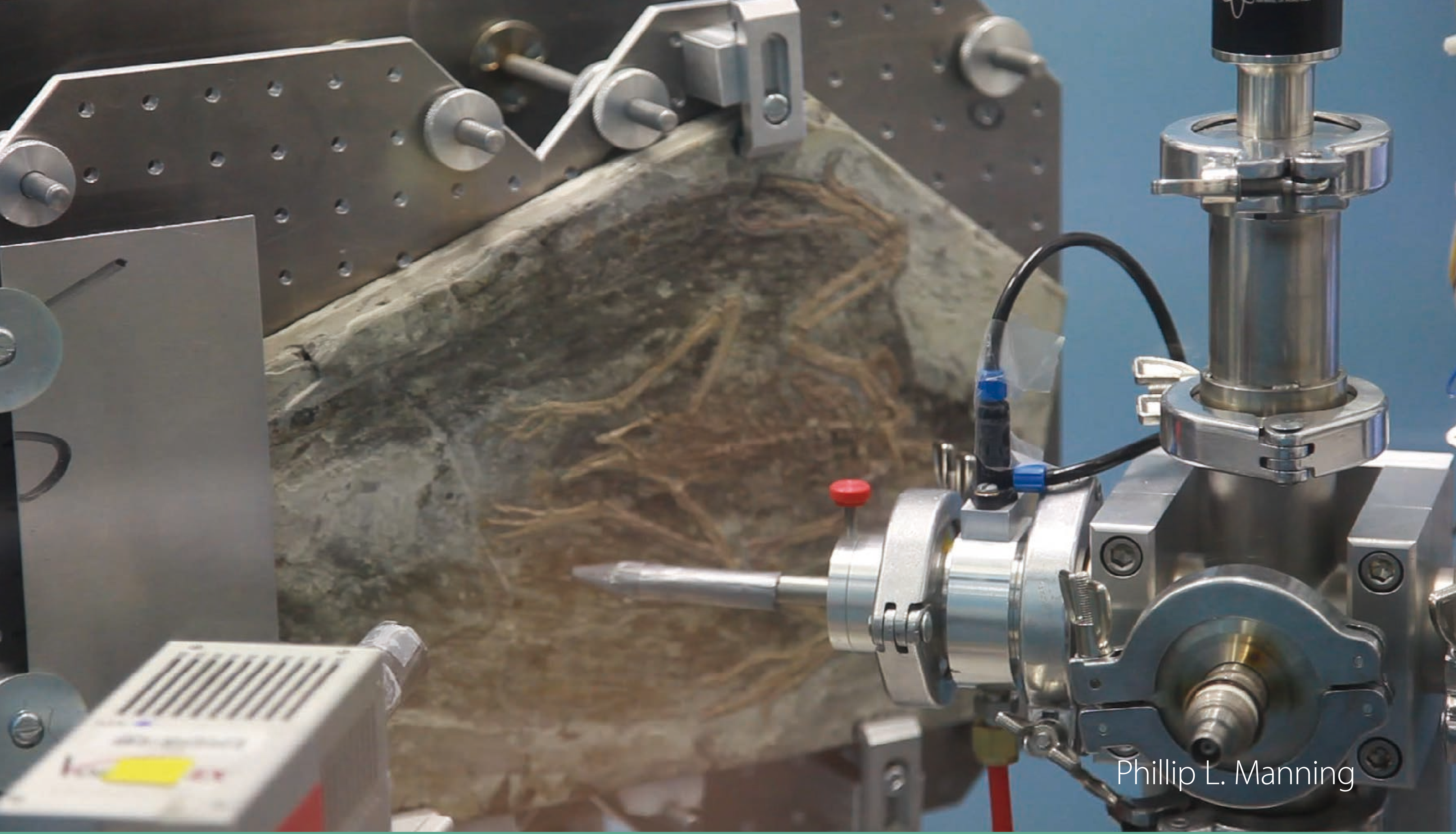
Phillip L. Manning

Copper, Calcium, Zinc

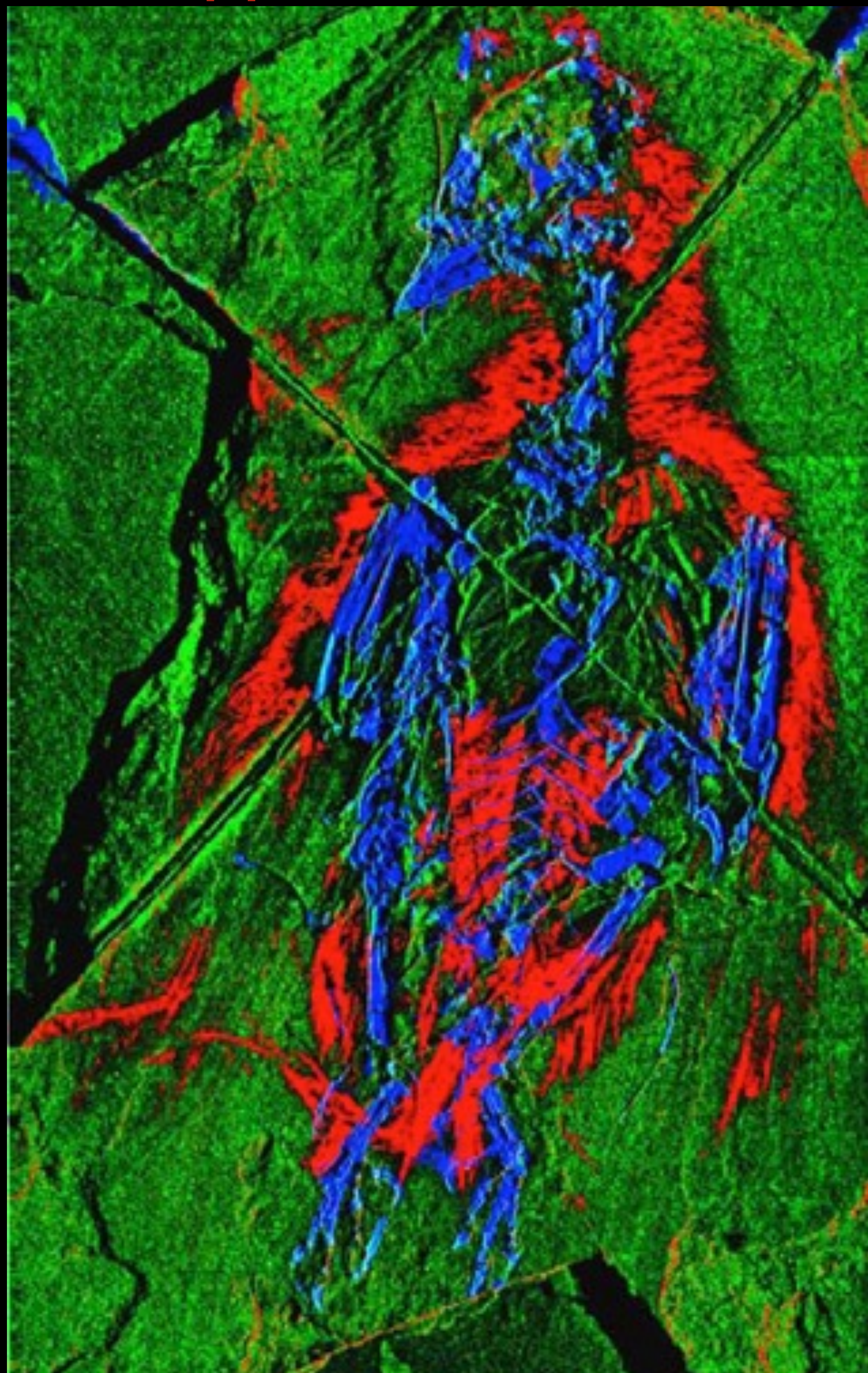

Phosphorus 2.010 KeV

Phillip L. Manning

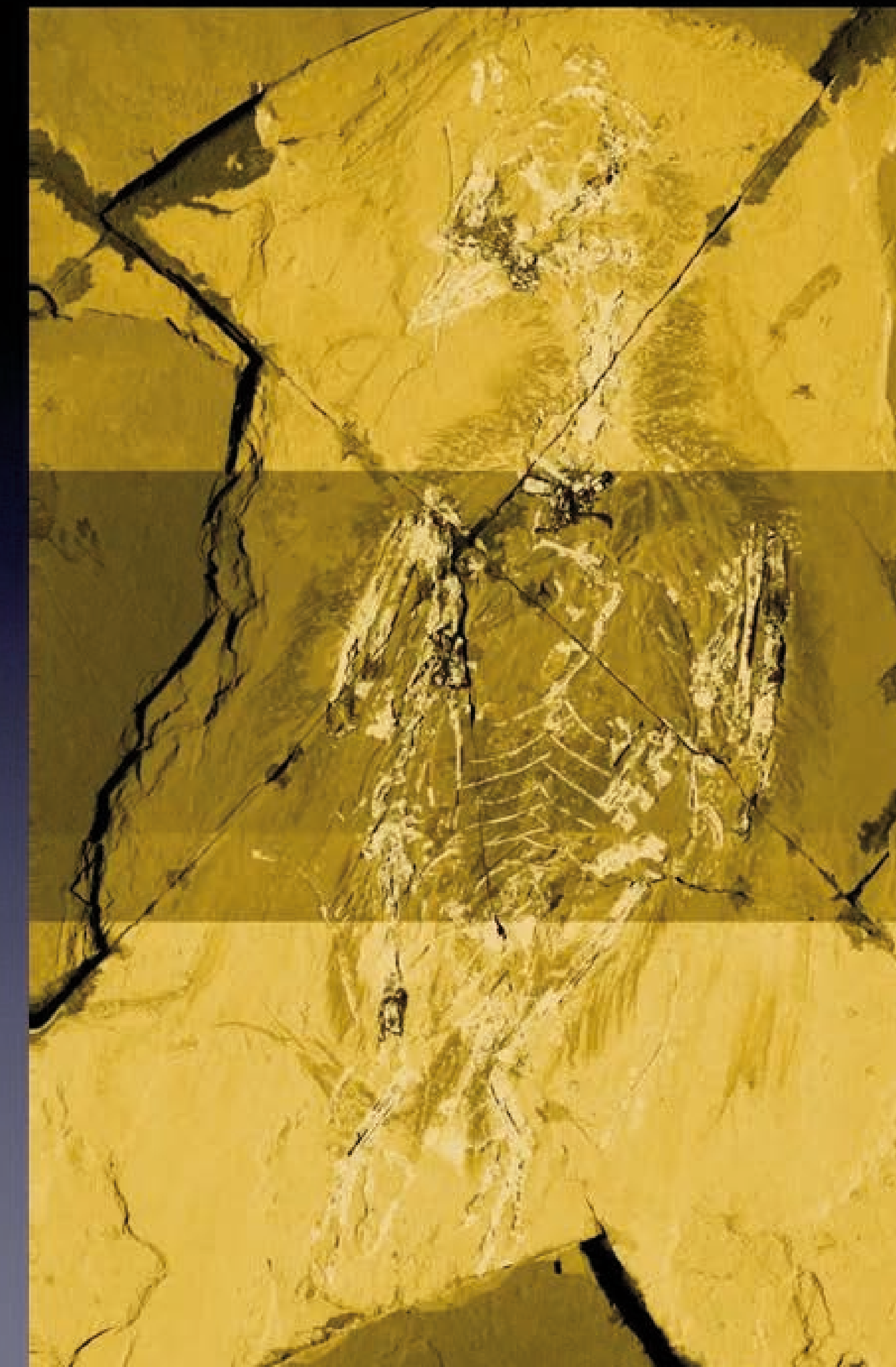

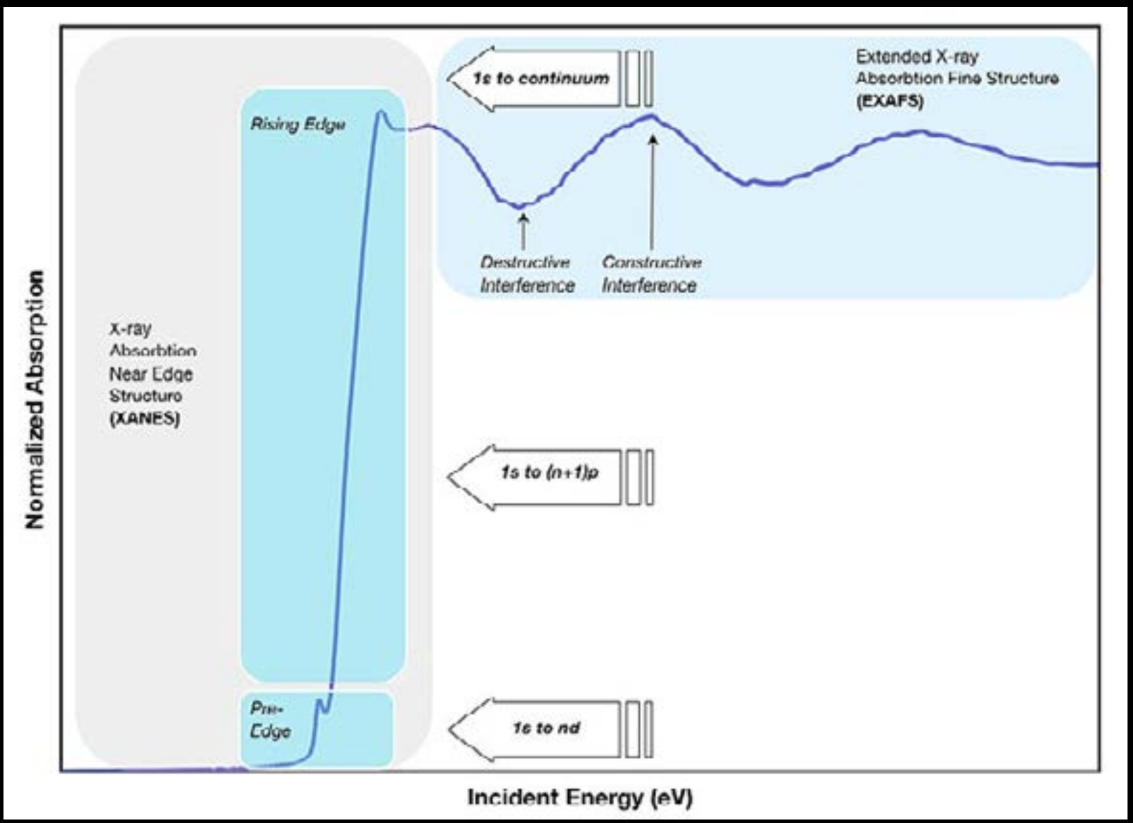


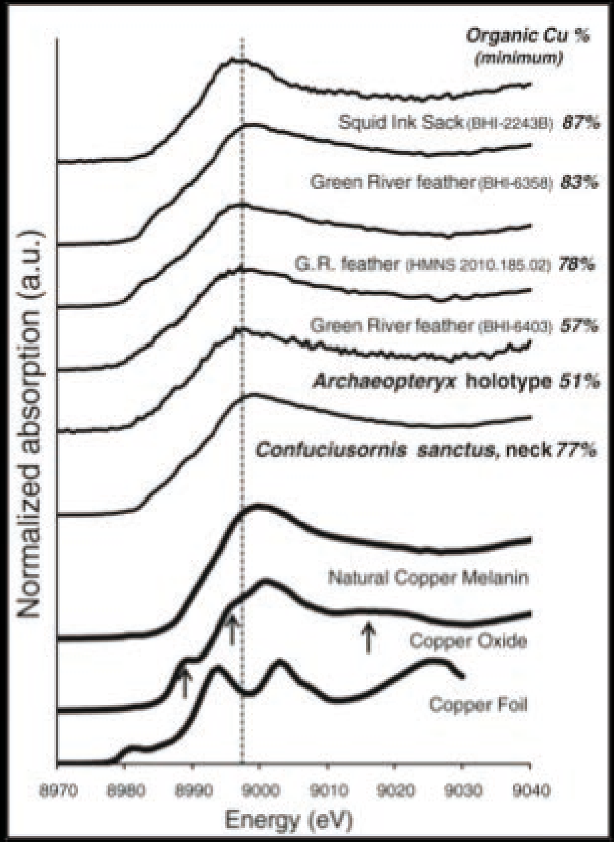


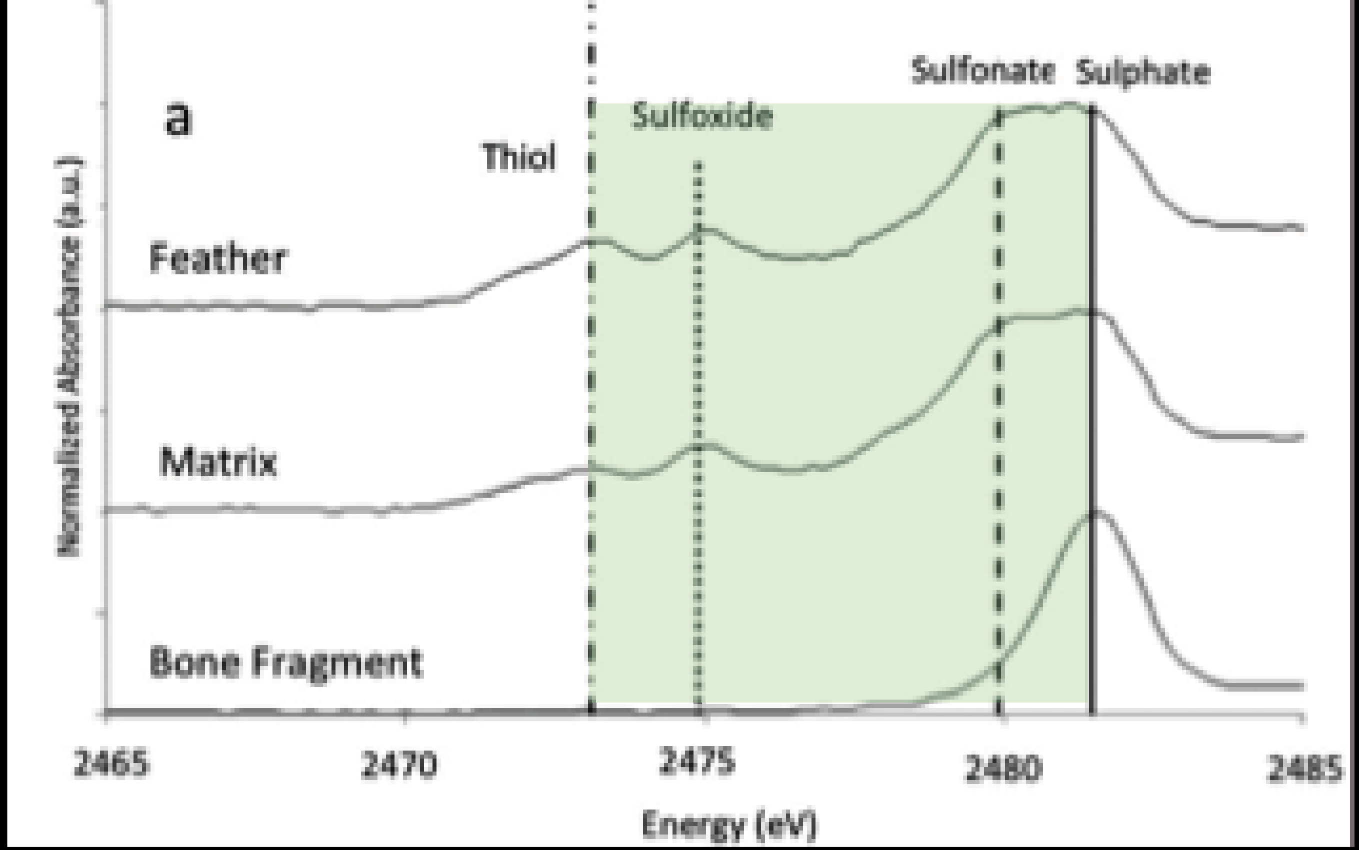


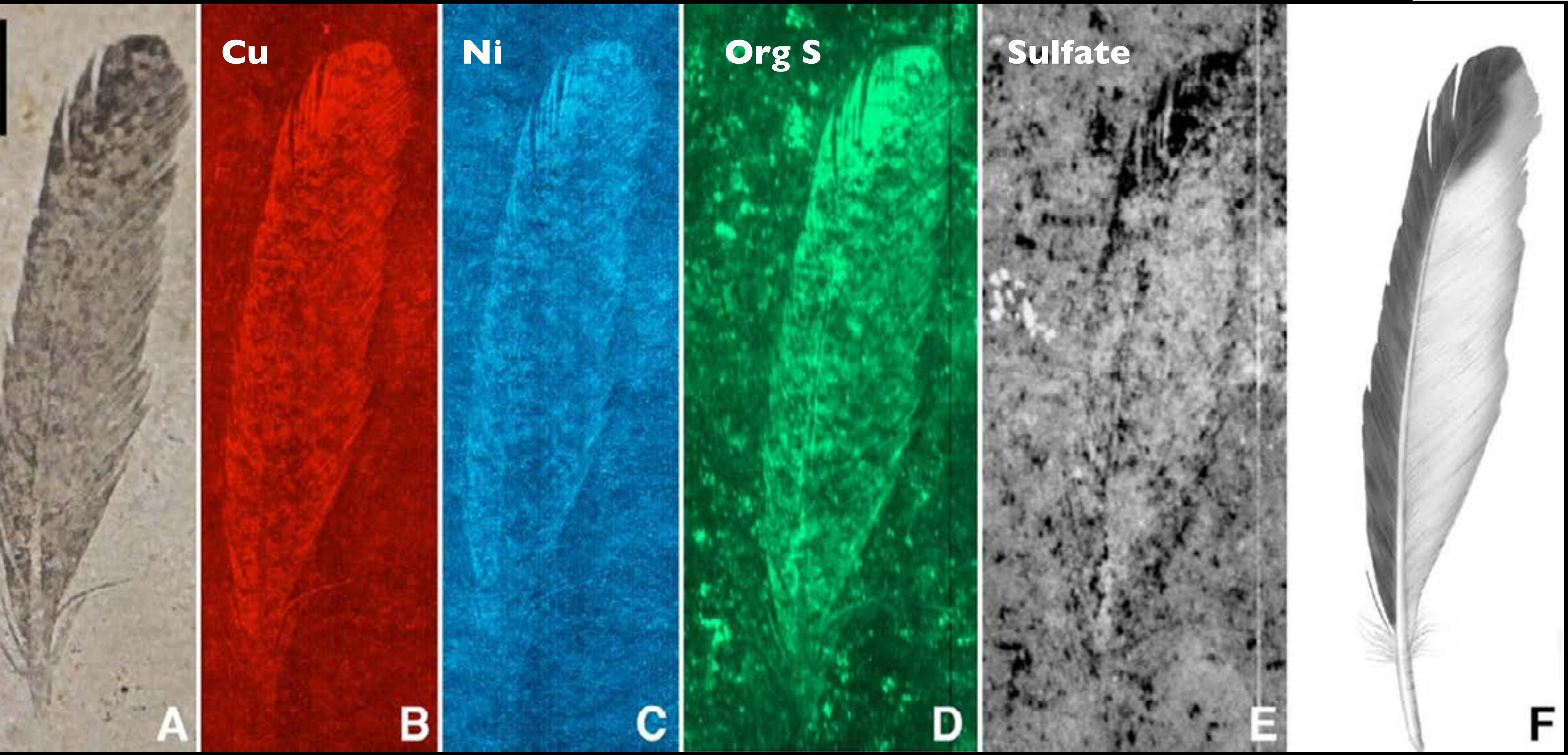


Manning, et al., 2013, JAAS

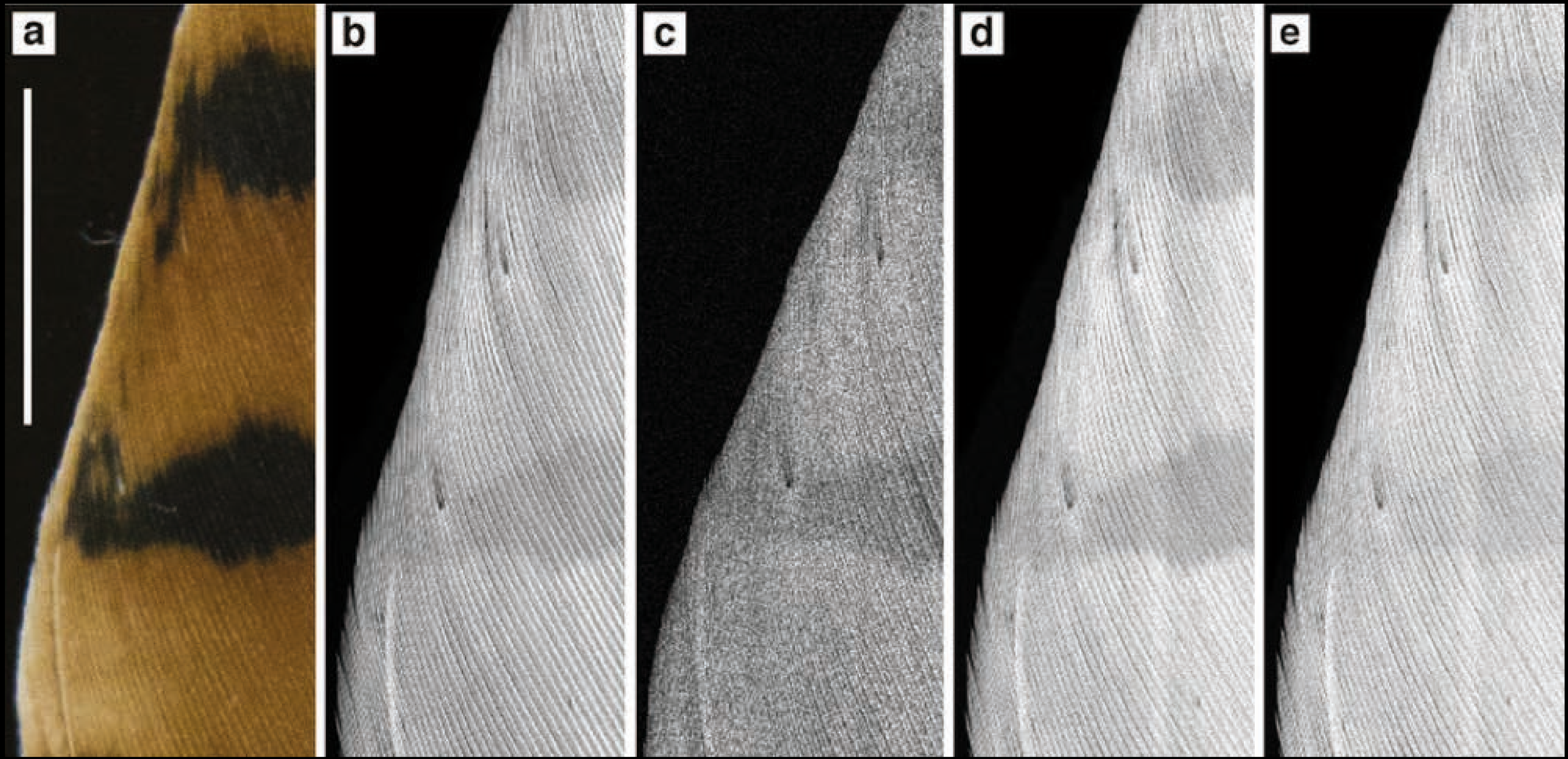


(**a**) Optical, (**b**) total sulfur (3150 eV), (**c**) 2476 eV, (**d**) 2473.5 eV, (**e**) 2472.3 eV. The total sulfur image shows that sulfur is elevated within and appears to correlate with red pigment compared to the dark stripes. Additionally, the distribution of specific oxidation states are not directly correlated. In particular, the striped pattern is more distinct in c and d compared to e. Pixel size = 50 microns. Map acquisition time = ~20 mins. Scale bar = 1 cm.

Edwards, et al., 2016, Nature Scientific Reports

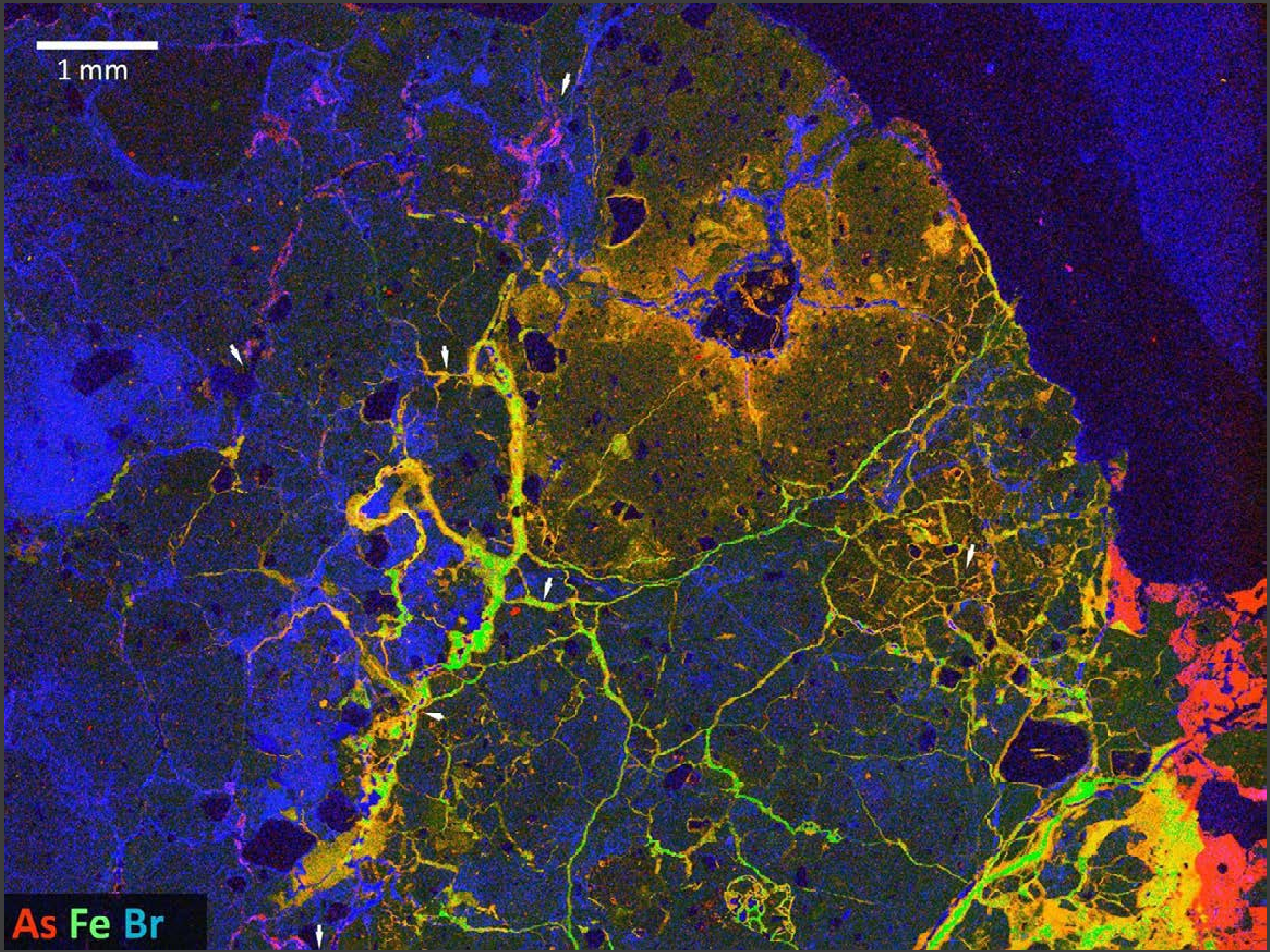


C. G. Ryan *et al*. Proc. 20th Int. Cong. X-ray Optics and Microanalysis, 1221, 9–17. AIP Conf. Proc., Apr 2010.

# Data acquisition schemes: step-by-step *vs.* continuous

step-by-step | continuous (on the fly)

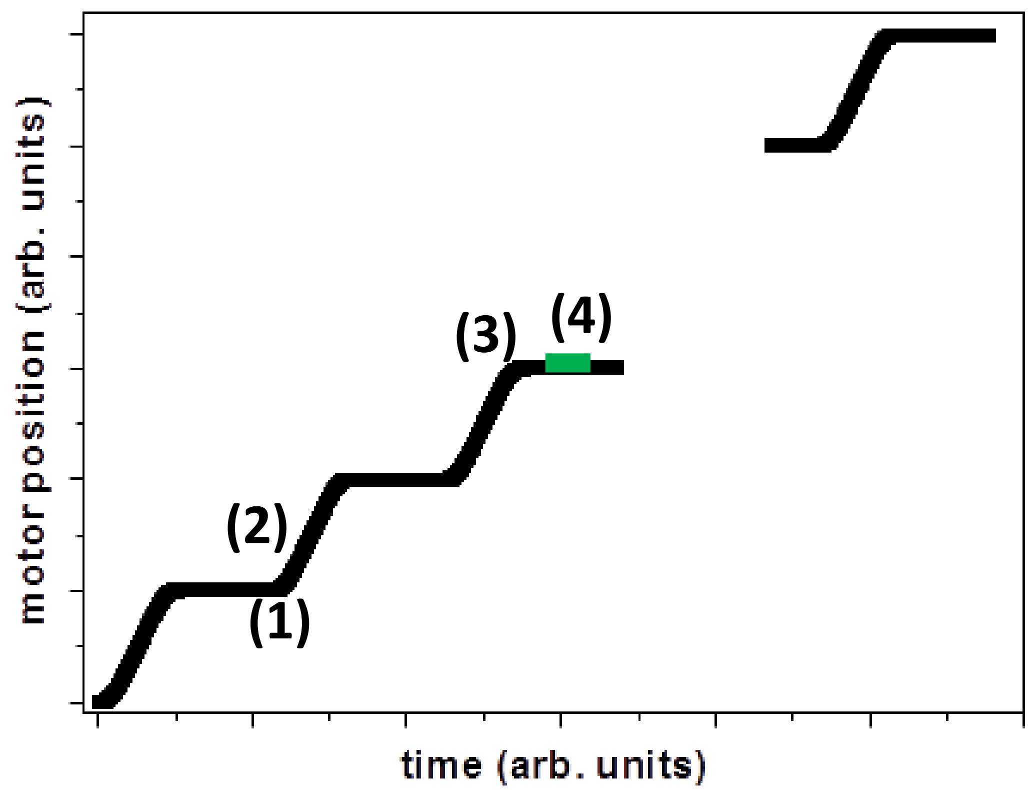


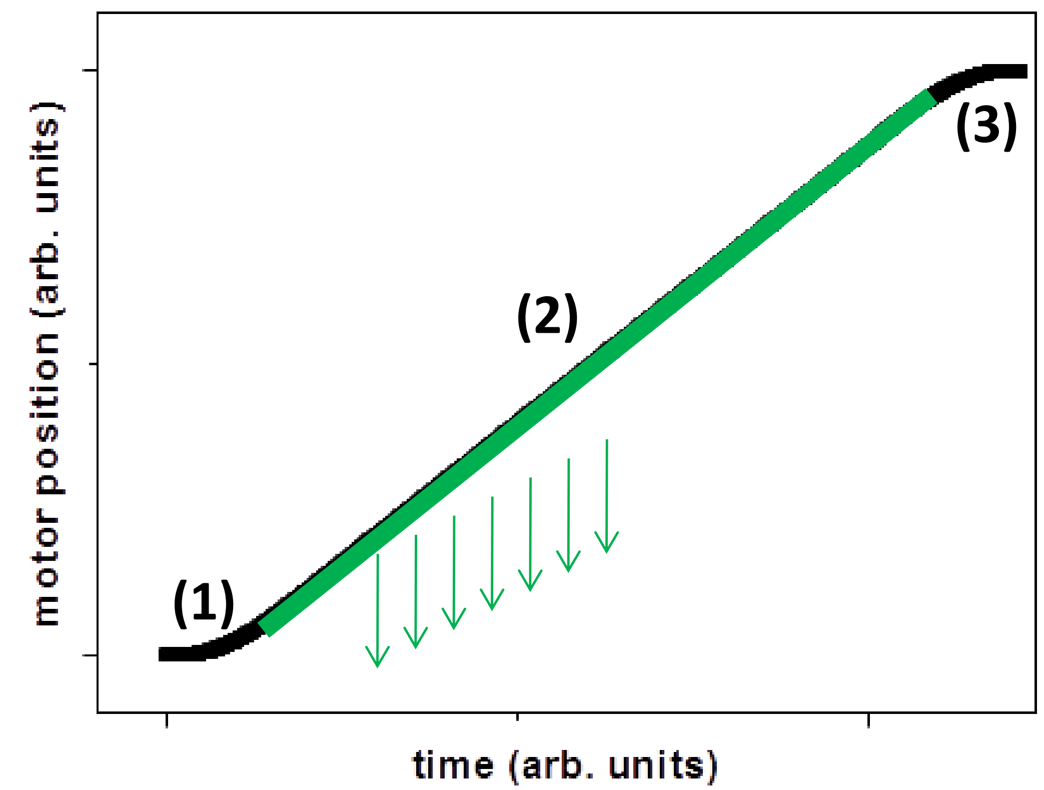


(1) motor acceleration phase
(2) motor steady speed
(3) motor decceleration phase
(4) data (detectors) acq.:
- send trig. signal
- acq. + wait det. ready
- save data, …

Typical 'deadtimes' ~ 0.5-0.7 ''
(e.g. DiffAbs beamline @ SynchrotronSOLEIL)

(1) motor acceleration phase
(2) motor steady speed
(3) motor decceleration phase
**continuous data acq.**

Data is buffered and saved / merged with motor position asynchroneously

C. Mocuta

## Fast data acquisition scheme: **the FlyScan platform** at Synchrotron SOLEIL

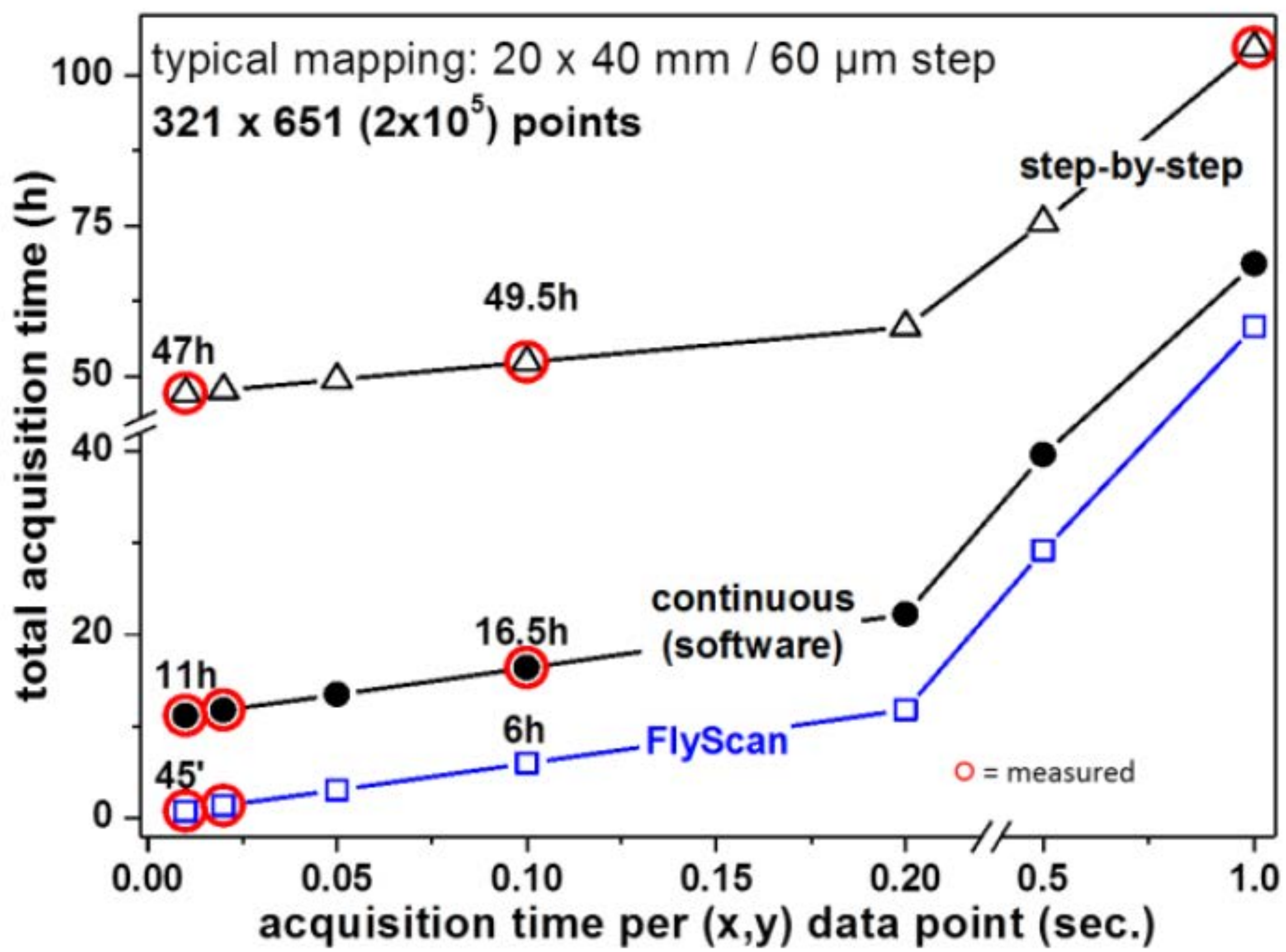


Performance comparison between several scanning techniques: step-by-step, continuous (software), and Flyscan.

The latest improvements yield to a ~ 15% supplementary gain in terms of acquisition speed.

Issues to address:

- data storage / mining / accessing
- data treatment

N. Leclercq *et al.*, 15 ICALEPCS (2015) Melbourne, Australia.

C. Mocuta

# palaeo-environmental conditions

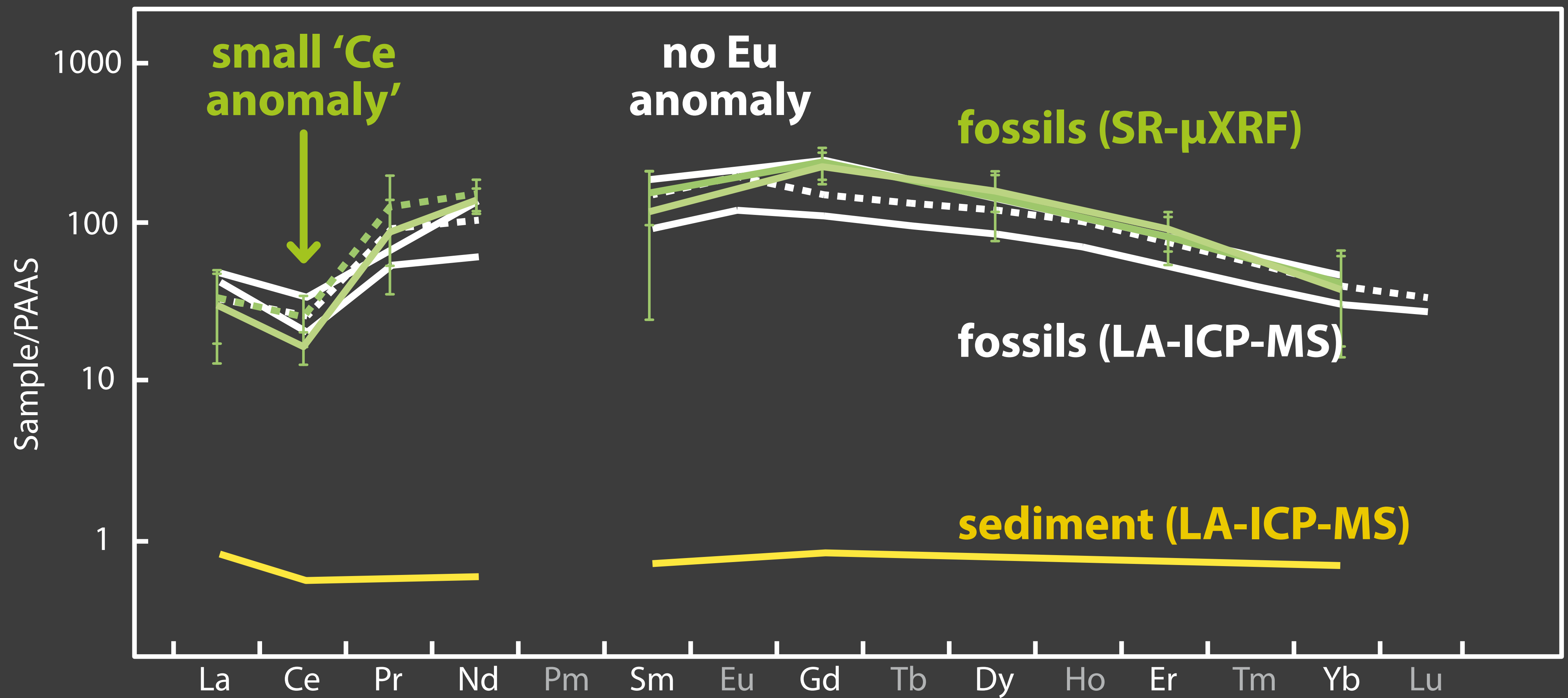


**slightly oxidizing** local conditions during rare earths' deposition

all REE are trivalent and share mostly similar physicochemical behaviour except Ce (III and IV) and Eu (II and III)

rare earth concentration profiles at **macroscale** and **microscale**

Fermi's golden rule:

$$\mu(E) \sim \sum_{Nfond} |\langle\Psi_{fond}| \boldsymbol{\varepsilon} \cdot \mathbf{r} |\Psi_{exc}\rangle|^2 \cdot \delta(h\nu - (E_{exc} - E_{fond}))$$

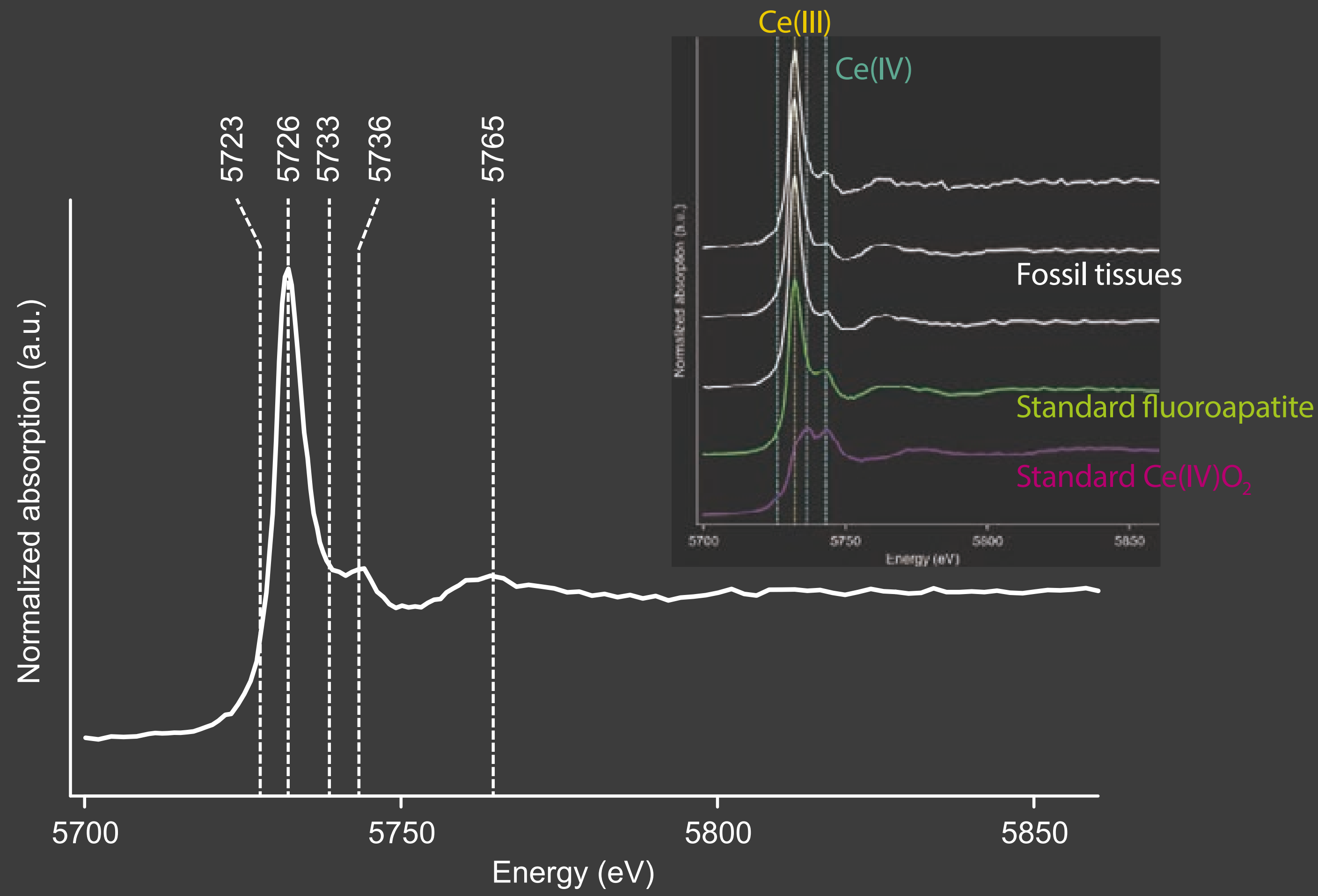


**Decapod crustacean "crab"**
Late Cretaceous, -95 Myr,
Djebel Oum Tkout Morocco

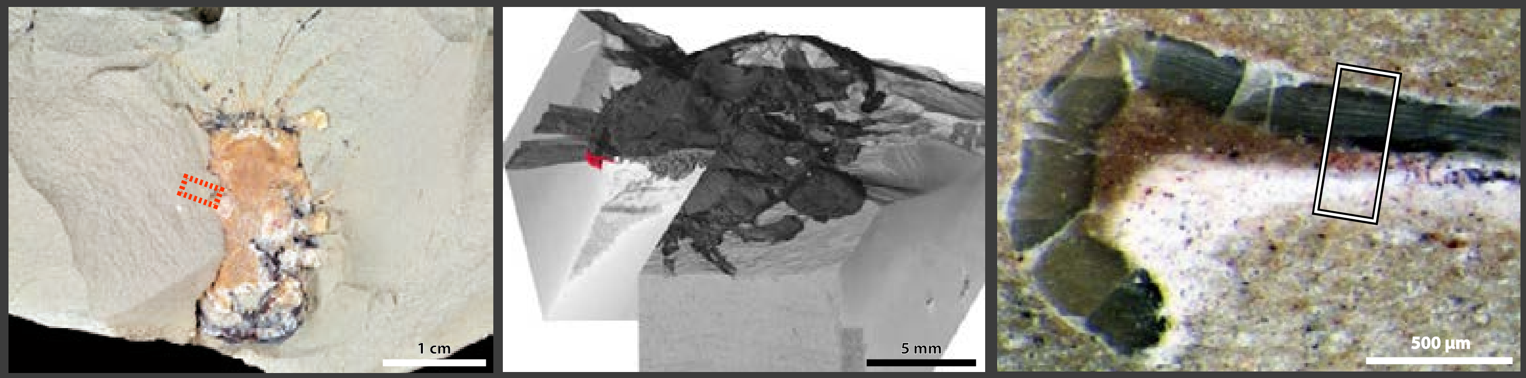


**XAS: local speciation**
Ce(III) + some Ce(IV)
in fossils, at a few µm lateral resolution

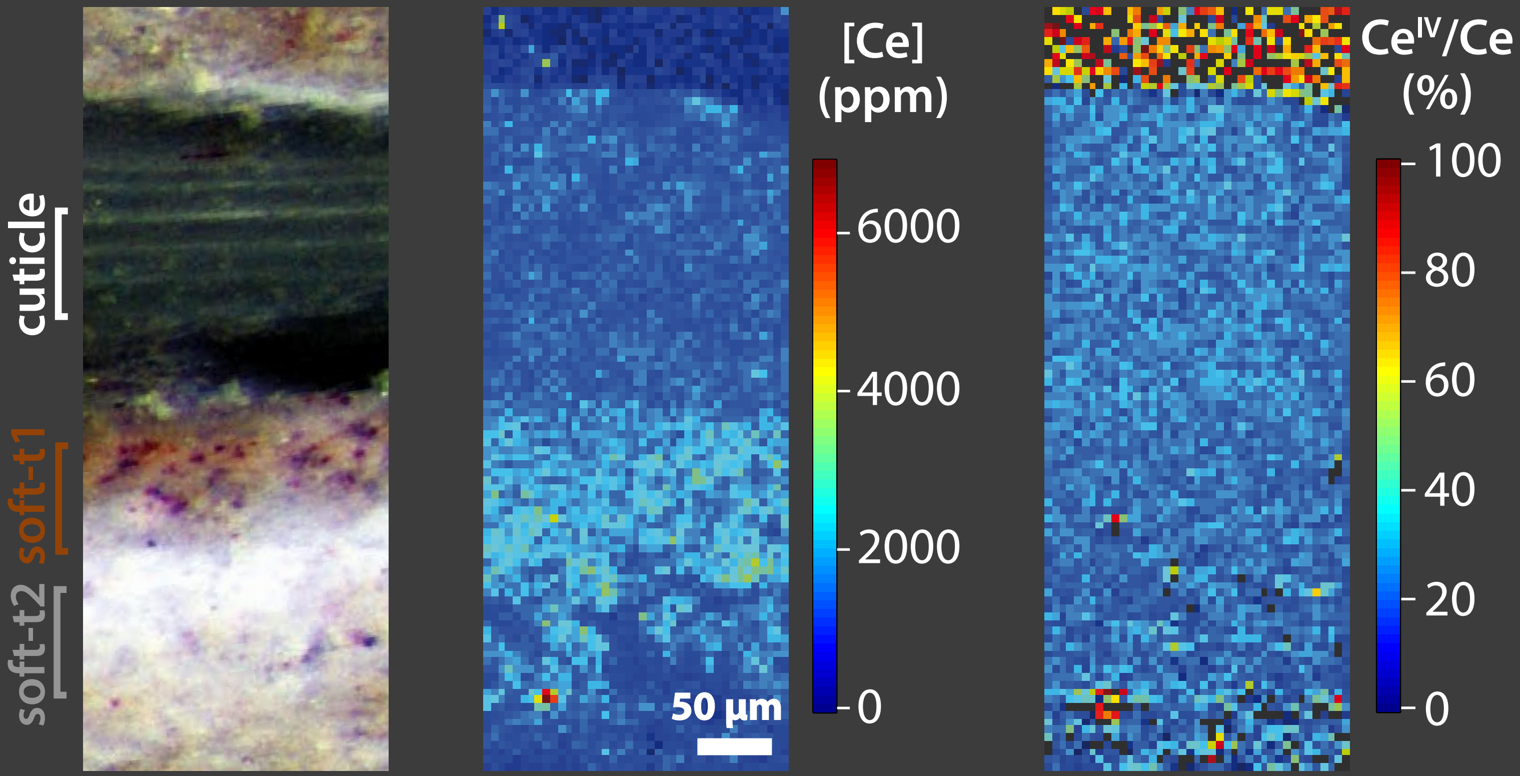


**comparison to REE profiles**
results are in phase (steady state?)
**$Ce^{4+}$ ubiquitously adsorbed**
+ as a few $CeO_2$ grains



► P. Gueriau et al. Anal. Chem. 2015.

# K-edge substraction

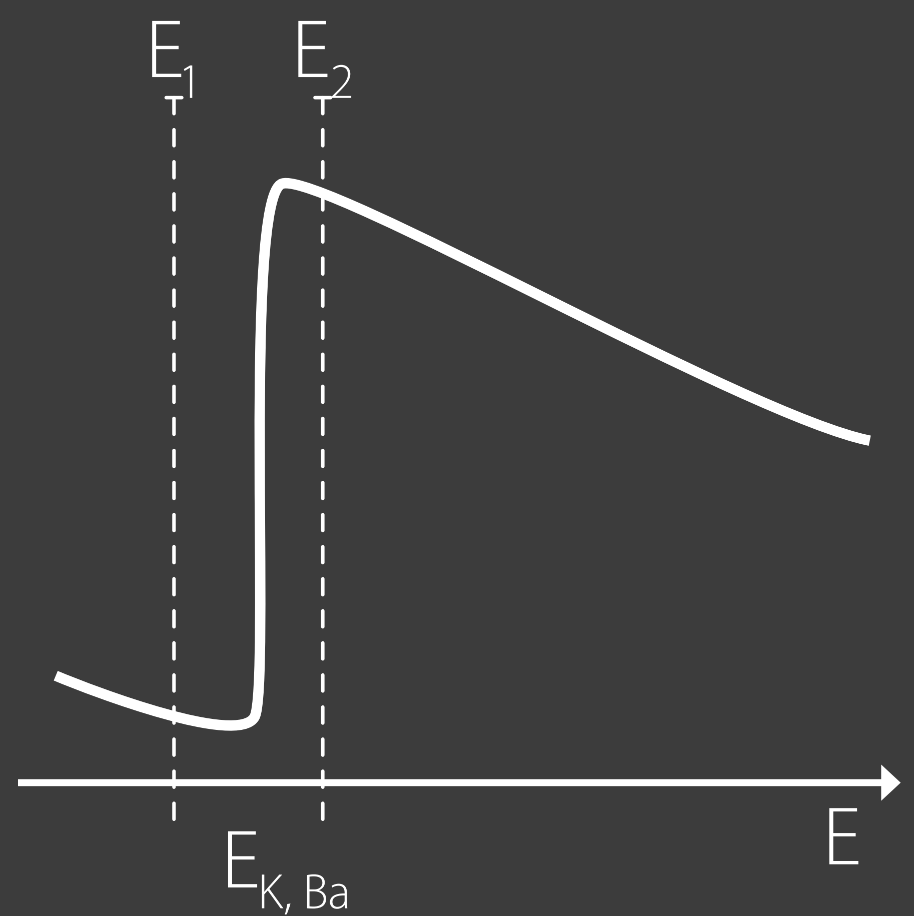


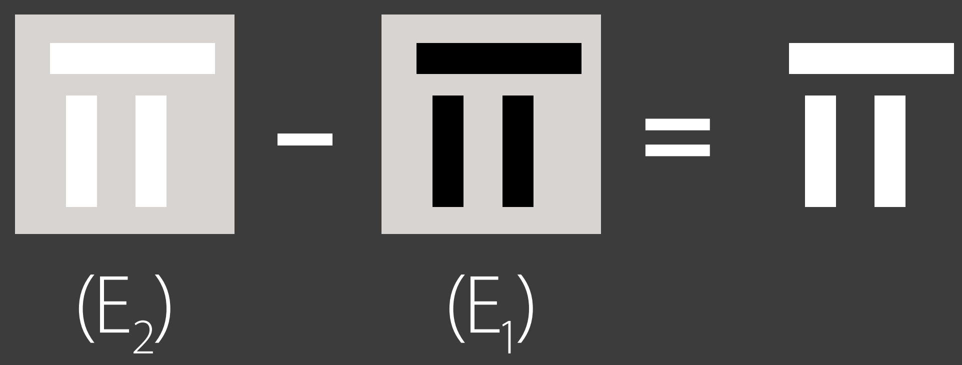


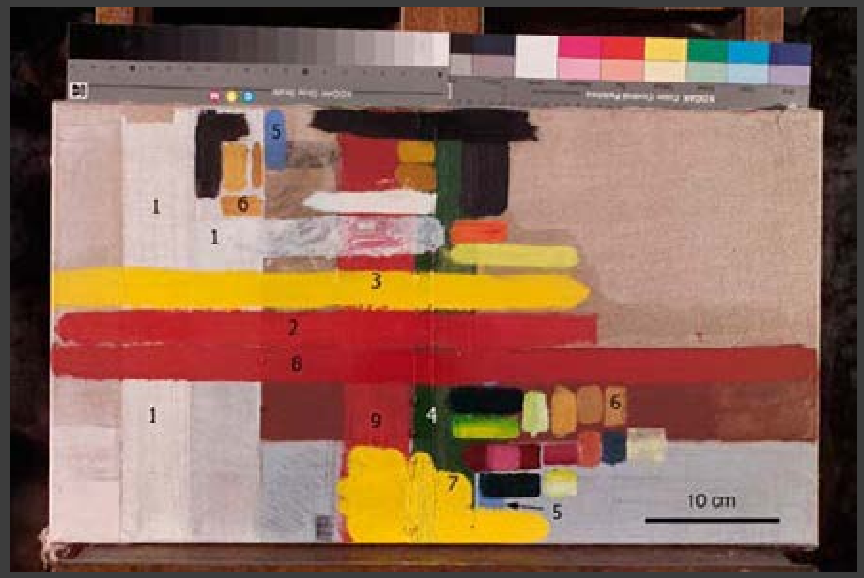

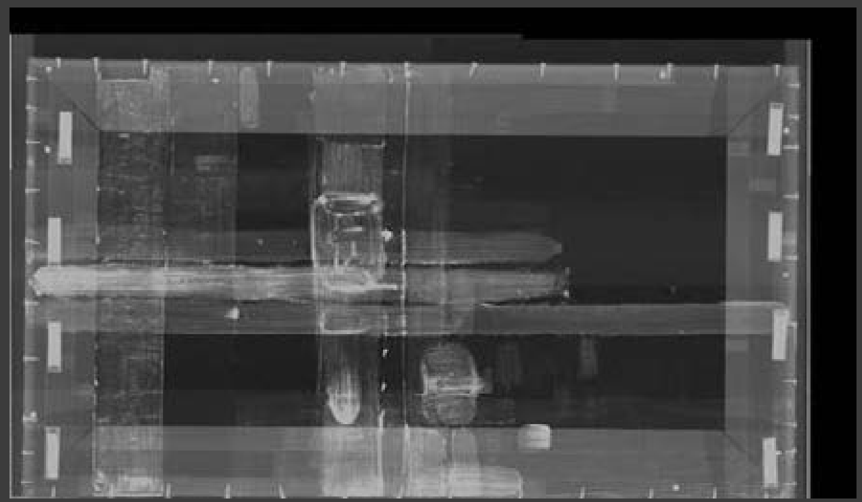

radiographie (50 keV)

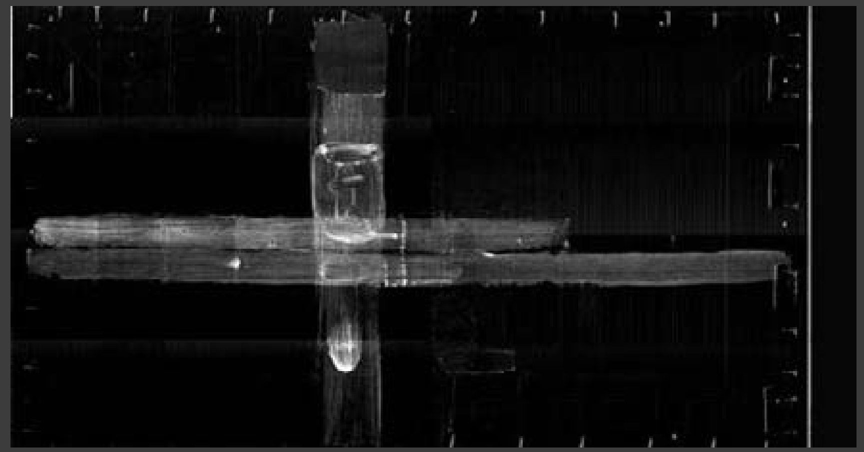

localisation Ba (38 keV)

localisation Pb (89 keV)

K. Krug et al. Appl. Phys. A, 2006.

## full-field XAS = TXM: speciation at each pixel!

transmission only: thin section


Roman Sigillata black gloss ceramic sherd

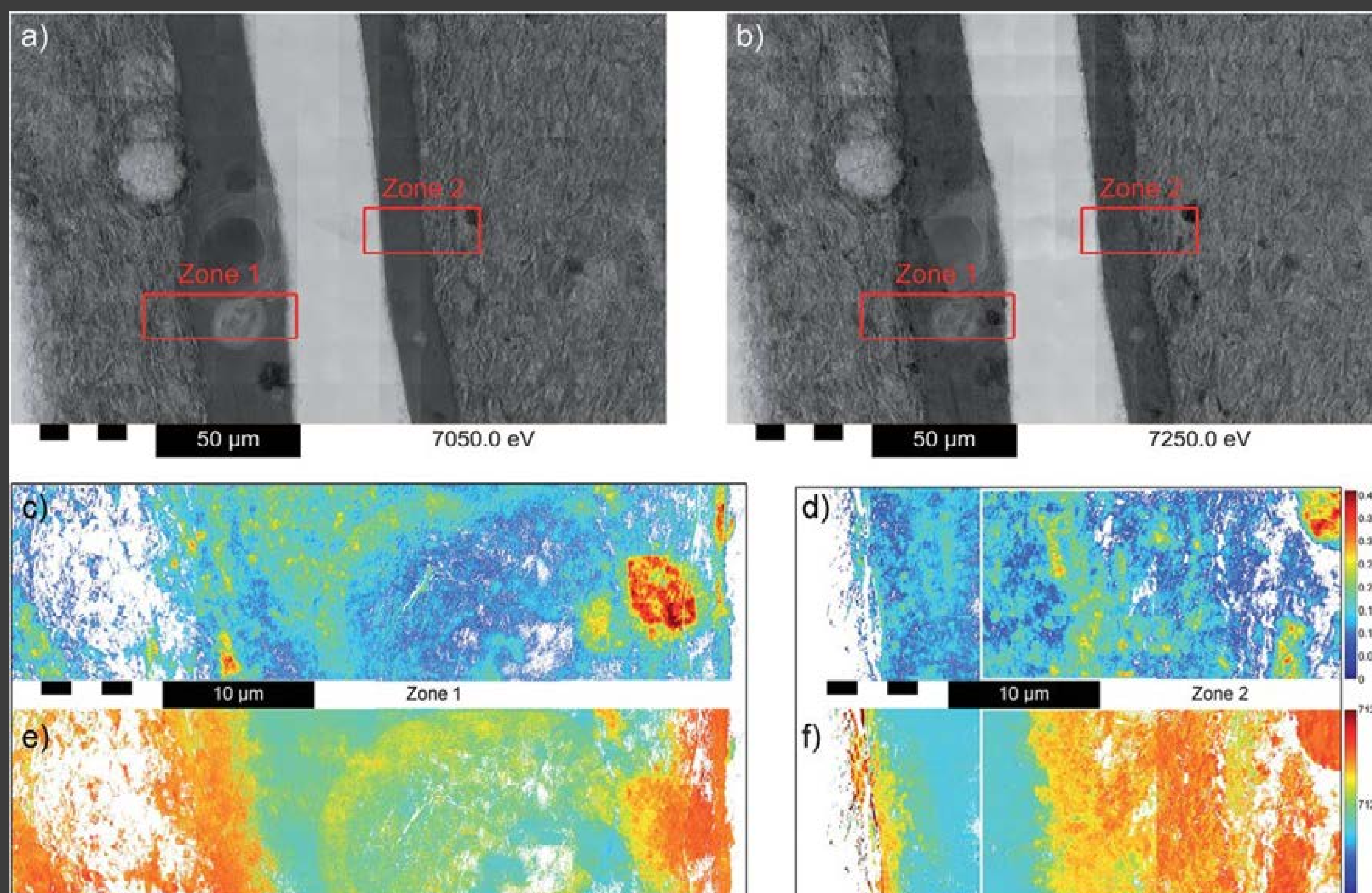


Fe K-edge jump intensity

Fe K-edge energy

F. Meirer et al. J. Anal. At. Spectrom., 2013.

**ancient carbonaceous systems**

art materials: pigments, binders, dyes, supports, textiles…

archaeological and palaeontological materials: cellulosic materials, proteins, etc.

…

**chemically complex and heterogenous due to their initial composition and effects of ageing**

# carbon speciation in ancient organic systems

## FT-IR spectroscopy

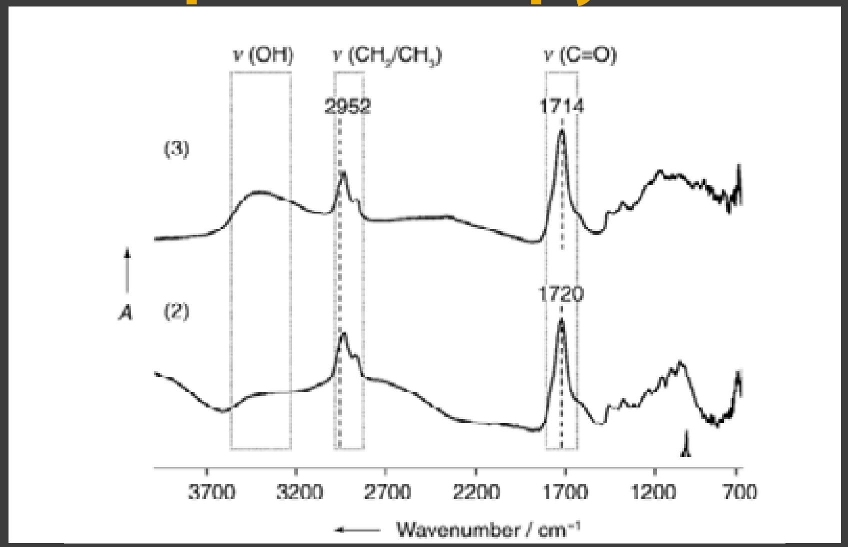


Echard et al. Angew. Chem. Int. Ed., 2010

## Raman spectroscopy

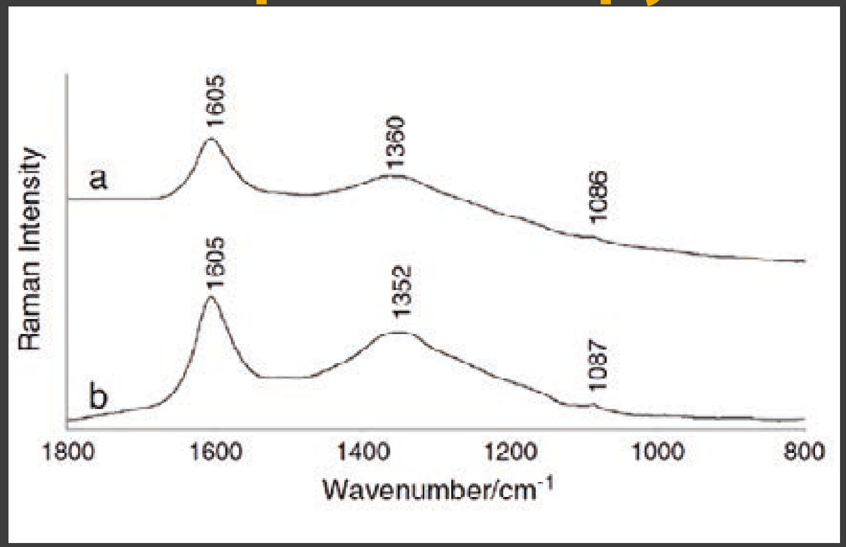


A. Coccato et al. J. Raman Spectrosc., 2015

## TOF-SIMS

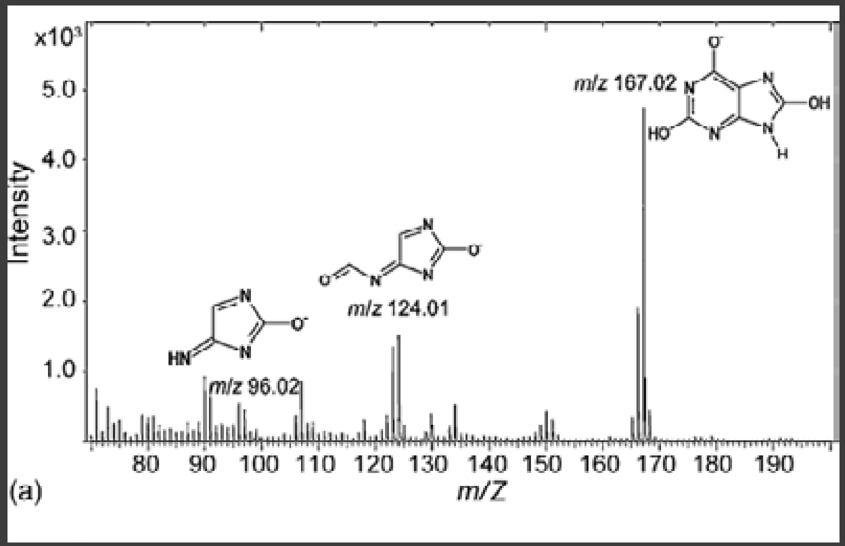


Mazel et al. Anal. Chim. Acta, 2015

## GC/MS…

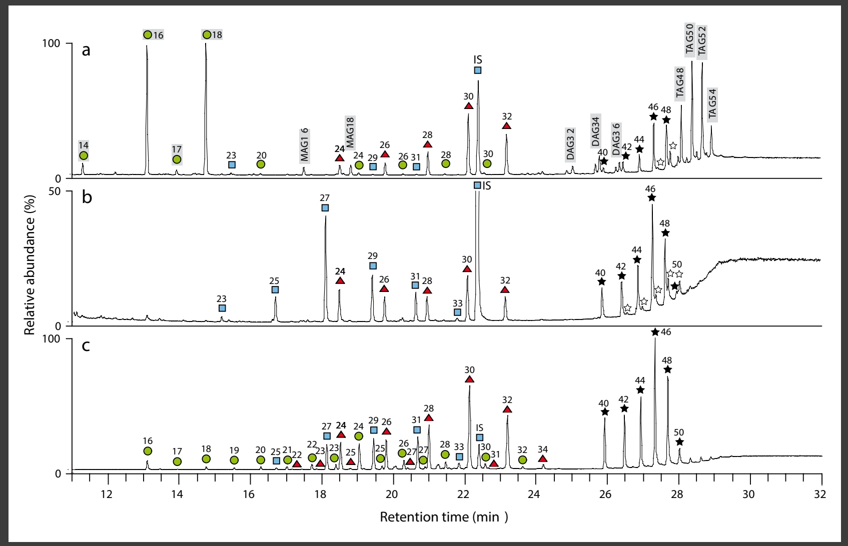


Roffet-Salque et al. Nature, 2015

**these methods are invasive or surface-sensitive (few µm's or below)**

natural carbon species (e.g. graphite) absorb almost the entire IR–UV range

over-representativeness of the (contaminated, altered) surface, impact of surface condition…

## Pyrolysis Gas Chromatography Mass Spectrometry (PyGCMS) of Hell Creek fossil dinosaur skin and surrounding matrix

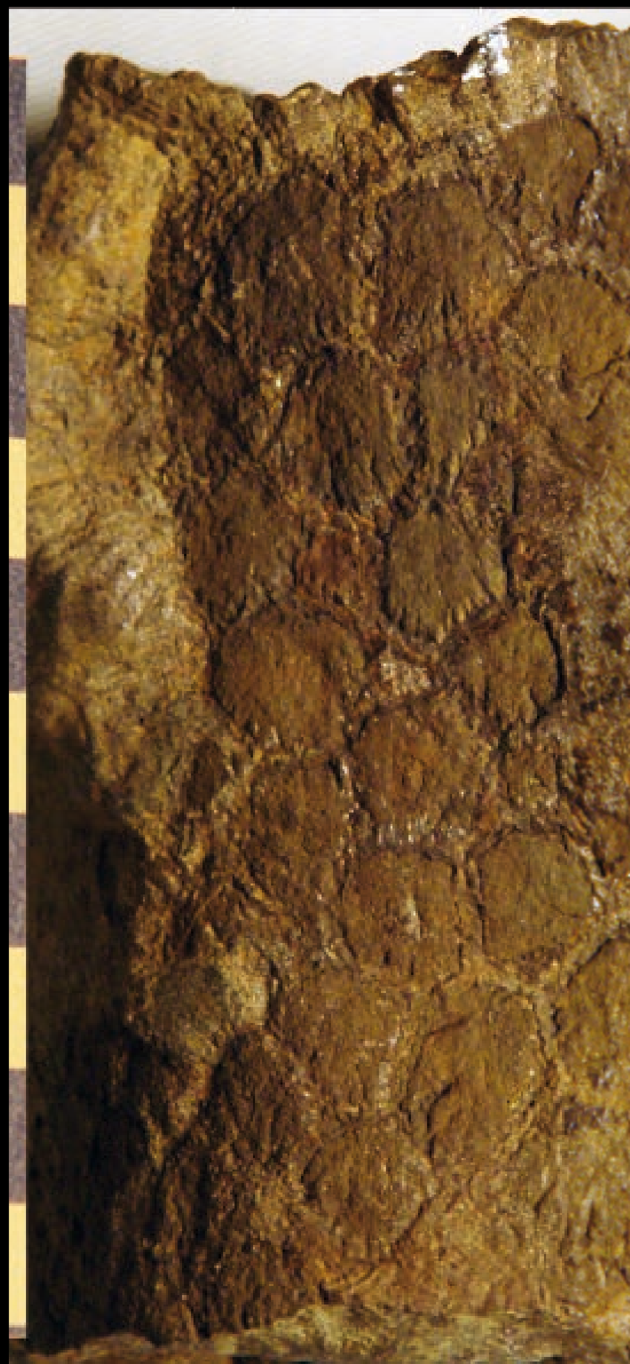

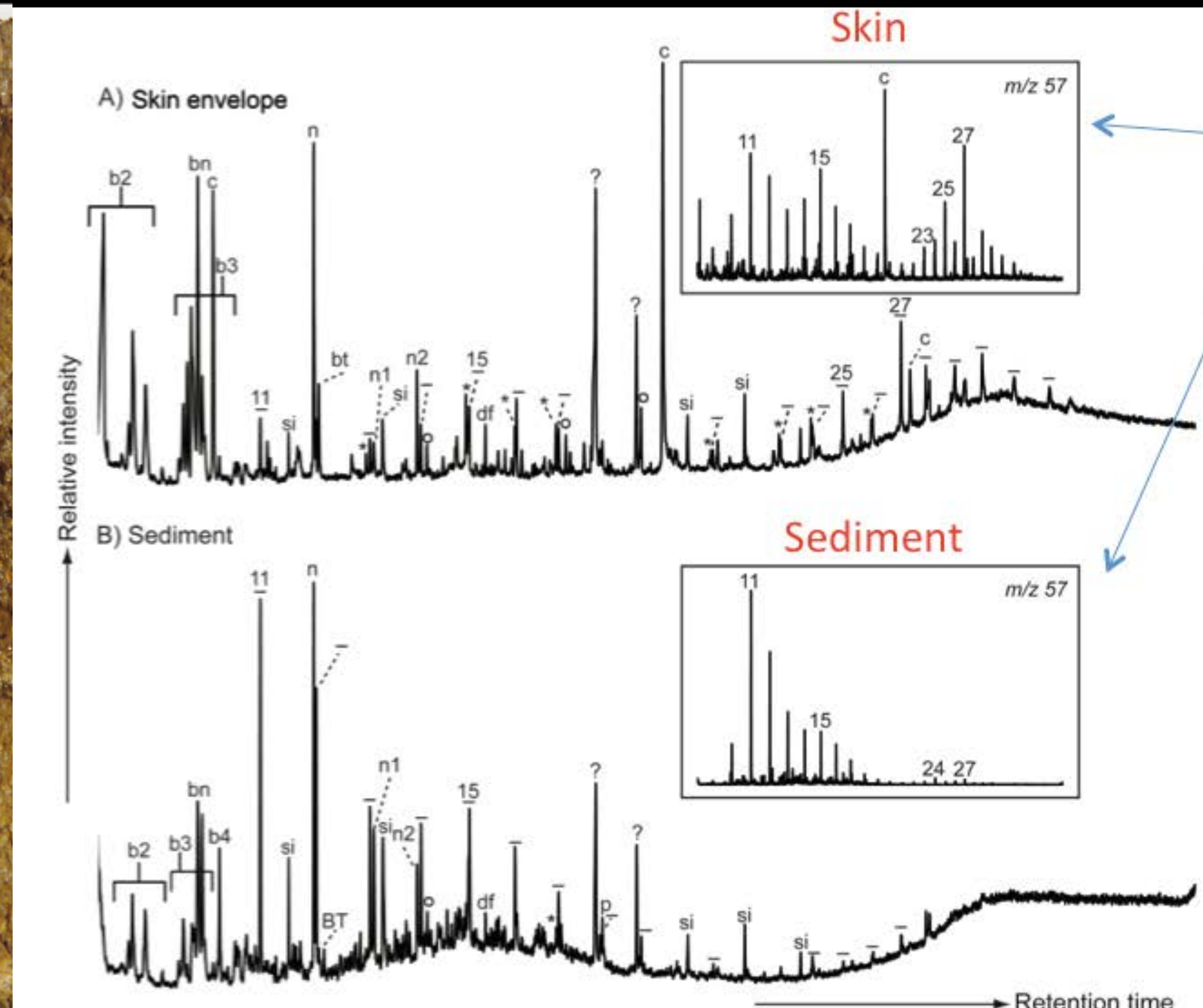


The simple hydrocarbon patterns are completely different.
These compounds (alkanes) are not biologically active and hence quite stable, and strongly support the conclusion that organic material from the organism has been retained over geological time.

Manning et al., 2009, Proc. Roy. Soc. B.

## “STXM” = Scanning Transmission X-ray Microscopy-based Carbon X-ray Absorption Near-Edge Spectroscopy

C K-edge: **285 eV**

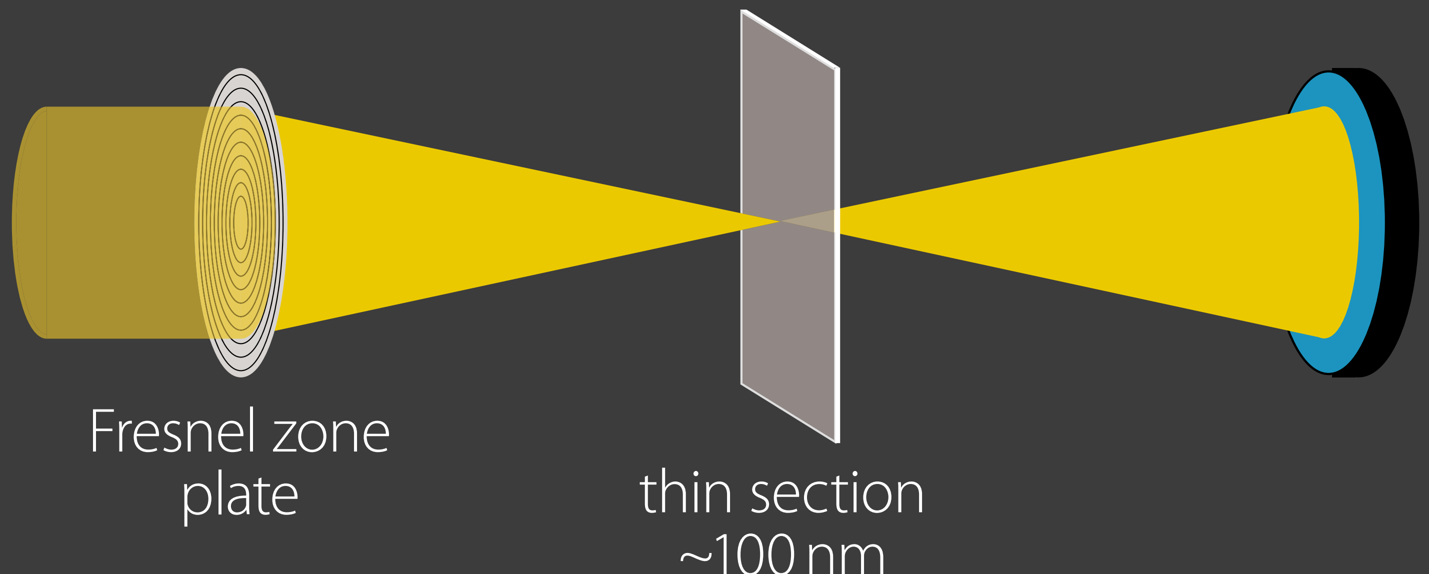


speciation at the carbon K-edge (~280 eV):

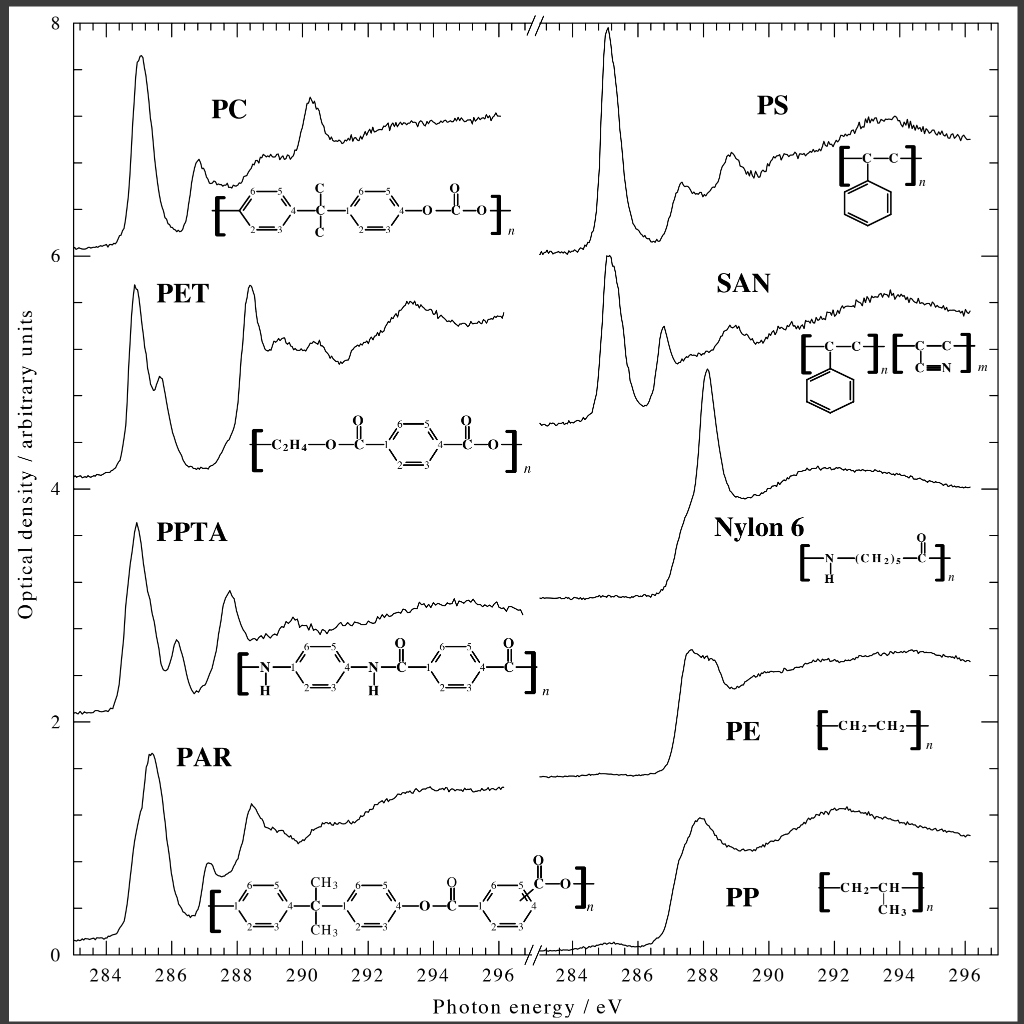


Koprinarov et al.

fossilized megaspore in Triassic metamorphic rocks from the Vanoise in the French Alps

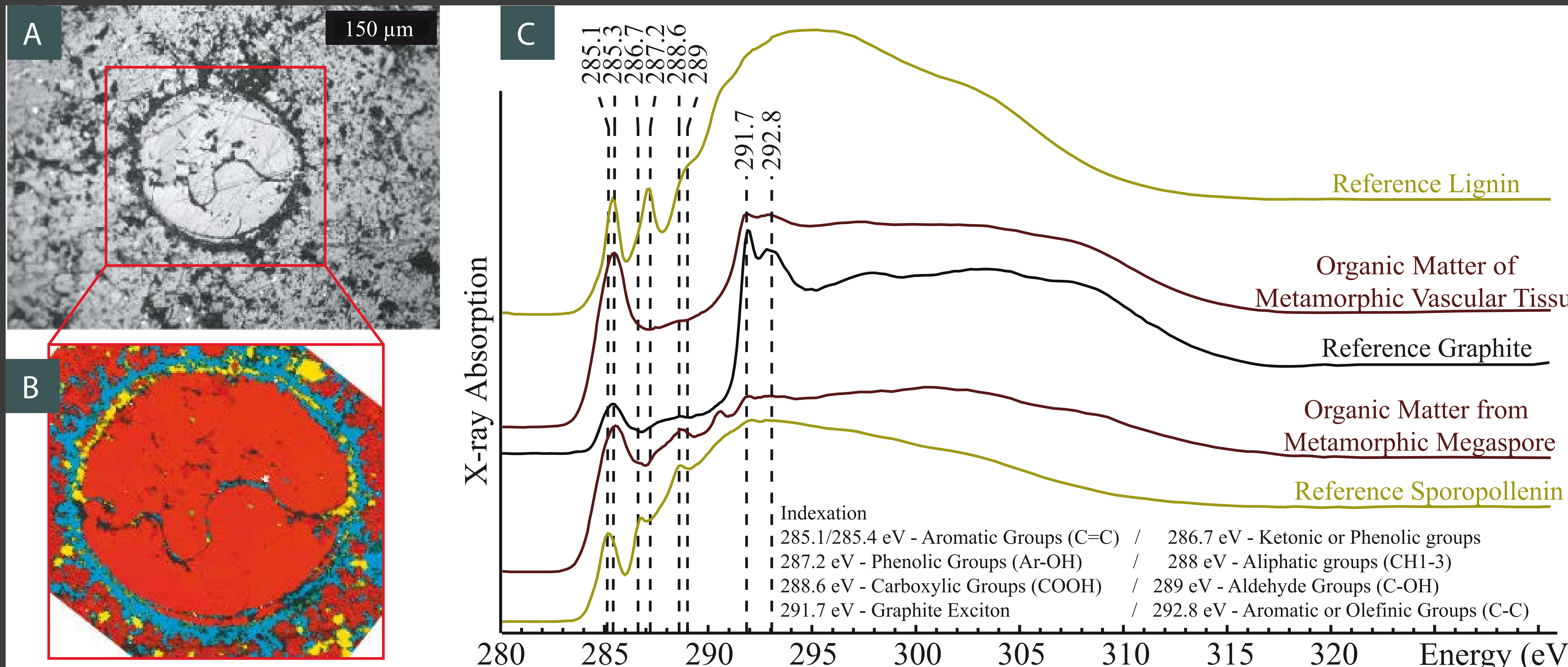


Raman map: graphitic carbon, calcite, and ankerite

**sporopollenin**: long chain fatty acids, phenylpropanoids, phenolics and traces of carotenoids.

S. Bernard & D. Papineau, 2014

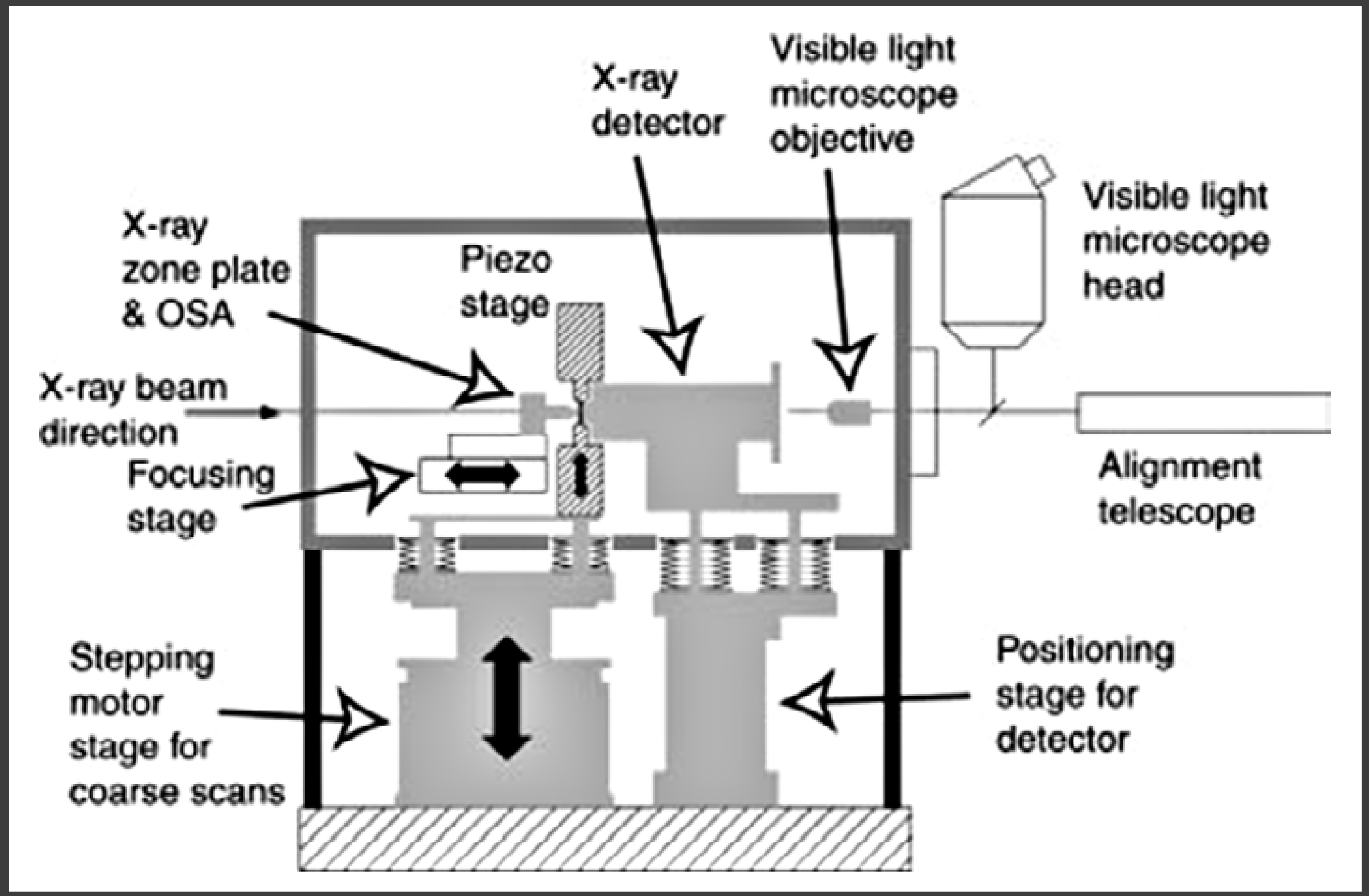


Maser, 2000

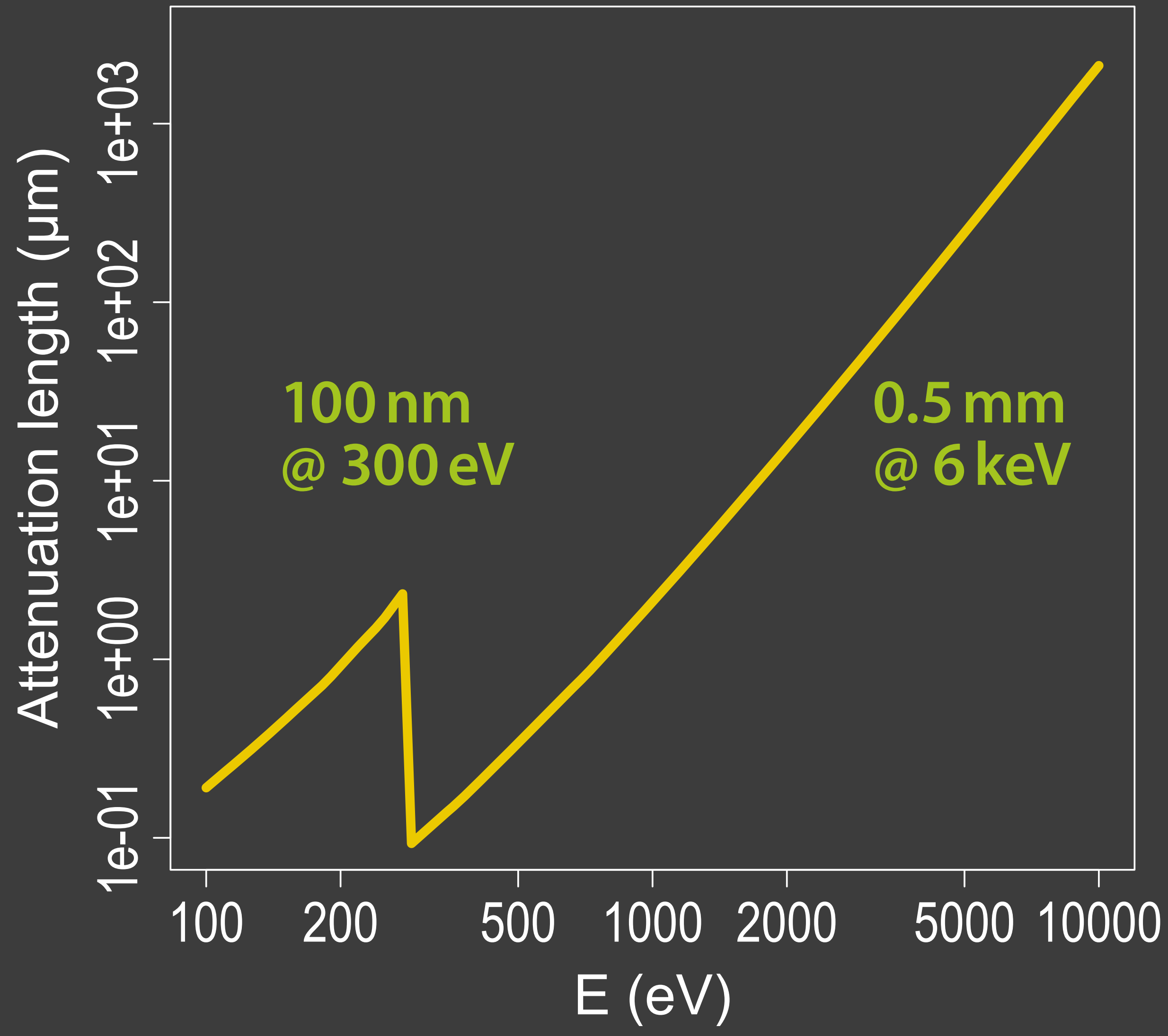


preparation using FIB, in vacuum, micromanipulation…

# X-ray Raman spectroscopy

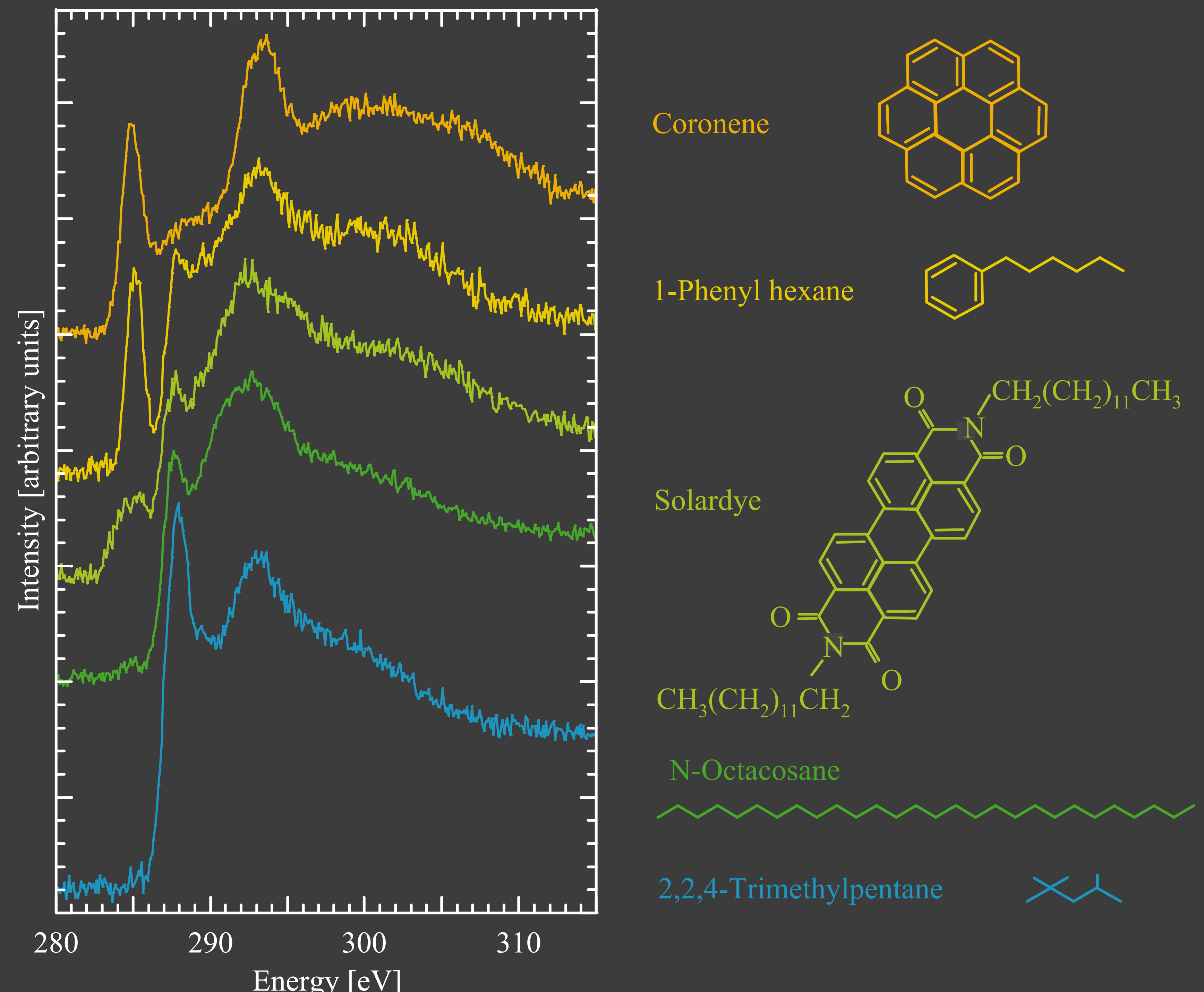


adapted from U. Bergmann and O. C. Mullins,
in Asphaltenes, Heavy Oils, and Petroleomics, 2007

# X-ray Raman spectroscopy

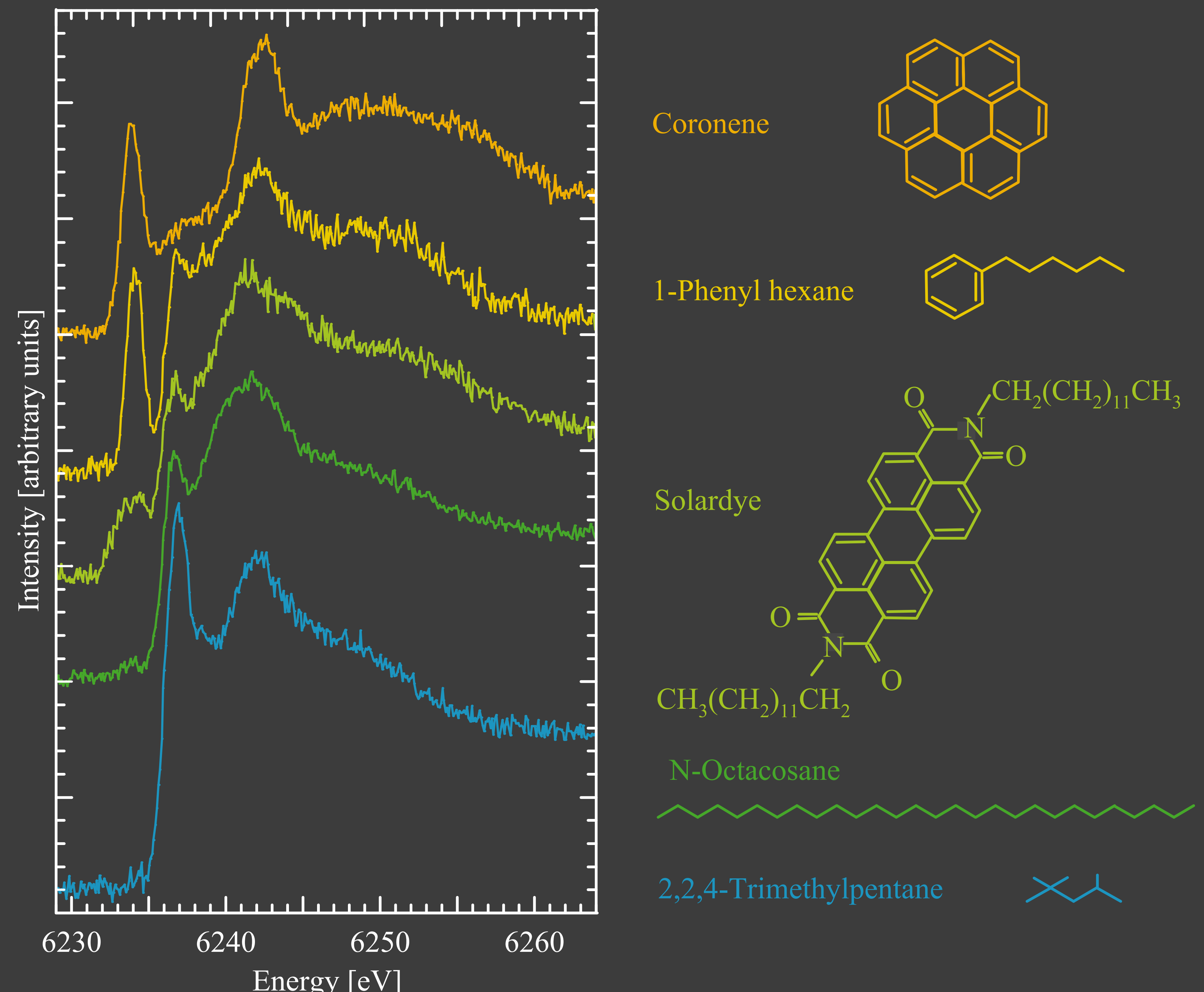


adapted from U. Bergmann and O. C. Mullins,
in Asphaltenes, Heavy Oils, and Petroleomics, 2007

# a final state spectroscopy

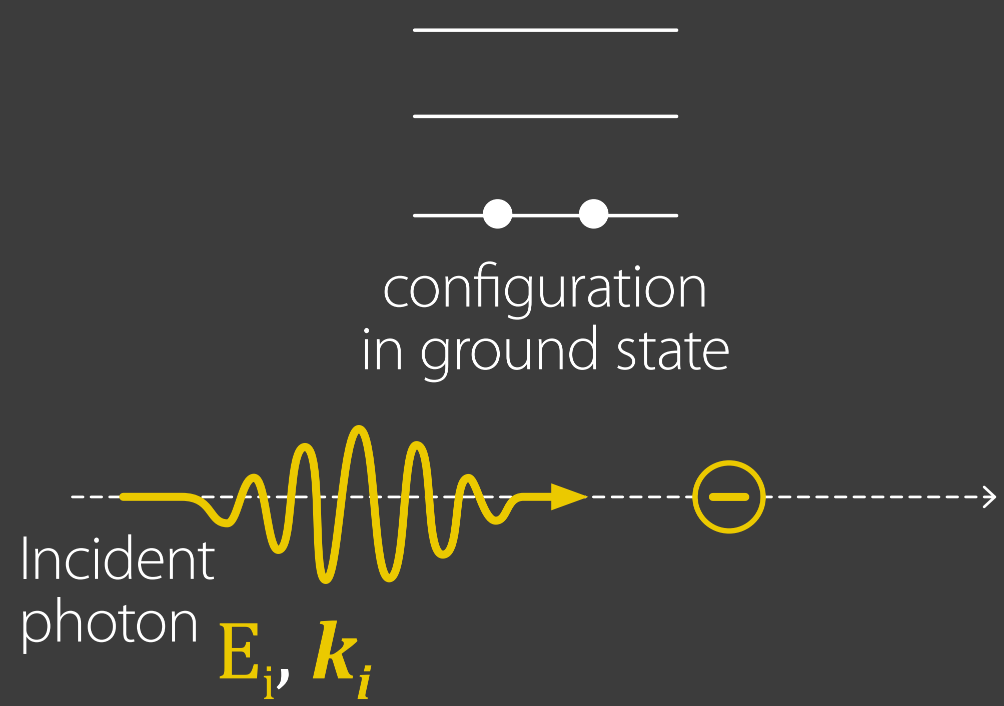

## a final state spectroscopy

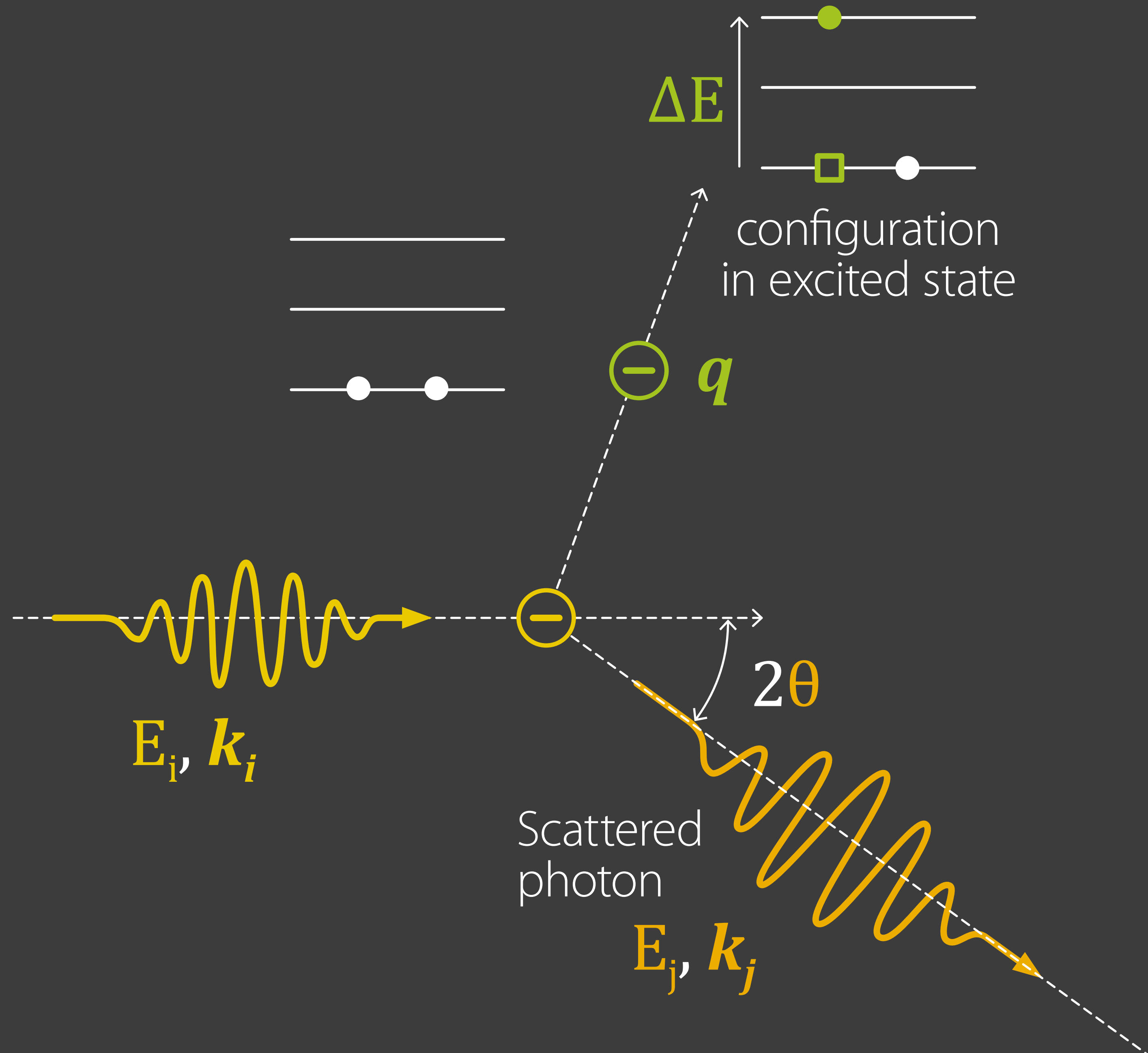

# a final state spectroscopy

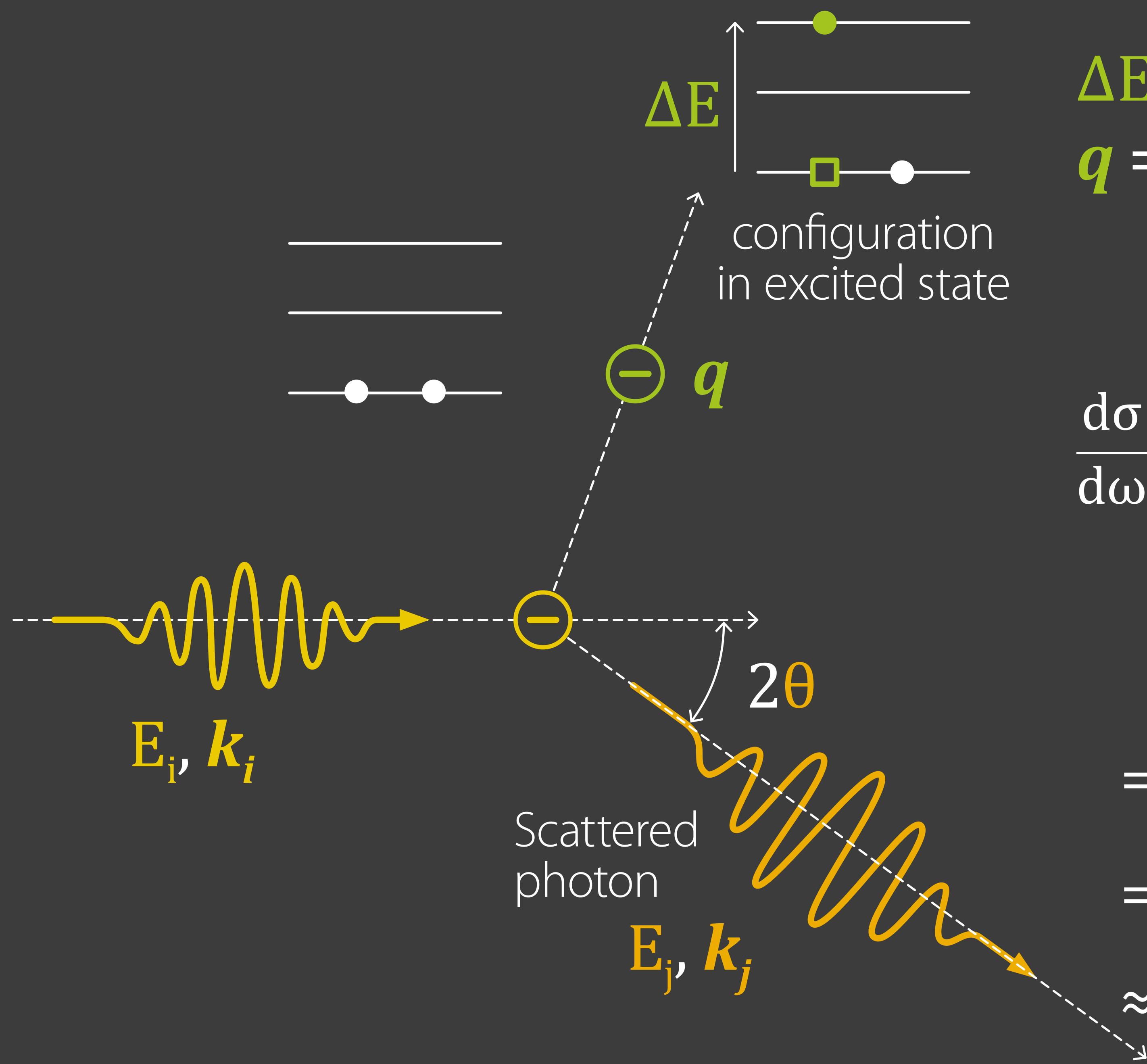


$\Delta E = E_i - E_j$

$\boldsymbol{q} = \boldsymbol{k_i} - \boldsymbol{k_j}$

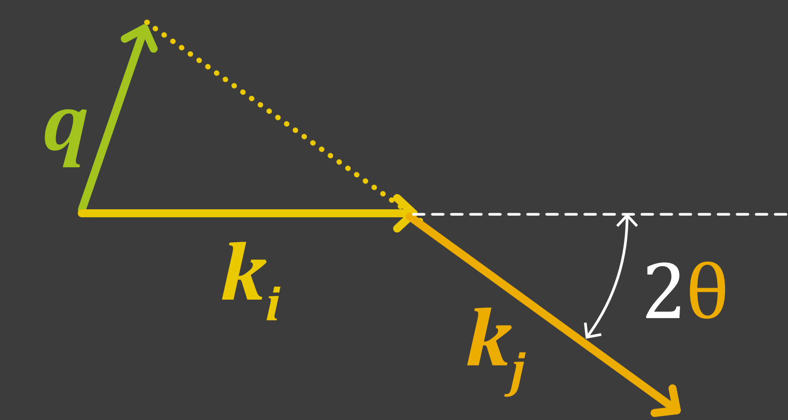


$$\frac{d\sigma}{d\omega} = \frac{4\pi^3 e^4 h}{m^2 \nu_i \nu_j}\left(1 + \cos^2\theta\right) \left\| \langle f \,|\, \exp\left[i\left(\mathbf{k_j} - \mathbf{k_i}\right)\cdot \mathbf{r}\right] |0\rangle \right\|^2$$

$$\times\ \delta\left(E_f - E_0 - h\left(\nu_i - \nu_j\right)\right)$$

Mizuno, 1967; Tohji, 1989; Bergmann, 2002

$$= |k_i - k_j|$$

$$= \sqrt{k_i^2 + k_j^2 - 2\,k_i\,k_j\,\cos 2\theta}$$

$$\approx 2\,k_i \sin\theta$$


experiments performed at:

- GALAXIES, **SOLEIL**, Saint-Aubin, FR
- ID20, **ESRF**, Grenoble, FR
- 6.2, **SSRL**, Stanford CA, USA

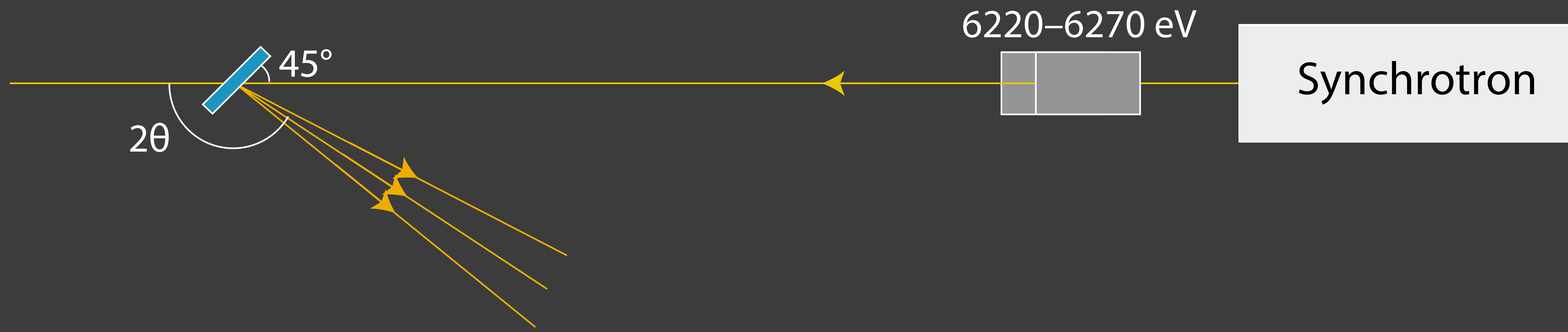


experiments performed at:
– GALAXIES, **SOLEIL**, Saint-Aubin, FR
– ID20, **ESRF**, Grenoble, FR
– 6.2, **SSRL**, Stanford CA, USA

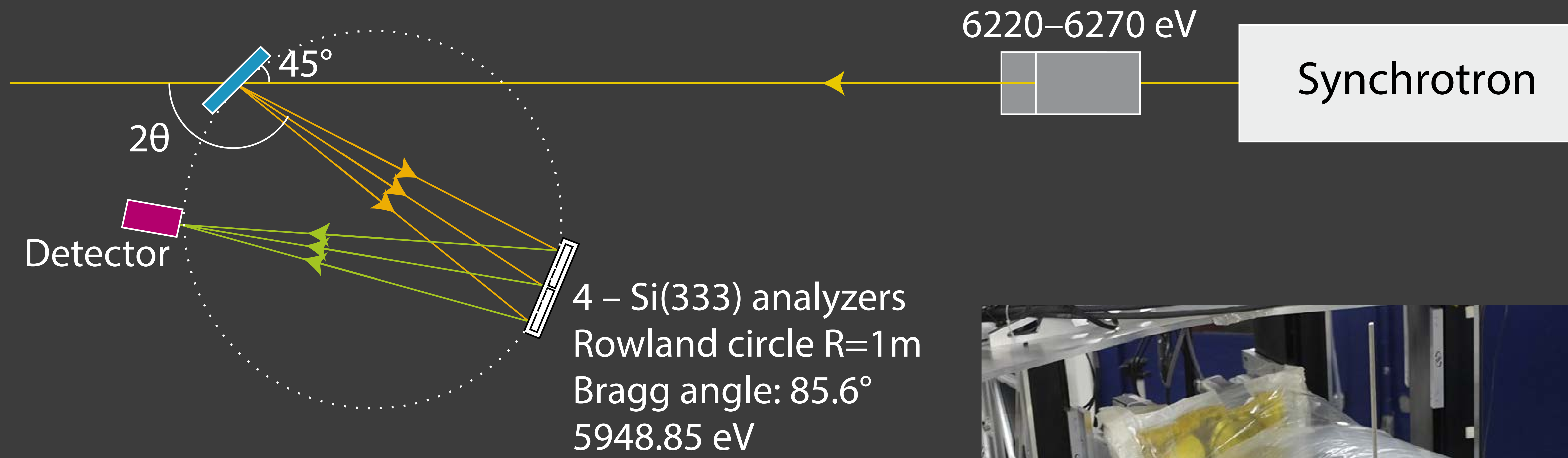


experiments performed at:

– GALAXIES, **SOLEIL**, Saint-Aubin, FR
– ID20, **ESRF**, Grenoble, FR
– 6.2, **SSRL**, Stanford CA, USA

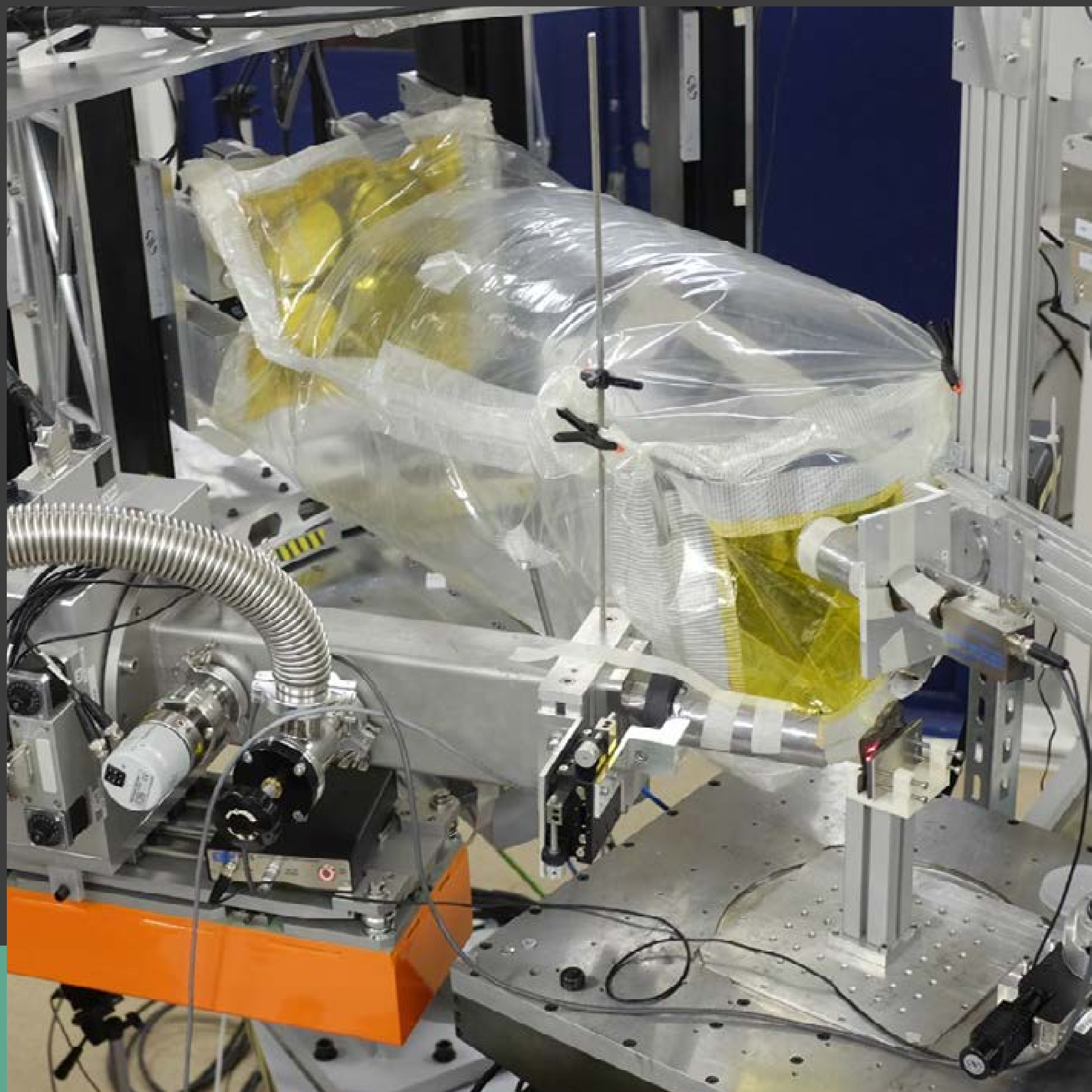

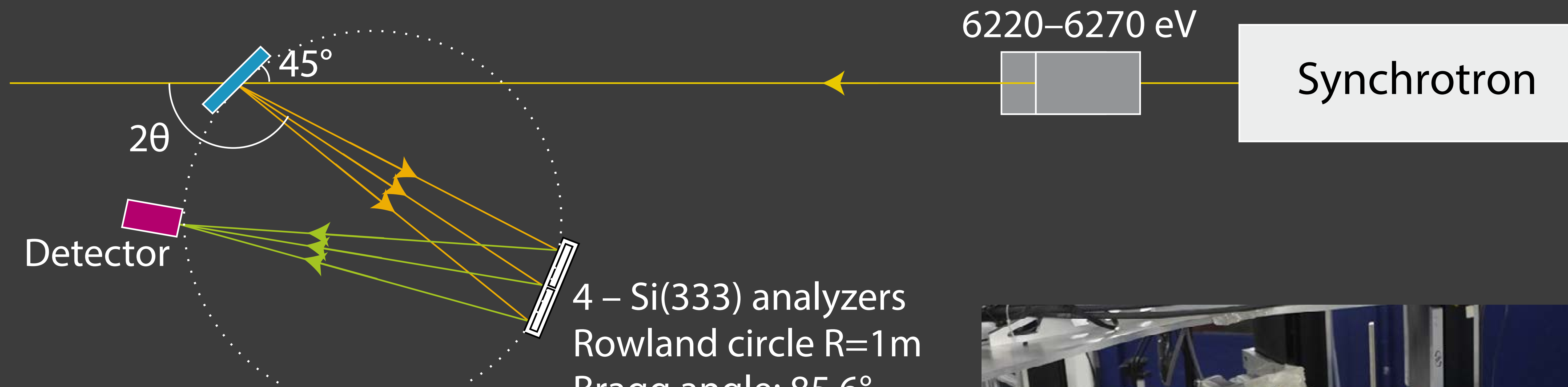


4 – Si(333) analyzers
Rowland circle R=1m
Bragg angle: 85.6°
5948.85 eV

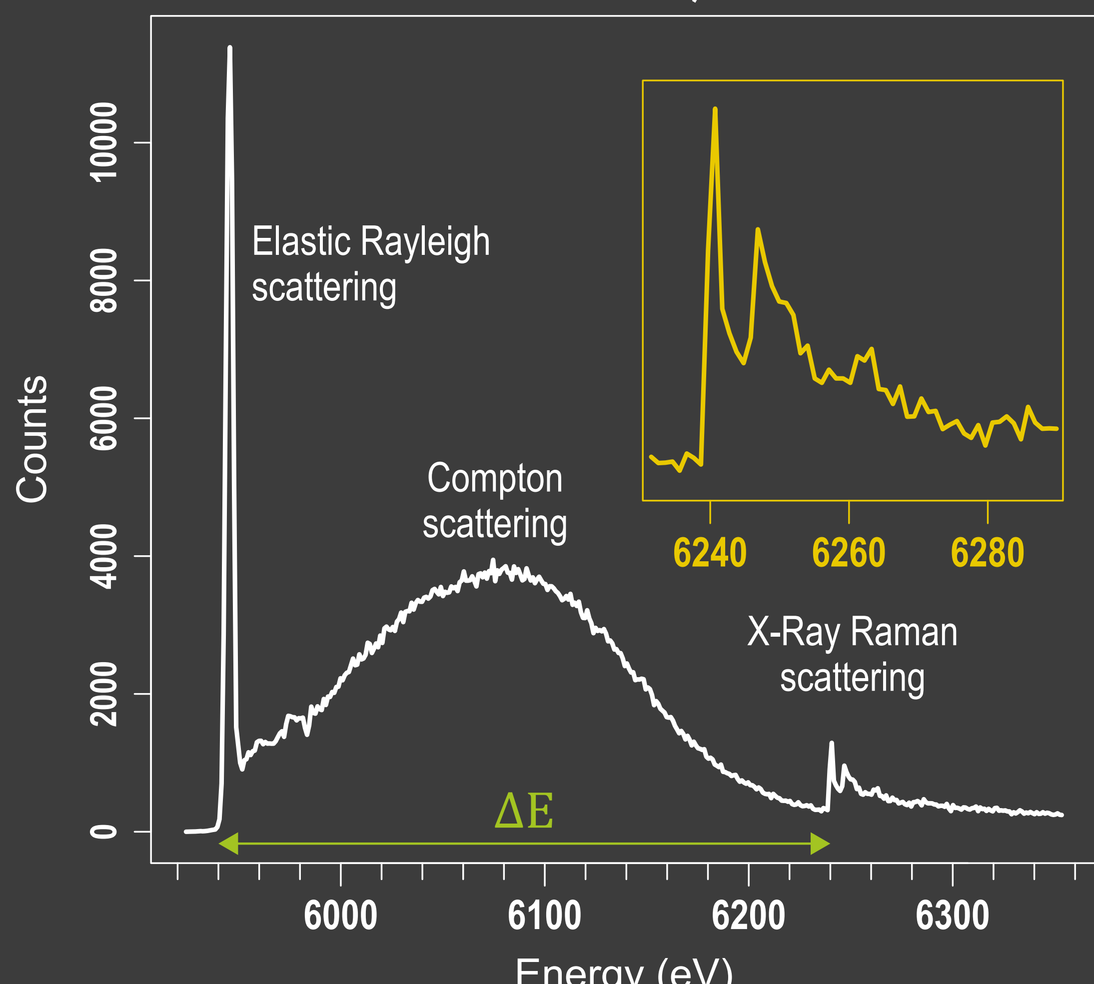


$\Delta E \approx 270–320$ eV

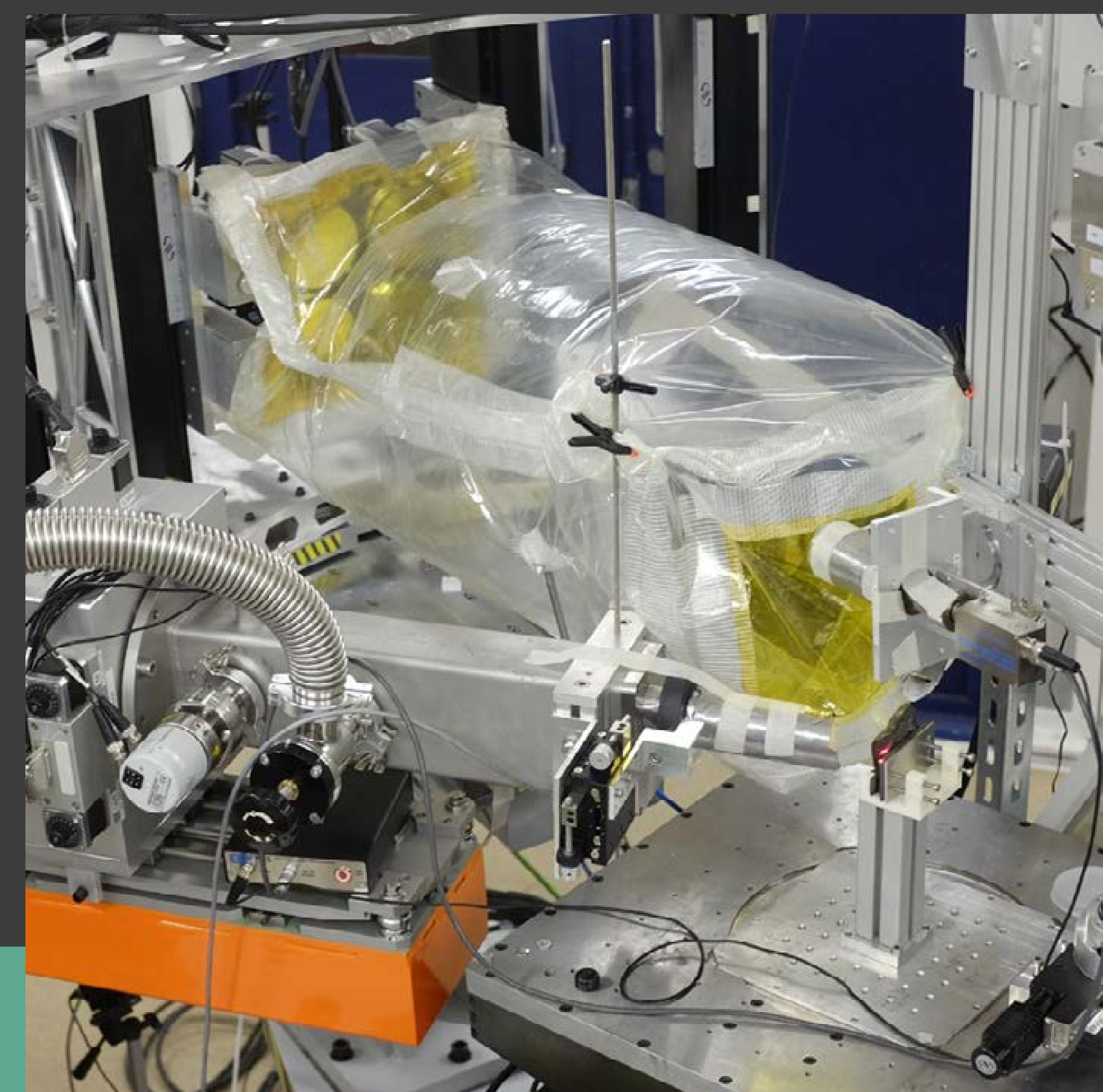

# "unprepared" fossil specimen

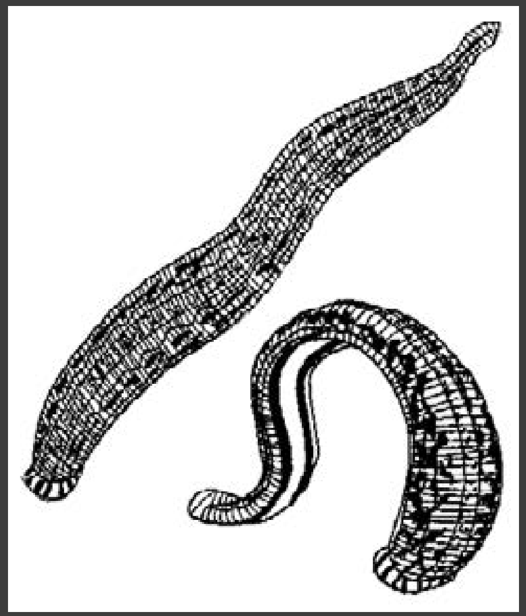

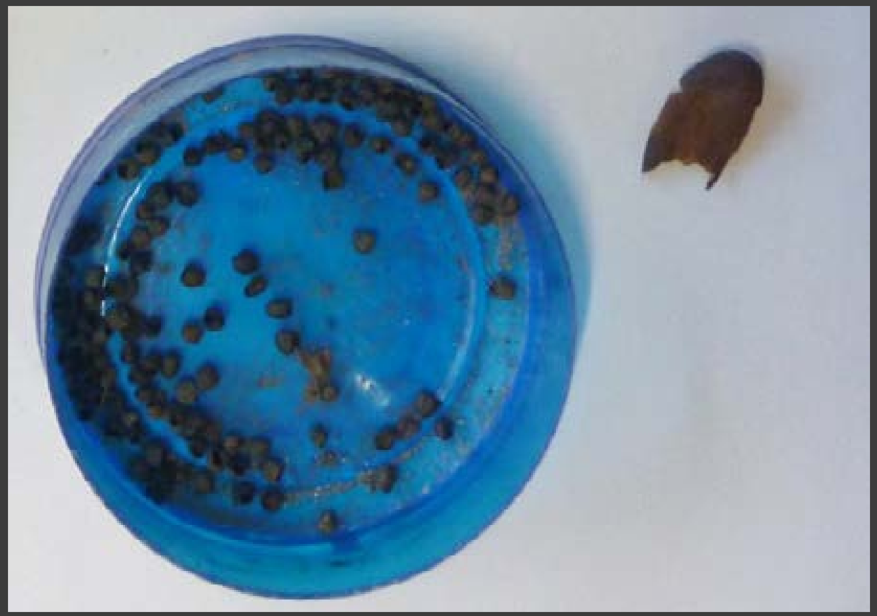

56-Myr old fossil
leech cocoon
Rivecourt (France)

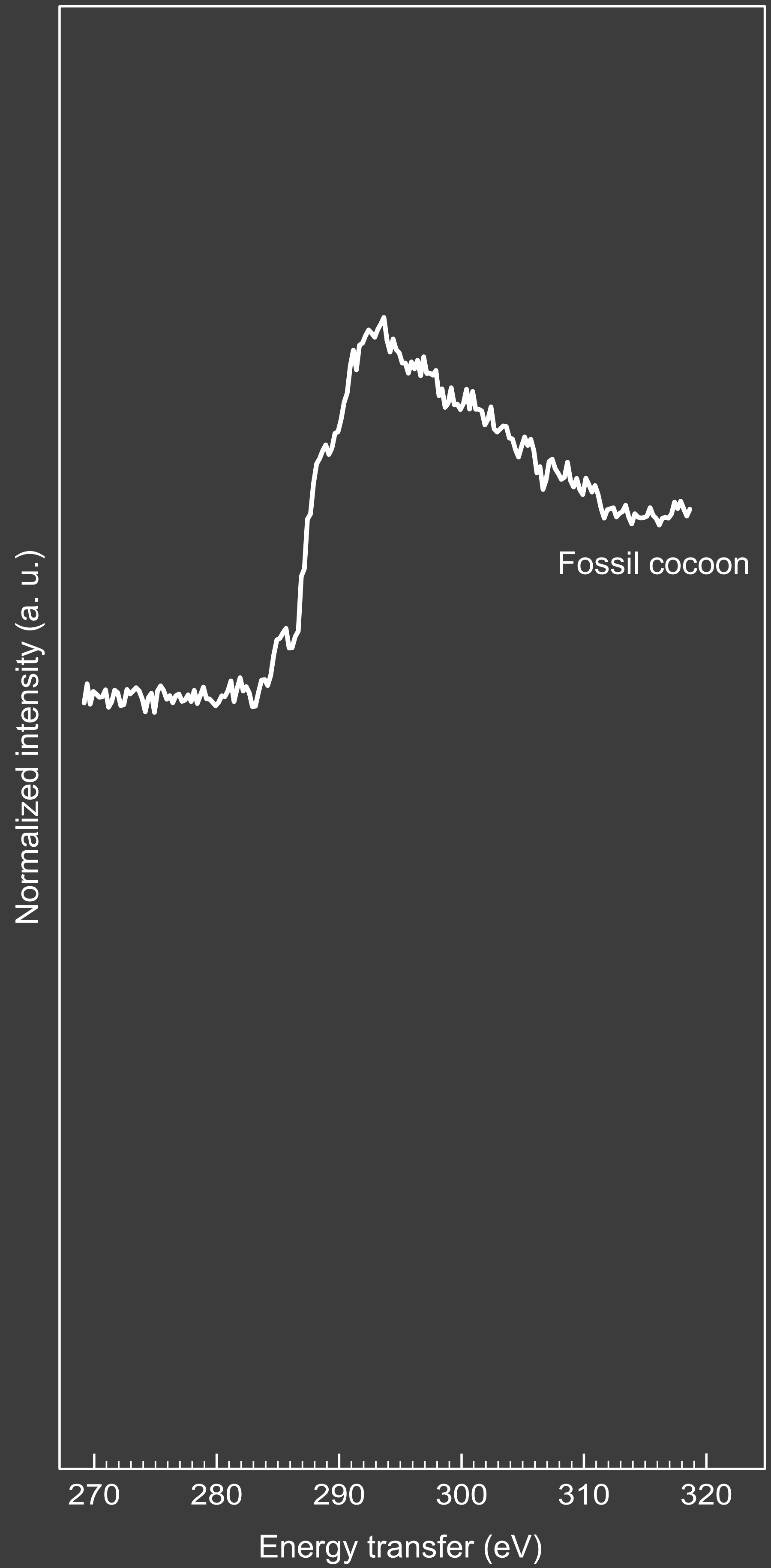




► P. Gueriau et al. Anal. Chem. 2017.

# “unprepared” fossil specimen

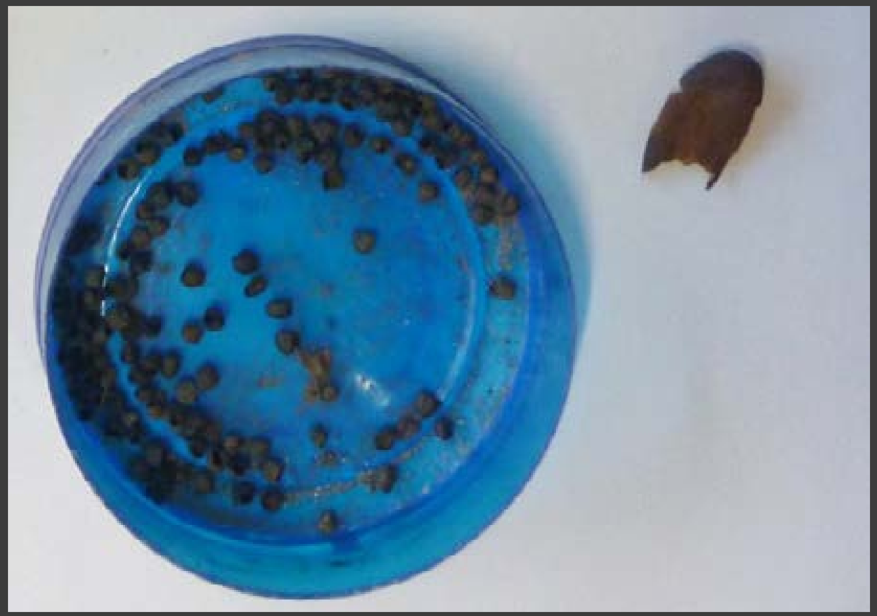

56-Myr old fossil leech cocoon Rivecourt (France)

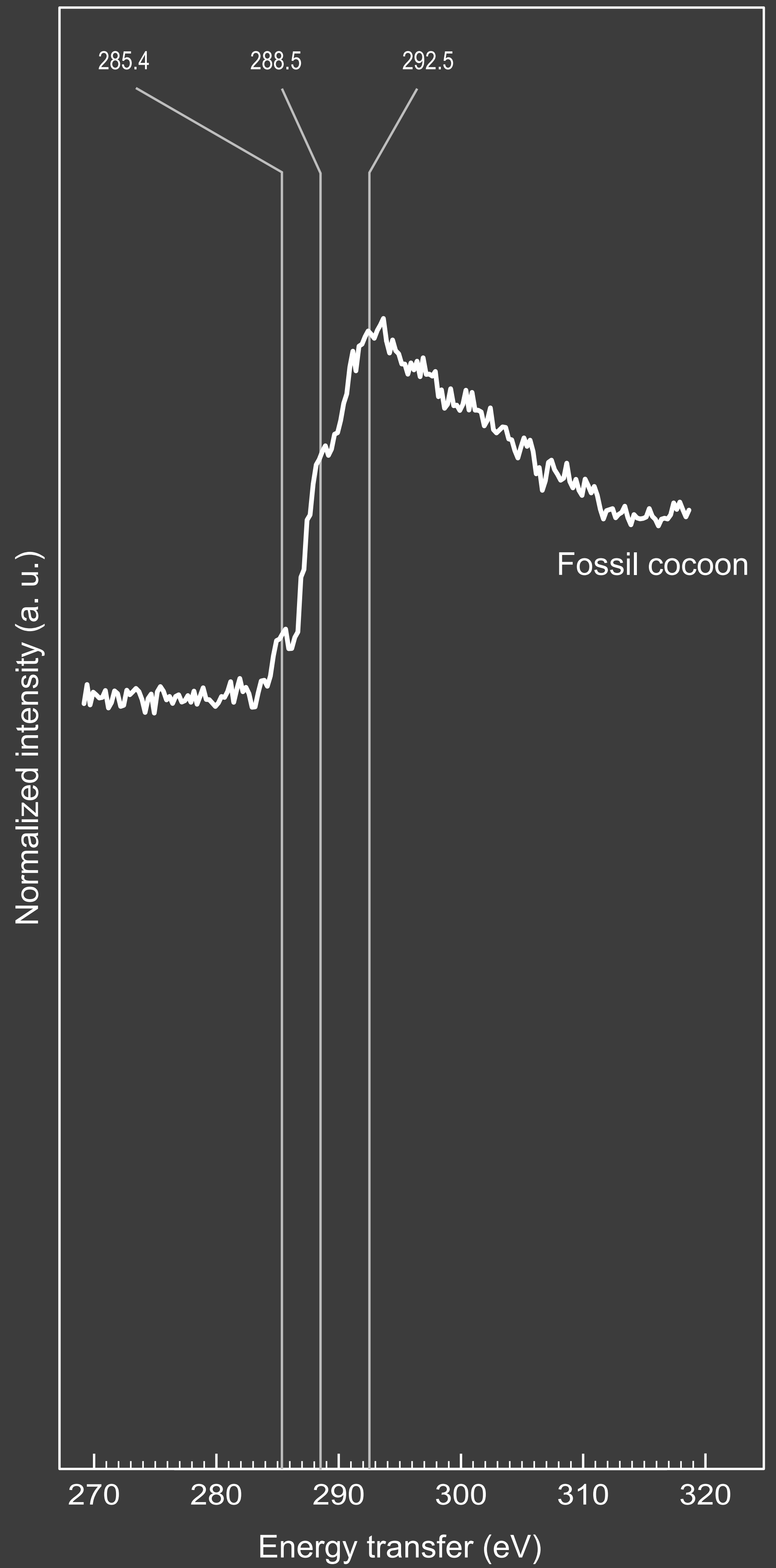


– low-intensity peak at ~285.4 eV: C=C 1s–π* from aromatic or olefinic C=C; unusual width from graphitic domains

– weak shoulder at ~287 eV

– low-intensity broad and complex feature at ~288.7 eV: 1s–π* in amide (288.3 eV) and carboxyl groups (288.7)

No significant signal at 290.3 and 300 eV: no carbonate minerals (XRD)



► P. Gueriau et al. Anal. Chem. 2017.

## “unprepared” fossil specimen

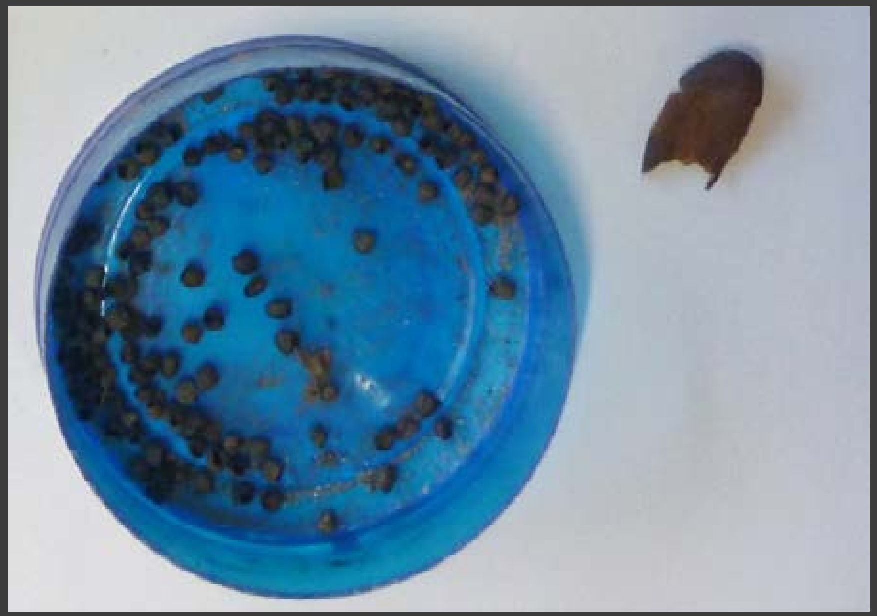

56-Myr old fossil leech cocoon Rivecourt (France)

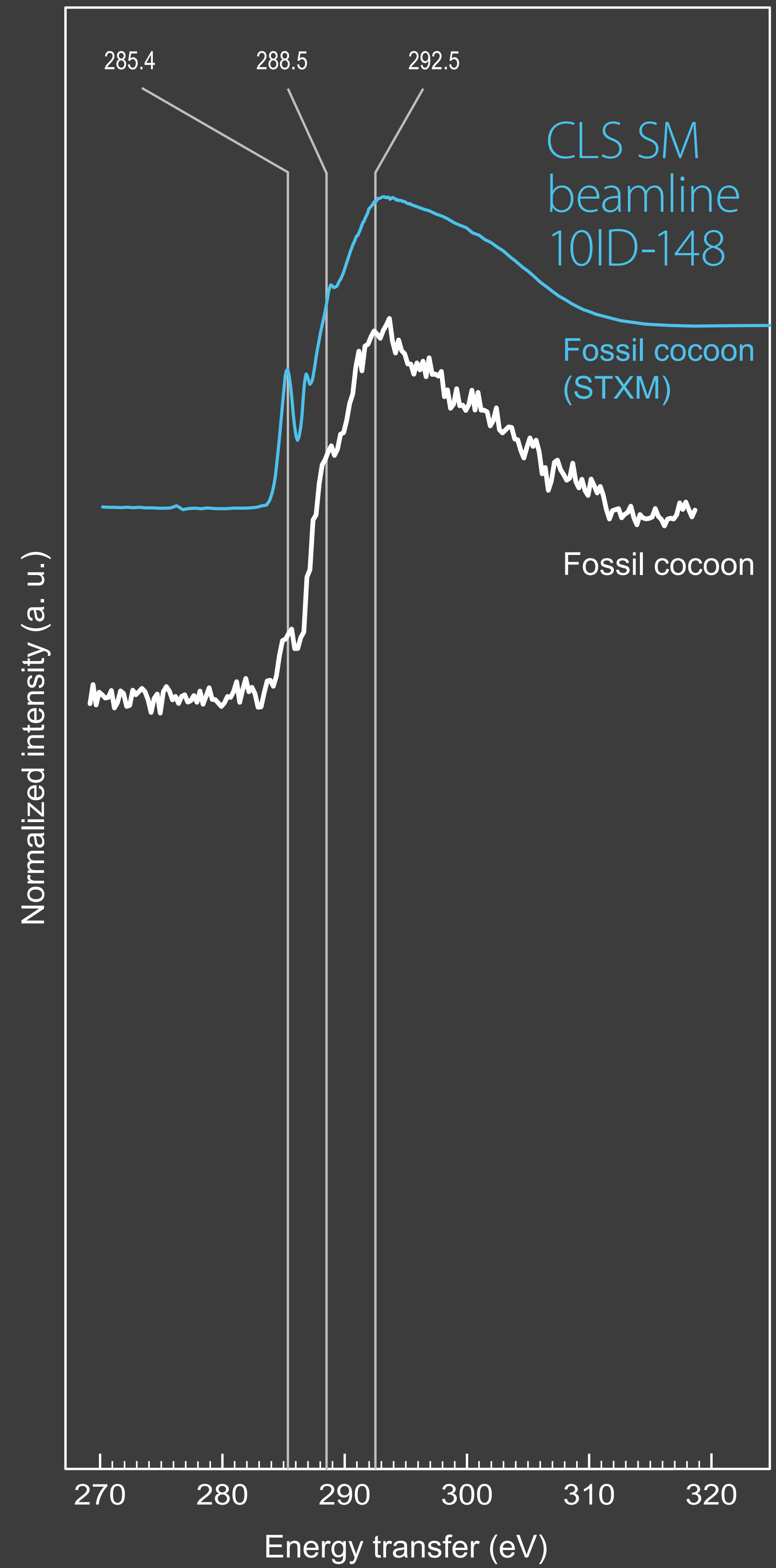


– low-intensity peak at ~285.4 eV: C=C 1s–π* from aromatic or olefinic C=C; unusual width from graphitic domains

– weak shoulder at ~287 eV

– low-intensity broad and complex feature at ~288.7 eV: 1s–π* in amide (288.3 eV) and carboxyl groups (288.7)

No significant signal at 290.3 and 300 eV: no carbonate minerals (XRD)



► P. Gueriau et al. Anal. Chem. 2017.

# “unprepared” fossil specimen

– low-intensity sharper peak at ~285.4 eV: low aromaticity
– intense broad feature at ~288.7 eV: amide and carboxyls
No significant signal at 290.3 and 300 eV: no carbonate minerals (XRD)

Fragment from the dry skin of a 49,000 yr-old fossil mammoth, Lyakhov island (Siberia)

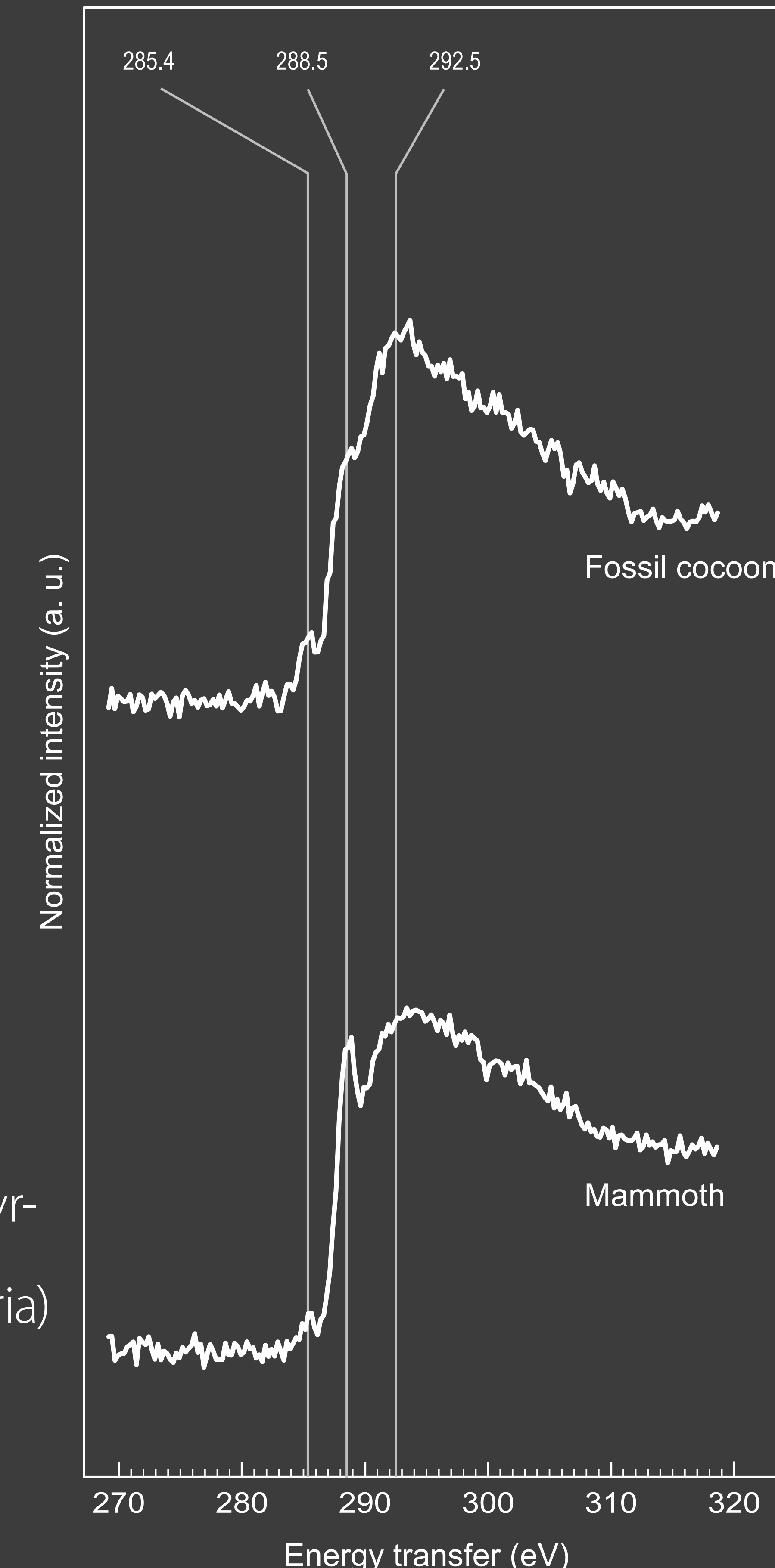




► P. Gueriau et al. Anal. Chem. 2017.

# “unprepared” fossil specimen

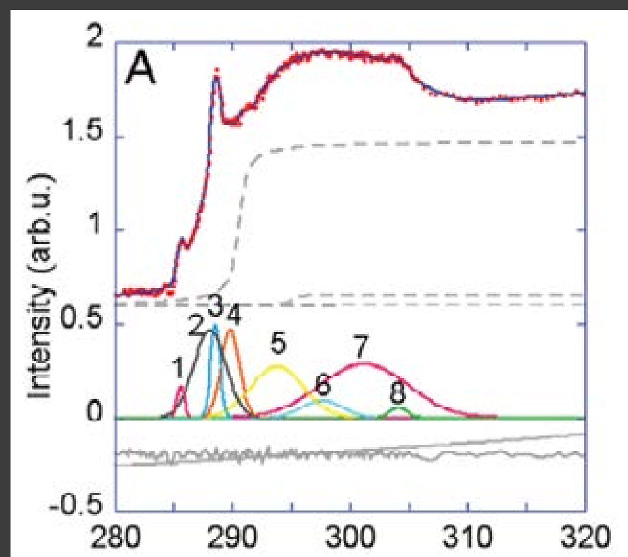


STXM spectrum of modern rat-tail tendon (Lam, ACS Chem. Bio., 2012)

very **good chemical preservation** of the organic compounds composing the ancient mammoth dry skin

Fragment from the dry skin of a 49,000 yr-old fossil mammoth, Lyakhov island (Siberia)

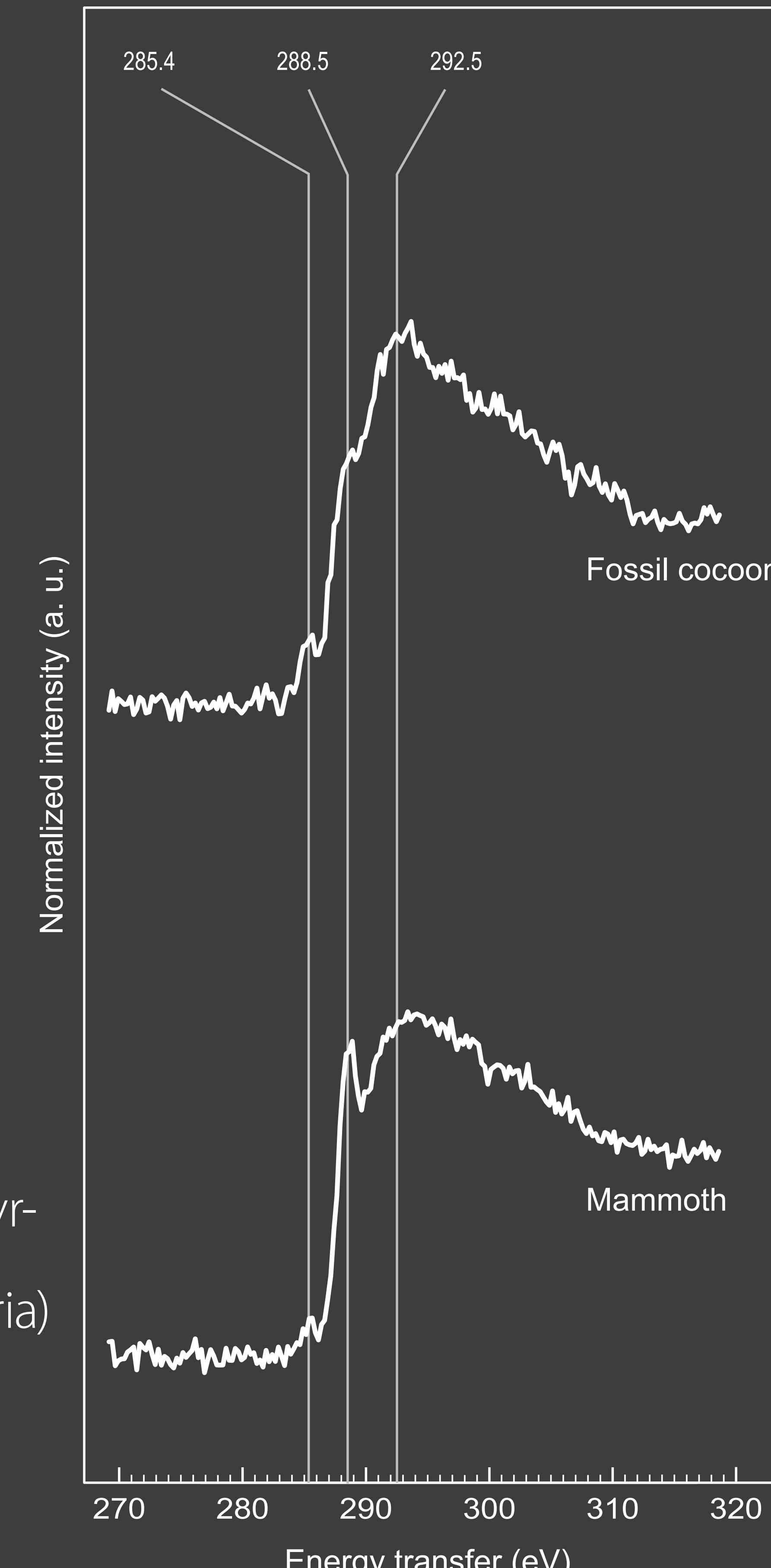




► P. Gueriau et al. Anal. Chem. 2017.

**spectral decomposition of the XRS-based XANES data**
– Gaussians to model features from diagnostic transitions
– arctangent contribution to model the C edge
– non-linear least squares procedure

satisfactory decomposition
reduction to a limited number of contributing features partly compensates the moderate energy resolution and S/N ratio

residual feature confirmed at **287.2 eV**

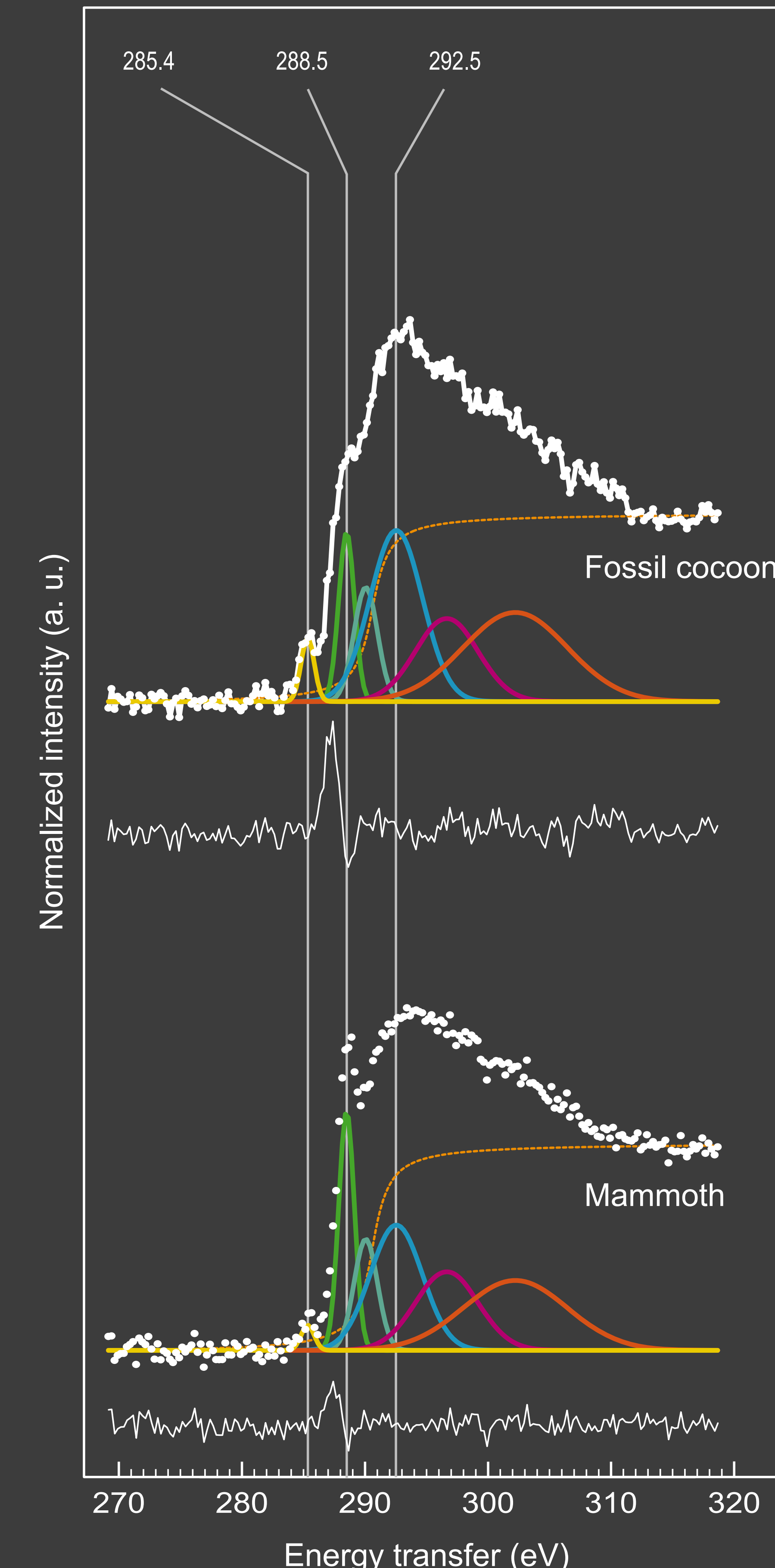




► P. Gueriau et al. Anal. Chem. 2017.

**shoulder at ~287 eV**

– adding peak to the model

– **287.2 eV**

– barely structured residue

1s–σ* transitions from bonds formed between carbon and heteroatoms, e.g. **sulphur** (1s–σ* C–S)

– weak in the mammoth sample

– intense in the cocoon sample

Leech cocoon membranes are unusually rich in sulphur (Mason et al., 2004)

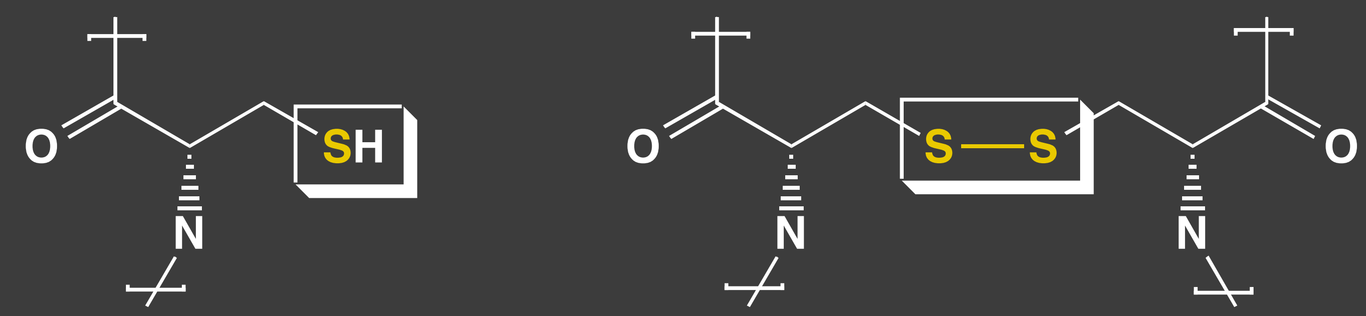


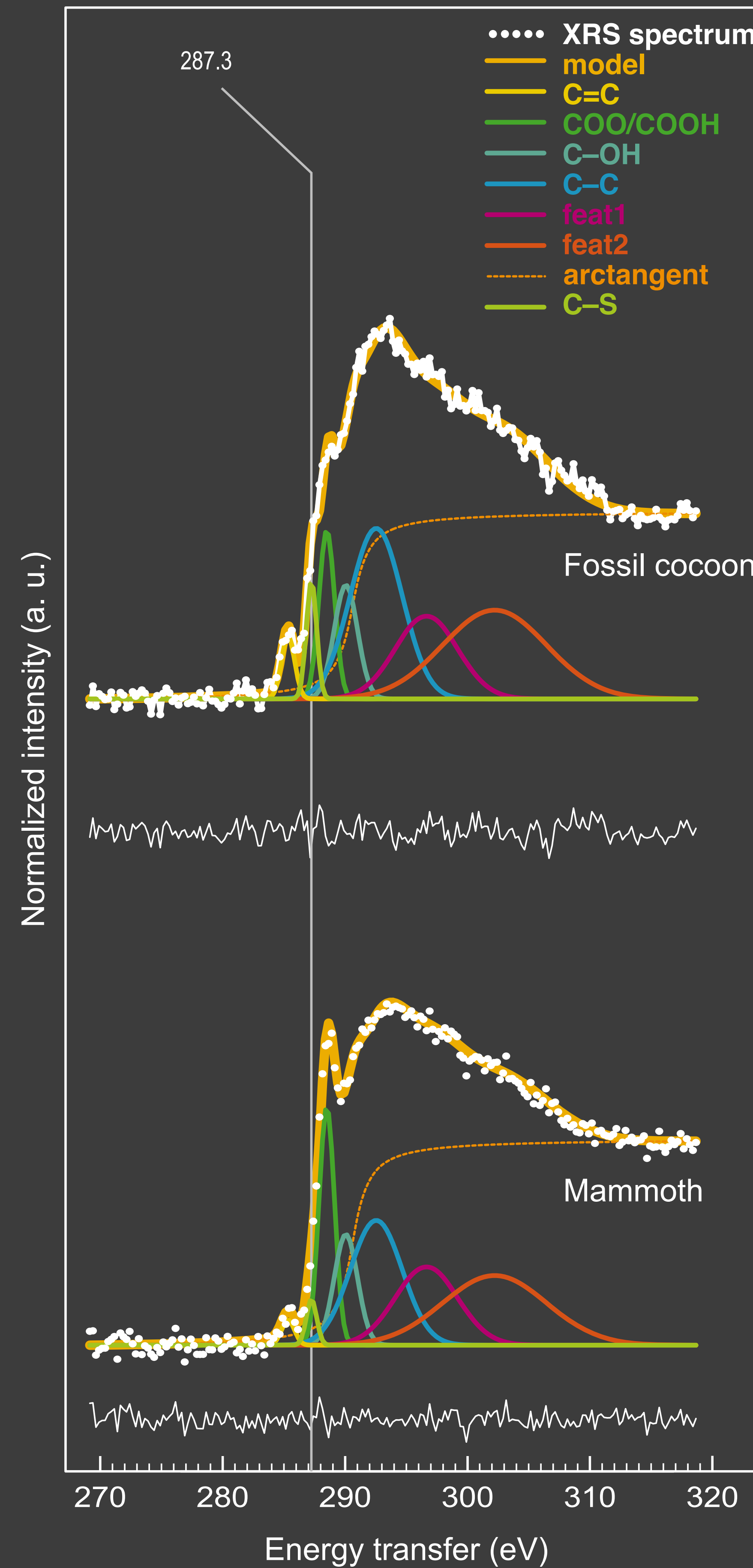




► P. Gueriau et al. Anal. Chem. 2017.

surface dose rate $D = n\, h\nu\, \mu/(s\, \rho)$

photon flux
incident photon energy
attenuation coefficient
beam footprint area
material density

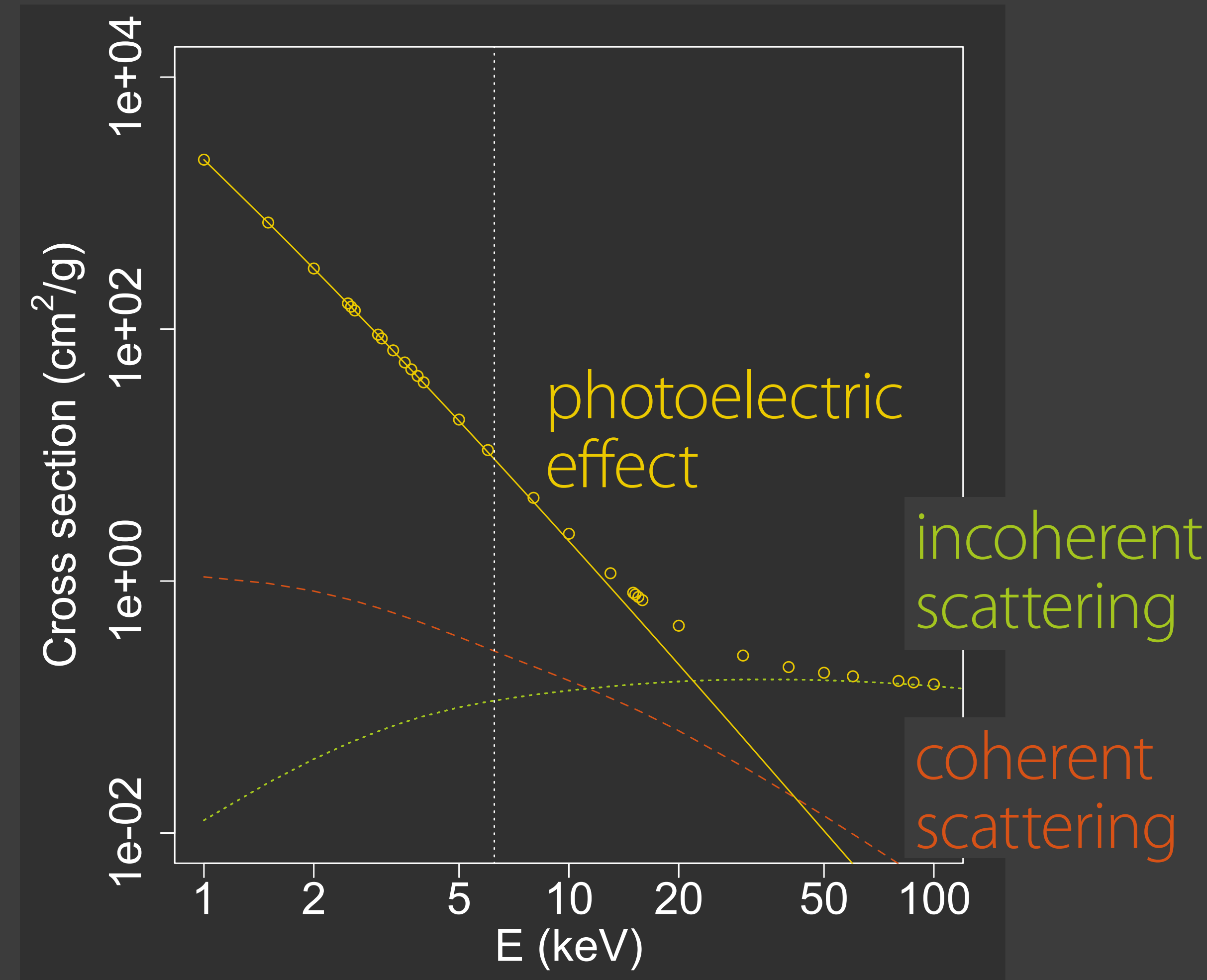


| Experiment | STXM | | XRS | |
|---|---|---|---|---|
| Compound | Surface dose rate (MGy/s) | Integrated surface dose (MGy) | Surface dose rate (MGy/s) | Integrated surface dose (MGy) |
| Chitin | 91 ± 18 | 64 ± 13 | 7.3 ± 1.5 | $7.2\times10^2 \pm 1.4\times10^2$ |
| Calcite | 39 ± 8 | 28 ± 6 | 71 ± 14 | $7.0\times10^3 \pm 1.4\times10^3$ |

**1. heritage materials are heterogeneous and chemically complex**

chemical and structural selectivity

a range of distinct methods to complement lab methods

**2. spectral imaging provide unprecedented information**

to explore multiscale samples

to validate results

**spectroscopy**
spectral
+ some spatial information

**imaging**
spatial
+ some spectral information

**spectral imaging**
spatial + spectral information

**3. beyond the synchrotron experiment**

sample preparation

data analysis

**4. heritage science is a field in itself**

inspiration of new methods

specific constraints, e.g. radiation damage, heterogeneity

## Collaborative interdisciplinary consortia


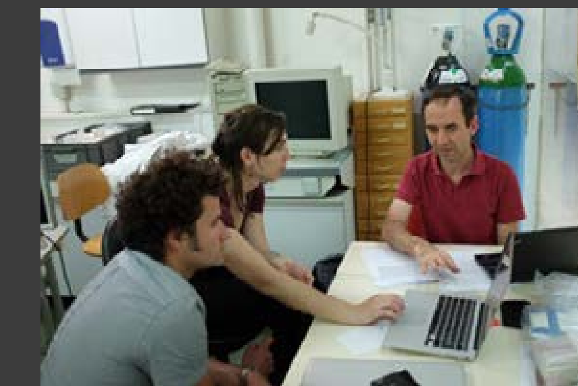

## Medium-term projects


integrated and coordinated use of resources
“time for interdisciplinarity”

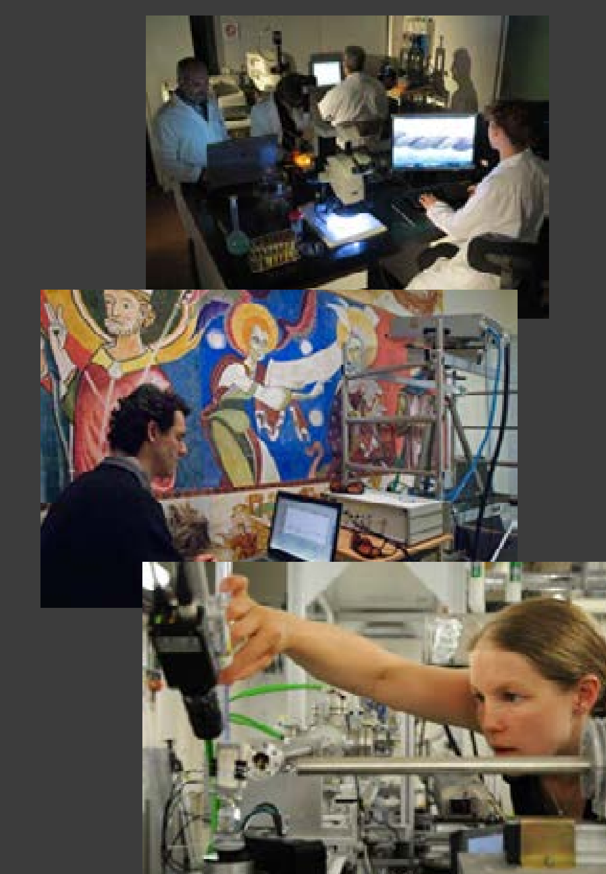

Support and services

Methodological research

E-RIHS
EUROPEAN RESEARCH INFRASTRUCTURE FOR HERITAGE SCIENCE



► L. Bertrand et al. J. Cult. Heritage, 2013.

PAST

"Raw" material

"Ancient" material

PRESENT

**heterogenous material**

⬇

**long-term behaviour**

⬇

**complex material at multiscale**


**analysis**

➡

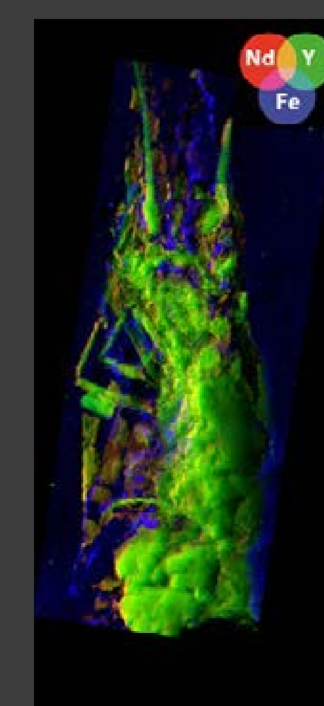


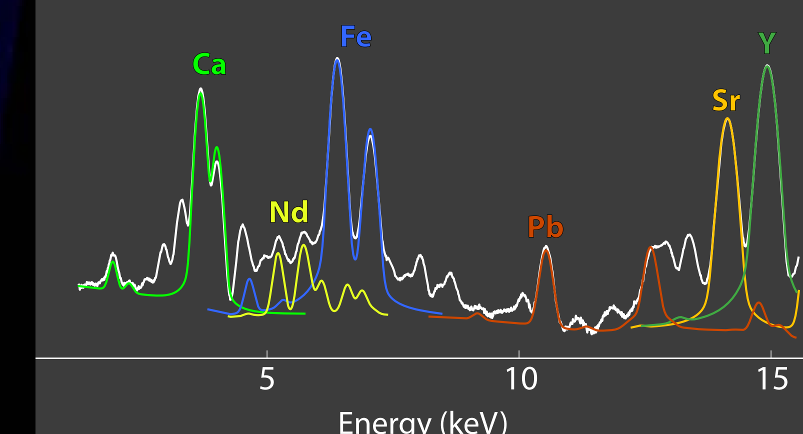


Observables



► L. Bertrand et al. J. Cult. Heritage, 2013.

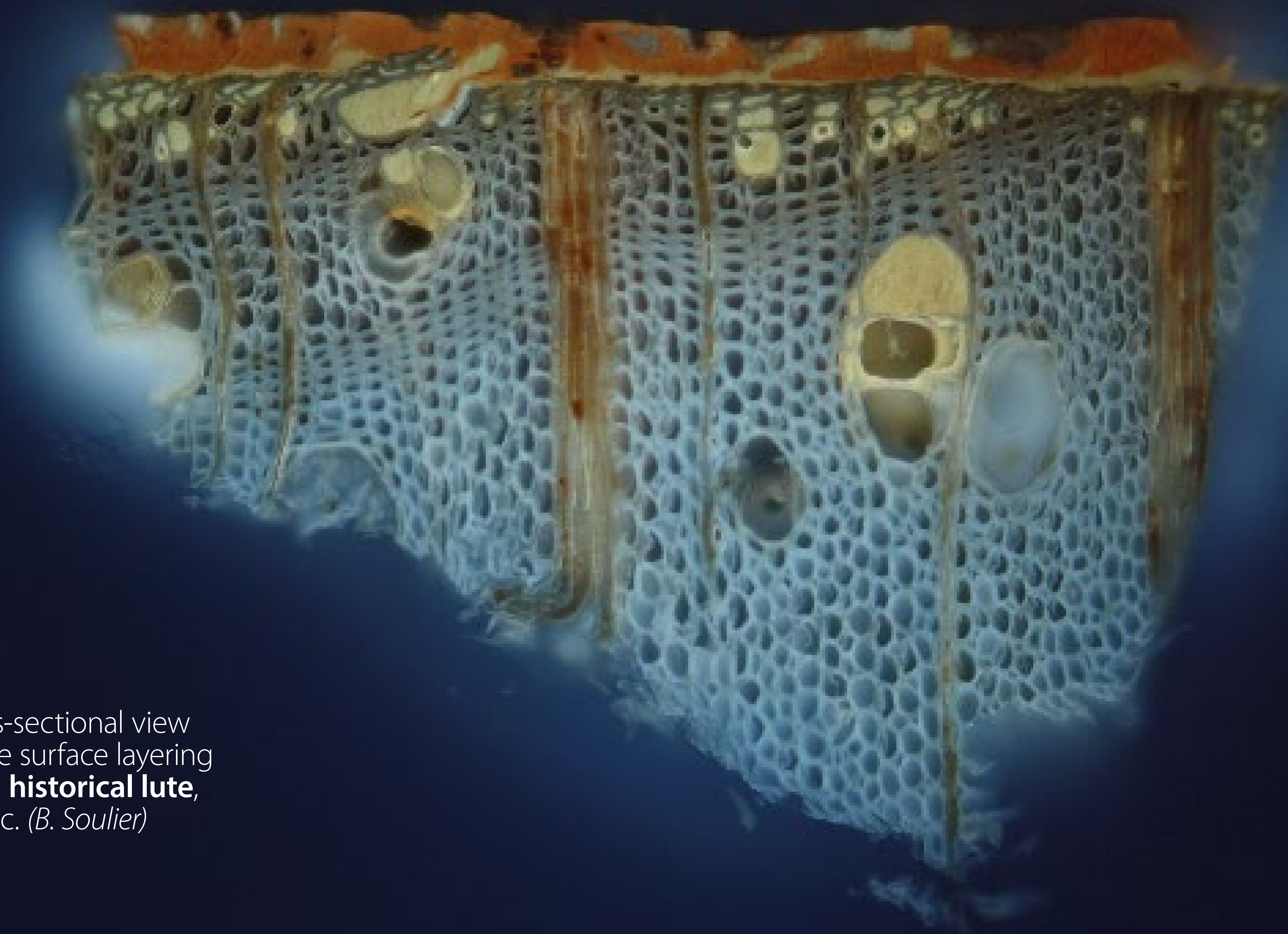

Cross-sectional view
of the surface layering
of an **historical lute**,
16th c. *(B. Soulier)*

Painted surface at a **rock art site**, Cederbeg, Republic of South Africa *(L. Bertrand)*

## synchrotron techniques are well adapted to ancient materials studies

sensitivity from traces to majors
imaging from sub-µm scale to cm's
excitation and emission tunability
kinetic experiments…

**composition**
few – 10s of features

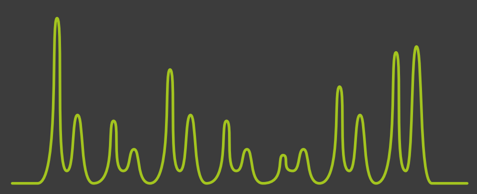

high specificity
&
low *a priori*
|
**versatility**

**abundance**
ppb – %

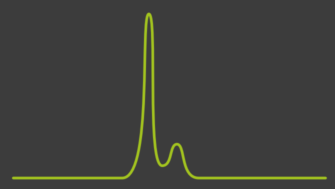

high detection limit
&
no saturation
|
**high dynamic range**

**morphology**
nm – cm

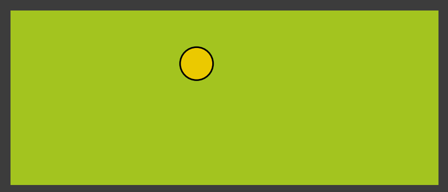

high spatial resolution
&
large field of view
|
**wide spatial dynamics**

## Improving the "length scale dynamics"

**Step Scan** ⇨ **Continuous Scan**
**Step Full field Scan**

Reducing dead times
i.e. unused exposure



► L. Bertrand et al. Phys. Rep., 2012.
► L. Bertrand et al. Top. Curr. Chem., 2016.